A CHEMICAL GENETIC APPROACH TO INTERROGATE THE STAPHYLOCOCCAL HEME SENSING SYSTEM

By
Matthew Carl Surdel

Dissertation
Submitted to the Faculty of the
Graduate School of Vanderbilt University
in partial fulfillment of the requirements
for the degree of

DOCTOR OF PHILOSOPHY
in
Microbiology and Immunology
December 2016
Nashville, Tennessee

Approved:

Timothy L. Cover, M.D.

Maria Hadjifrangiskou, Ph.D.

Eric P. Skaar, Ph.D., M.P.H.

Gary A. Sulikowski, Ph.D.

To Al and AlVerne Bohn,

my loving grandparents who we miss dearly.

ACKNOWLEDGEMENTS

This work would not have been possible without the support of my mentor Eric Skaar, PhD, MPH. He has been a great mentor through my endeavors in the lab, and outside the laboratory. His advice and guidance has helped make me the scientist I am, and will continue to help me become the future physician I will become. I would also like to thank the current and former members of the Skaar laboratory for their continued support and guidance through completion of the work presented in this dissertation.

I have had numerous mentors throughout my education thus far, all of which have been incredible. Dr. Sophia Sarafova helped me realize my love of science while studying in her laboratory at Davidson College. At Vanderbilt University, the MSTP leadership team has provided huge support; specifically I would like to thank Dr. Terry Dermody, and Dr. Chris Williams, and Melissa Krasnove. Finally, I would like to thank those who served on my thesis committee throughout the Ph.D. process: Dr. Tim Cover, Dr. Maria Hadjifrangiskou, Dr. Anthony Richardson, Dr. Eric Skaar, Dr. Gary Sulikowski, and Dr. John Williams.

The work presented here would not have been possible without numerous collaborators and their laboratory members: Harry Dailey (University of Georgia), Duco Janson (Vanderbilt University), D. Borden Lacy (Vanderbilt University), Anthony Richardson (UNC-Chapel Hill), and Gary Sulikowski (Vanderbilt University).

The following reagents were provided by the Network on Antimicrobial Resistance in *Staphylococcus aureus* for distribution by BEI Resources, Nebraska Transposon Mutant Library Screening Array, NR-48501, *Staphylococcus*

epidermidis Strain HIP04645, NR-45860. Core Services performed through Vanderbilt University Medical Center's Digestive Disease Research Center were supported by NIH grant P30DK058404 Core Scholarship. The light source was developed by Philip Samson of the Vanderbilt Institute for Integrative Biosystems Research and Education.

My work was supported by Public Health Service award T32 GM07347 from the National Institute of General Medical Studies for the Vanderbilt Medical-Scientist Training Program, R01AI069233, and R01AI073843.

TABLE OF CONTENTS

LIST OF TABLES

LIST OF FIGURES

CHAPTER I. INTRODUCTION

STAPHYLOCOCCUS AUREUS IS A SIGNIFICANT THREAT TO PUBLIC HEALTH

Staphylococcus aureus is a Gram-positive bacterial pathogen that asymptomatically colonizes the anterior nares of approximately a third of the population (1). Upon breaching host defenses, *S. aureus* is capable of causing a wide range of diseases, ranging from superficial skin and soft tissue infections (SSTIs) to invasive diseases with considerable mortality. *S. aureus* is a leading pathogen associated with invasive, life-threatening blood stream infections and ventilator-associated pneumonia (2-4). Together disease caused by *S. aureus* results in approximately 40,000 deaths annually in the United States alone (5-8).

The emergence of antimicrobial resistance is a significant public health threat. It is currently estimated that at least half of *S. aureus* clinical isolates are resistant to methicillin, and furthermore resistance to last line antibiotics such as vancomycin is on the rise (5, 6, 9-12). Taken together, the therapeutic options available for treatment of staphylococcal infections have decreased substantially such that The Centers for Disease Control and Prevention categorized methicillin resistant *S. aureus* (MRSA) as a "Serious Threat" to the United States (13). Importantly, MRSA is responsible for approximately 50% of deaths due to any antibiotic resistant organism in the United States (13). There is a dire need for a further understanding the pathogenesis of this organism in an effort to identify novel therapeutic targets.

PROPIONIBACTERIUM ACNES IS A HUGE HEALTHCARE BURDEN

Propionibacterium acnes, the causative agent of acne, is a Gram-positive bacterium that colonizes virtually the entire population. Over 90% of the world's population will suffer from *P. acnes* infection over the course of their lifetime (14-16). Although not life threatening, *P. acnes* leads to the development of disfiguring lesions that have a tremendous impact on the individual. Because of this, acne poses significant social and economic burdens. Acne is associated with low self-esteem, poor work and school performance, and higher unemployment rates (14, 17). Direct costs due to acne are estimated to exceed $4B each year (14, 18). In addition, there is a dramatic effect on quality of life for patients suffering from acne, which has been quantified monetarily to exceed $12B a year (18).

Although there is a vast array of treatments for acne, effectiveness and side effects limit much of their use. Antibiotic resistance in *P. acnes* is a growing threat and it is estimated that 50% of *P. acnes* isolates are resistant to current therapeutics (19). In addition, current treatments have significant drawbacks due to their often extensive side effect profiles. Oral isotretinoin, the most effective treatment for acne, has the most extensive side effects, including joint pain, headaches, and depression (20). In addition, isotretinoin is a strong teratogen, preventing use in women of reproductive age, one of the largest populations affected by acne (20). Given the incredible social and economic burden caused by acne, it is clear that new therapeutic strategies for the treatment of acne are urgently needed.

HEME HOMEOSTASIS IS ESSENTIAL TO BACTERIAL DISEASE

Bacteria require the essential nutrient heme to colonize the vertebrate host (21-24). Heme serves as a cofactor for numerous processes within the cell, as well as an iron source during infection. The heme requirement can be satisfied by two mechanisms: importing exogenous heme through dedicated machinery or synthesizing endogenous heme *de novo* from metabolic precursors. Both acquisition and synthesis of heme are required for *S. aureus* to cause disease (21, 25-27).

S. AUREUS ACQUIRES HEME FROM THE HOST

Within the human host, *S. aureus* is in a constant battle to acquire nutrient metals (28). Humans have developed intricate defense mechanisms to sequester nutrients from invading pathogens in a process termed "nutritional immunity" (12). *S. aureus* requires exogenous heme as an iron source in order to successfully cause disease; however, the majority of heme is complexed to hemoglobin within the host. Hemoglobin is stored within red blood cells (RBCs), providing yet another layer of defense that *S. aureus* must overcome to gain access to this essential nutrient. *S. aureus* has developed a system to overcome this by secreting hemolysins, which lyse RBCs and liberate hemoglobin. The iron-regulated surface determinant (Isd) system of *S. aureus* then extracts and imports exogenous heme (27, 29). Intact heme is a required cofactor for cytochromes in the electron transport chain, is necessary for catalase in order to detoxify reactive oxygen species (ROS), and is also a cofactor for bacterial nitric oxide synthase (bNOS) (22, 30). The Isd system can further break down heme to release iron, a required nutrient metal (31).

GRAM-POSITIVE BACTERIA UTILIZE A UNIQUE HEME BIOSYNTHESIS PATHWAY

Heme is required by all kingdoms of life. Heme biosynthesis was long thought to proceed through a pathway conserved across all species. Therefore, antibacterial strategies were not focused on targeting heme biosynthesis due to potential off-target effects in humans. However, in the last two years Dailey *et al.* and Lobo *et al.* independently published reports that the majority of Gram-positive organisms synthesize heme through a noncanonical pathway, utilizing three distinct terminal enzymes that differ from the classical pathway (32, 33).

Early heme biosynthesis proceeds through the same mechanism in both the classical and noncanonical pathways (Figure 1). However, upon production of coproporphyrinogen III (CPGIII) the two pathways diverge. In the classical pathway, CPGIII is converted to protoporphyrinogen IX (PPGIX) by HemF/N. PPGIX is then converted to protoporphyrin IX (PPIX) through a six electron oxidation catalyzed by protoporphyrinogen oxidase (annotated as HemG, HemJ, or HemY). Finally, ferrochelatase (HemH) assists in coordinating an iron atom in the porphyrin ring, resulting in heme. In organisms that utilize the noncanonical pathway however, CPGIII is instead converted to coproporphyrin III (CPIII) by coproporphyrinogen oxidase (HemY), followed by coordination of an iron atom by HemH to produce copro-heme. The final enzyme, HemQ, was recently discovered and is specific to the noncanonical pathway. HemQ catalyzes the decarboxylation of copro-heme to form heme (21, 24, 32-34).

Although often annotated in a similar fashion, there are two distinct genes that encode HemY leading to differences in structure and function, one in each pathway. In the classical pathway HemY serves as a protoporphyrinogen oxidase. Interestingly, it has

been observed previously that Gram-positive HemY retains unique characteristics, making it distinct from the classical HemY. Multiple studies have found that Gram-positive HemY has the ability to oxidize both PPGIX as well as CPGIII (34-37). Importantly, Gram-positive HemY converts CPGIII at a rate 9-fold higher than PPGIX (32). Upon further investigation, Dailey *et al.* found that these are in fact structurally and functionally distinct enzymes, which led to the characterization of the noncanonical pathway (32). The divergence of the classical and noncanonical pathways has opened the door to the exciting possibility of Gram-positive specific therapies targeting the terminal steps of heme biosynthesis.

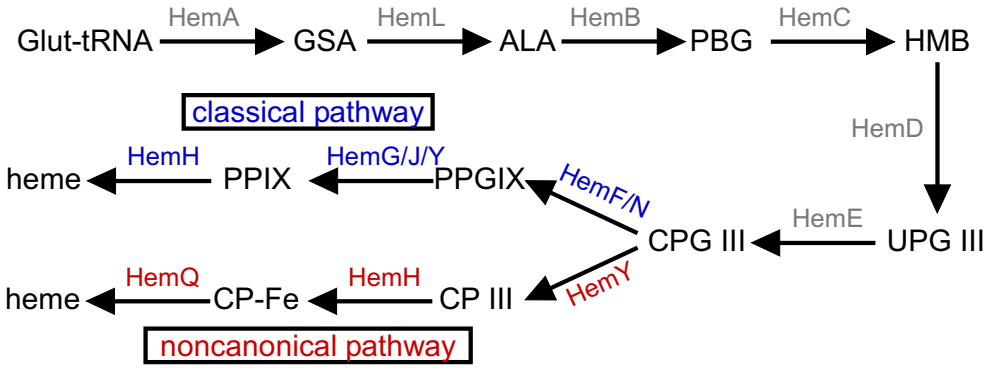

Figure 1. Gram-positive heme biosynthesis utilizes a noncanonical pathway.
Recently it was uncovered that heme biosynthesis in Gram-positive bacteria proceeds through a noncanonical pathway (red), as opposed to the classical pathway (blue) utilized by all other organisms (21, 32, 33).

ALTHOUGH REQUIRED, HEME IS TOXIC

Although required to successfully colonize the host, excess heme is toxic to the bacteria. Thus, the ability to sense and respond to increased levels of heme is critical to the survival of many Gram-positive pathogens. A major mechanism by which bacteria sense and respond to their environment is through the use of two-component systems (38-41). Two-component systems are present in almost all bacterial genomes (41). A prototypical two-component system utilizes a membrane bound sensor histidine kinase to sense specific stimuli. Upon activation by a signal, the kinase undergoes autophosphorylation. The kinase facilitates phosphotransfer to and therefore activation of a cognate response regulator, which induces a desired response. One of the most common responses induces is modification of the transcriptional program of the bacteria (38, 40). There is significant interest in understanding the specific mechanisms that facilitate two-component system signal transduction. In addition, despite the thousands of two-component systems identified, only a handful have known ligands (40, 42, 43).

S. aureus senses heme through a two-component system, the heme sensor system (HssRS). Upon activation, the membrane histidine kinase, HssS, activates the response regulator, HssR, which induces the expression of the heme-regulated transporter (*hrtAB*). *hrtAB* encodes an efflux pump that alleviates heme toxicity (44, 45). The coordinated efforts of HssRS and HrtAB enable *S. aureus* to grow in the presence of high heme concentrations. As with the majority of two-component systems, the signal that activates the sensor histidine kinase, in this case HssS, remains unknown (Figure 2) (44, 46). Previously it has been identified that deletion of components of HssRS affect the virulence of the pathogen (46). Determining the mechanisms by which pathogens cope

with heme stress will lead to insight into novel therapeutic targets. As heme sensing systems are conserved across numerous medically relevant pathogens, this work may be applicable to numerous infectious agents.

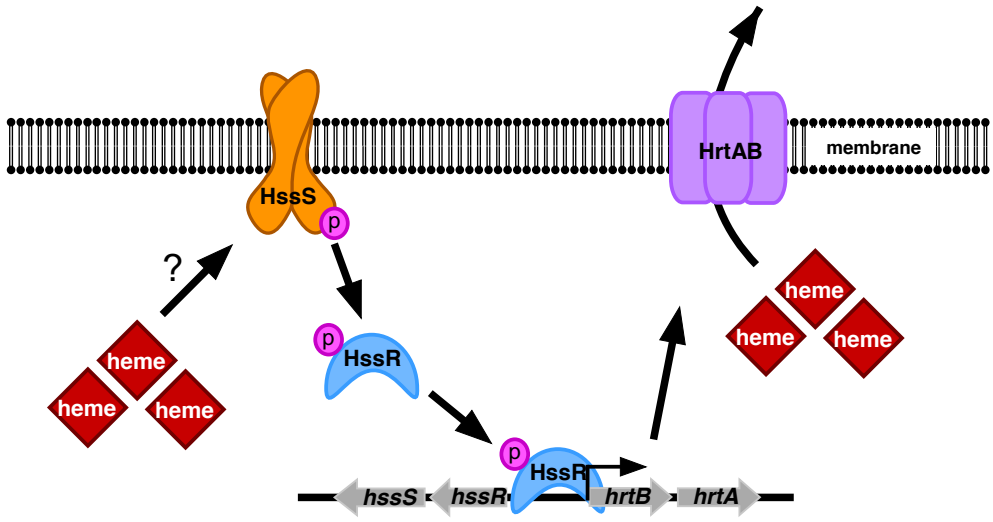

Figure 2. The *S. aureus* heme detoxification system.

Heme exposure induces the autophosphorylation of HssS, followed by phosphotransfer to HssR. Upon activation, HssR induces the expression of *hrtAB* to alleviate heme toxicity.

HIGH-THROUGHPUT SCREEN (HTS) IDENTIFIES SMALL MOLECULE ACTIVATORS OF THE *S. AUREUS* HEME SENSING SYSTEM

In order to probe the mechanism of HssRS activation, a high-throughput screen (HTS) was previously performed utilizing the Vanderbilt Institute for Chemical Biology (VICB) small molecule library, consisting of approximately 160,000 compounds (47). A P_{hrt} driven luminescent reporter (p*hrt.lux*) was developed and transformed into *S. aureus* (47, 48). Heme induces robust luminescence in wild-type *S. aureus* harboring p*hrt.lux*, and this response is dependent upon an intact two-component system (Figure 3). Using this assay, 250 positive hits were identified. The top 110 hits were subjected to secondary and tertiary screens to eliminate molecules that generated non-specific luminescence. Positive hits were further selected based on chemical-tractability, lack of offending functional groups, and absence of significant biological activity based on SciFinder and PubChem searches. Ultimately, twelve lead compounds were identified for further interrogation. The small molecules VU0038882 (‘882) and VU0043981 (‘3981) were selected for focused follow-up (Figure 3).

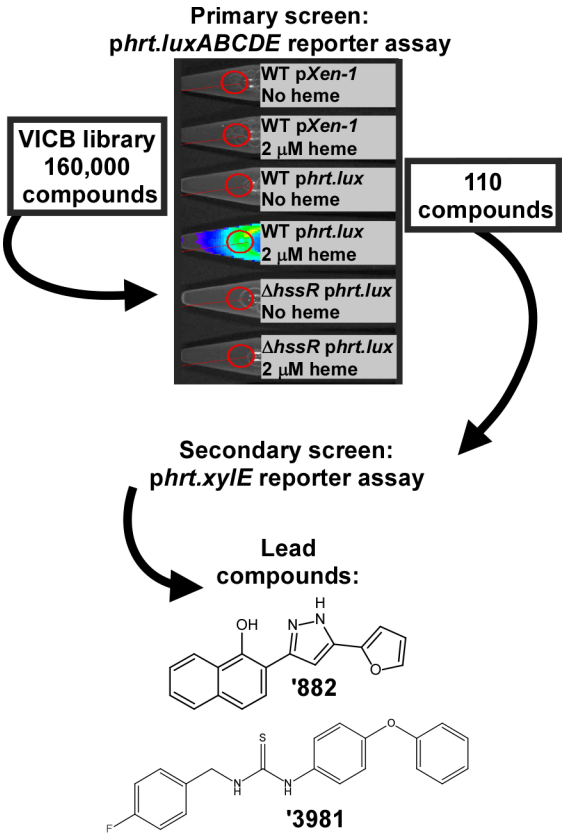

Figure 3. High throughput screen identifies small molecule activators of HssRS.
A whole cell bioluminescence assay to identify HssRS activators was used to screen the Vanderbilt Institute for Chemical Biology small molecule library of approximately 160,000 compounds. Top hits were confirmed in a secondary screen employing the p*hrt.xylE* reporter construct. Lead compounds '882 and '3981 were identified for focused follow-up. Figure adapted from Mike *et al.* (47).

‘882 INCREASES ENDOGENOUS HEME BIOSYNTHESIS

In order to further the understanding of HssRS activation, previous studies have utilized molecule ‘882 (47, 49). Mike *et al.* characterized ‘882 as an HssRS activator and identified that ‘882 induces two major phenotypes in bacterial cells. First, ‘882 exhibits toxicity toward respiration deficient strains of *S. aureus* (47). Second, ‘882 activates HssRS (47). Upon further interrogation, it was determined that these two phenotypes are in fact unrelated (49).

Mike *et al.* hypothesized that ‘882 may activate HssRS by increasing endogenous heme biosynthesis (47). Upon ‘882-treatment, *S. aureus* accumulates 15-fold more heme than untreated cells. In addition, ‘882 does not activate HssRS in strains lacking an intact heme biosynthesis pathway. Importantly, this was the first instance that endogenously produced heme was shown to activate HssRS. Taken together, ‘882 was identified as an activator of endogenous heme biosynthesis. Despite significant efforts, the authors were unable to identify the target of ‘882 (47).

OVERCOMING THE HURDLE OF SMALL MOLECULE TARGET IDENTIFICATION

Identifying the targets of small molecules is a major obstacle in biomedical research (50-52). Phenotypic high-throughput screens utilizing small molecule libraries often result in the identification of numerous molecules with unknown targets. Several approaches have been successful in identifying intracellular targets of small molecules, including overexpression libraries, transposon mutagenesis, and the isolation of spontaneous resistance mutants (53-59). However, the strategies do not work in all circumstances, thereby requiring a multifaceted approach in order to successfully identify

the target of a small molecule. Taken together, creative and novel methods for identifying cellular targets of small molecules are often necessary in order to be successful in this endeavor. Identifying targets of small molecules has the potential to enable the development of novel therapeutics strategies to target infectious diseases.

SKIN AND SOFT TISSUE INFECTIONS (SSTIS) ARE A BURDEN TO SOCIETY

The skin is the largest organ in the human body and is the first barrier to infection. Disruption of this physical blockade allows bacteria to colonize and invade into host tissues. Skin and soft tissue infections (SSTIs) represent a group of infections relating to the skin and the underlying tissues, including the epidermis, dermis, fascia, and underlying fat (9, 15, 60). The most common etiological agents of SSTIs are Gram-positive bacteria. Specifically, *S. aureus* and *P. acnes* are among the most prevalent causative agents of SSTI (9, 14, 15, 60). In fact, SSTIs are the most common infectious cause of clinic visits in the United States (15). Although the exact prevalence is difficult to determine due to the wide variability among disease presentation, it is estimated that approximately 10% of hospitalized patients suffer from an SSTI, and SSTIs lead to approximately 14.2 million ambulatory care visits in the United States (15). With the growing rates of antibiotic resistance, identifying novel strategies to treat SSTIs is of paramount importance. Photodynamic therapy (PDT) has gained significant interest as a therapeutic strategy to treat SSTIs (16).

PHOTODYNAMIC THERAPY (PDT) IS A PROMISING THERAPEUTIC STRATEGY

The first clinical trial with PDT occurred over 100 years ago, and since then PDT has developed to treat a variety of diseases, including neoplasms, inflammatory, and infectious diseases (16, 61-65). PDT utilizes a photosensitizer molecule that is activated by light, leading to the production of reactive oxygen species (ROS) that results in cell death (16).

Various photosensitizers have been developed, however, the only currently US Food and Drug Administration approved photosensitizers are aminolevulinic acid (ALA) derivatives, which serve as prodrugs (16). When given to a patient, ALA enters the cell and increases the flux through the entire heme biosynthetic pathway (Figure 1). This results in increased production of porphyrins, such as PPIX in mammalian cells and CPIII in bacterial cells, that serve as photosensitizers within the cell. When used to treat skin cancers, the goal of the therapy is to kill human cells. However, the major hurdle facing treatment of infectious disease is that ALA targets both human and bacterial cells, leading to a large number of unwanted side effects, including itching, edema, and inflammatory responses (16, 64). Regardless of the side effects, PDT has become more popular for treatment of acne and other SSTIs that are recalcitrant to current antibiotic therapy (16, 20, 61-63, 66, 67). Identification of new photosensitizers specific to bacteria have the ability to greatly advance the use of PDT for the treatment of infectious diseases and the recent identification of a Gram-positive specific heme biosynthesis pathway has opened the door to bacterial specific PDT strategies.

Recently, the use of PDT is also expanding beyond SSTIs. Gastrointestinal endoscopes have been developed that emit wavelengths that activation porphyrins in

patients to detect cancer, and further been interrogated for their ability to treat gastrointestinal infections (68, 69). Osteomyelitis and infection of orthopedic devices are some of the most common invasive bacterial infections, and many researchers are developing PDT strategies to combat these infections (66, 70-75). Applications are being developed to treat many other diseases as well, including parasitic, dental, and sinus infections (67, 76). Taken together, PDT has the potential to significantly expand the treatment of numerous infections.

CONCLUSIONS

S. aureus and *P. acnes* are significant healthcare threats. There is an urgent need to understand the pathogenesis of these organisms in an effort to identify novel therapeutic strategies. Through interrogating heme homeostasis, the work described here uncovers pathways and treatment strategies that advance our understanding of the pathogenesis of these organisms, and furthermore provides mechanisms by which these bacteria may be targeted in an effort to expand the current antibacterial armamentarium.

CHAPTER II. FUNCTIONAL CHARACTERIZATION OF A TWO-COMPONENT SYSTEM THROUGH USE OF A SUICIDE STRAIN

INTRODUCTION

The ability to sense and respond to environmental stimuli is essential to bacterial survival. The major mechanism through which bacteria sense and respond to their environment is through the use of two-component systems (38-41). Two-component systems are present in virtually every bacterial species, with certain species encoding up to 200 two-component systems (41). A prototypical two-component system consists of a membrane bound sensor histidine kinase and a cytoplasmic response regulator. Upon stimulation, the histidine kinase undergoes autophosphorylation, followed by phosphotransfer to the response regulator. The activated response regulator induces the desired response, such as altering transcription of target genes (38, 40).

Membrane bound histidine kinases generally consist of a homodimer. Each subunit contains a sensor domain, a linker domain, and a kinase core domain, although many variations on this general structure do exist (38-41). For membrane bound histidine kinases, the sensor domain is often extra-cytoplasmic. After receiving the signal, the linker domain passes the signal through the membrane into the cytoplasm. The mechanism by which the signal is relayed is not well understood (40). The kinase core domain consists of multiple sub-domains, including the dimerization and phosphotransfer domains. Upon the signal passing through the linker domain, a conserved histidine residue found in the dimerization domain undergoes autophosphorylation.

Phosphotransfer to the response regulator is then catalyzed by the phosphotransfer domain of the histidine kinase.

Response regulators consist of two major domains. First, the receiver domain facilitates the association of the response regulator to the dimerization domain of the histidine kinase. The interaction of these two domains is important for specificity of the response regulator to its cognate histidine kinase. Despite significant advancements in this realm, the specific mechanisms governing many aspects of specificity remain to be elucidated (38-40, 77, 78). The phosphate group is then transferred to a conserved aspartate residue, resulting in a conformational change that activates the output domain. The output domain can induce a wide range of outputs, including DNA-binding, RNA-binding, protein-binding, or enzymatic activity (40). DNA-binding response regulators are diverse, even with significant diversity existing within subfamilies. DNA-binding response regulators recognize a wide variety of DNA sequences to alter transcription. One of the most well characterized families of response regulators is the OmpR family. OmpR response regulators generally form homodimers and bind direct repeat DNA sequences (38-40, 44, 46). Typically, the response regulator will regulate transcription of target genes as well as the genes encoding the two-component system it belongs to, thus increasing signal transduction in response to the environmental cue (38, 79). Despite the thousands of two-component systems identified, there is not a full understanding of the mechanisms by which the histidine kinase senses and responds to stimuli.

Another challenge facing the study of two-component systems is identifying the specific signals that activate the histidine kinases (40). Only a handful of ligands have been identified that directly bind a histidine kinase and activate it, despite having

identified thousands of two-component systems (40, 42, 43). In the case of transmembrane histidine kinase, the signal is often thought to be extracellular; however, recent studies have shown that many two-component systems can sense intracellular stimuli or membrane perturbations as well (38, 40, 43, 47). The high diversity in signals adds to the difficulty in identifying specific ligands that activate histidine kinases.

Many methods have been developed to interrogate two-component system function. The most common method is to monitor phosphorylation using ^{32}P *in vitro* (80). Histidine kinases undergo autophosphorylation in the presence of ATP, thus the rate of autophosphorylation can be interrogated using radio-labeled ATP, gel electrophoresis, and autoradiography. This method can be used to interrogate potential ligands, as the presence of a ligand increases the rate of autophosphorylation. Approximately one third of histidine kinases contain a transmembrane domain (38, 43, 81, 82). In order to interrogate transmembrane histidine kinase, two methods are often used. By truncating the histidine kinase, researchers study the intracellular domain; however, in this case ligands cannot be interrogated. Alternatively, recombinantly expressed histidine kinases can be reconstituted within liposomes, or membrane vesicles can be created using strains over expressing the histidine kinase (42, 83). The rates of phosphotransfer to the response regulator can be measured using similar methods. Despite the limitations, much has been learned from utilizing these methodologies. Directed mutagenesis has been used to identify residues and domains required for various aspects of two-component system function. Significant effort has focused on developing *in vivo* systems to interrogate two-component systems, such as using fluorescence resonant energy transfer (FRET). Despite this, no widely applicable *in vivo* system has been successful (80). Taken together,

developing tools to interrogate two-component system structure and function will lead to significant advancements in our understanding of bacterial responses to environmental stimuli.

Two-component systems are virtually ubiquitous in bacteria, and are absent in mammals (43, 84). In addition, altering two-component system function can modulate virulence in a number of pathogenic bacteria (42, 46, 85-89). Two-component systems regulate a variety of processes, including resistance to antibiotics, attachment to host tissues, toxin production, and the response to vertebrate immune systems (90). Taken together, there is significant interest in understanding two-component systems to further our understanding of bacterial physiology as well as identifying bacterial specific therapeutic targets.

S. aureus is a major human pathogen that is responsible for numerous diseases in the vertebrate host (3, 4, 9, 10, 91). *S. aureus* encodes sixteen two-component systems that respond to a wide variety of signals, including antibiotic stress, hypoxia, and quorum sensing signals (40, 44, 46). As discussed above, identifying the specific ligands of these systems is difficult. Of these sixteen two-component systems, only one has one well characterized ligand. The Agr two-component system is activated by the autoinducing peptide utilized for quorum sensing (40, 92).

S. aureus requires proper heme homeostasis to successfully colonize the host. Previously, a system that responds to heme in *S. aureus* was identified (46). When exposed to high levels of heme, the two-component system HssRS is activated, which induces the expression of *hrtAB* to alleviate heme toxicity. Previous work has identified numerous requirements of HssRS activation (44-47, 49, 93). Specifically, directed

mutagenesis has identified numerous residues required for HssRS function, and furthermore defined the promoter and direct repeat sequence that the response regulator, HssR, binds (44, 47). A complete understanding of HssRS signaling remains to be elucidated.

The ability to sense and respond to heme is critical for pathogenesis, yet the mechanism of heme sensing remains unknown. Small molecule '882 was identified in a high-throughput screen as an activator of staphylococcal HssRS. '882 increases endogenous heme synthesis (47, 49). Here we report the construction of a P_{hrt} driven suicide strain to interrogate HssRS function. Using this unique unbiased genetic selection strategy, we have uncovered residues of HssRS and P_{hrt} required for detection of exogenous heme and endogenous heme. Further studies will interrogate the functional repercussions of these mutations on autophosphorylation, phosphotransfer, and DNA-binding. Understanding how pathogens cope with heme toxicity will lead to insights into potential therapeutic targets. Based upon the conservation of heme sensing systems across numerous medically relevant pathogens, this work may provide information for understanding and manipulating heme sensing in many infectious agents.

METHODS

A version of the following Methods is under review at Nature Chemical Biology for inclusion in "Antibacterial photosensitization through activation of coproporphyrinogen oxidase."

Bacterial strains, plasmids and growth conditions

Cloning was performed in *Escherichia coli* DH5α (Invitrogen™). Strains, plasmids, and primers used are described in Table 1, Table 2, and Table 3, respectively. All *S. aureus* strains were grown in tryptic soy broth (TSB) or agar (TSA), *E. coli* strains were grown in lysogeny broth (LB) or agar (LBA).

Table 1. Bacterial strains used in Chapter II.

Bacterial Strain	Description	Reference
Wild-type	*Staphylococcus aureus* strain Newman	(94)
Δ*hrtB*	In-frame deletion of *hrtB* in Newman background	(95)
RN4220	*S. aureus* cloning intermediate	(96)
hrtAB::relE	*S. aureus* strain Newman expressing two copies of *relE* at the *hrtAB* locus	This study
Δ*hssRS*	In-frame deletion of *hssRS* in Newman background	(93)

Table 2. Plasmids used in Chapter II.

Plasmids	Reference
phrt.XylE	(46)
pKORI	(97)
pES006	(47)
pMS001	This study

Table 3. Primers used in Chapter II.

Primer Name	Sequence
MS001	GGGGACAAGTTTGTACAAAAAAGCAGGCTGATTTGCTTAGGACGTGCTGC
MS001b	GATTTGCTTAGGACGTGCTGC
MS019	GCGTCTTTACAAGCCACATATGGATTCACTTCTCCCTATTTCTTC
MS020	GGGAGAAGTGAATCCATATGTGGCTTGTAAAGACGC
MS006	GGGGACCACTTTGTACAAGAAAGCTGGGTGGCCAACTTAAGCCAGG
MS006b	GGCCAACTTAAGCCAGG
MS023	GCGGCGCATATGGCGTATTTTCTGGATTTTGACG
MS024	CGCCGCCATATGGCTTTGGTTCAGAGAATGCG
R-C4Y-F	GCTATGGTGCAATATCTTGTTGTCGATGACGATCC
R-C4Y-R	GGATCGTCATCGACAACAAGATATTGCACCATAGC
R-L5F-T	GCTATGGTGCAATGTTTTGTTGTCGATGACG
R-L5F-B	CGTCATCGACAACAAAACATTGCACCATAGC
R-A49T-F	CAGCGTGTCGATATTACAGTGGTAGATATTATGATGG
R-A49T-R	CCATCATAATATCTACCACTG TAA TAT CGA CAC GCT G
R-C64Y-F	GGACGGCTTTCAATTATATAATACATTAAAAAATGATTATGATATACCAG
R-C64Y-R	CTGGTATATCATAATCATTTTTTAATGTATTATATAATTGAAAGCCGTCC
R-L84H-T	CAGCGCGGGATGCACATAGTGACAAAGAGCG
R-L84H-B	CGCTCTTTGTCACTATGTGCATCCCGCGCTG
R-G94D-T	GCGTTTATAAGCGATACTGACGATTATGTAACC
R-G94D-B	GGTTACATAATCGTCAGTATCGCTTATAAACGC
R-D97N-F	GCGTTTATAAGCGGTACTGACAATTATGTAACCAAACCC
R-D97N-R	GGGTTTGGTTACATAATTGTCAGTACCGCTTATAAACGC
R-V105F-F	CGATTATGTAACCAAACCCTTTGAGTTTAAGGAACTTATTTTTAGAATTCG
R-V105F-R	CGAATTCTAAAAATAAGTTCCTTAAACTCAAAGGGTTTGGTTACATAATCG
R-E107K-T	CCCTTTGAGGTTAAGAAACTTATTTTTAGAATTCG
R-E107K-B	CGAATTCTAAAAATAAGTTTCTTAACCTCAAAGGG
R-W179C-F	CGTGAACAAATAATAGAAAAAATTTGTGGCTATGATTATGAAGGAGATGAGCG
R-W179C-R	CGCTCATCTCCTTCATAATCATAGCCACAAATTTTTTCTATTATTTGTTCACG
R-G185V-T	GGCTATGATTATGAATGAGATGAGCGAACAG
R-G185V-B	CTGTTCGCTCATCTCATTCATAATCATAGCC
R-G185E-F	GGGCTATGATTATGAAGAAGATGAGCGAACAGTTGACG

R-G185E-R	CGTCAACTGTTCGCTCATCTTCTTCATAATCATAGCCC
R-R196L-F	CAGTTGACGTTCATATTAAGCTACTACGCCAAAG
R-R196L-R	CTTTGGCGTAGTAGCTTAATATGAACGTCAACTG
R-G215R-F	GCCACACTTACAATTGAAACAGTAAGAAGACAAGGCTATAAGGTGG
R-G215R-R	CCACCTTATAGCCTTGTCTTCTTACTGTTTCAATTGTAAGTGTGGC
S-R152L-T	GCAGTATTTATGCTTCCAGATATTGGAG
S-R152L-B	CTCCAATATCTGGAAGCATAAATACTGC
S-R201G-T	GCTAGCGACCGAAGGCTTAATTGATGGTG
S-R201G-B	CACCATCAATTAAGCCTTCGGTCGCTAGC
S-R215C-F	GGTGATTTTGAAACACCTATCAAACAAACATGCAAAGATGAAATTGGAAC
S-R215C-R	GTTCCAATTTCATCTTTGCATGTTTGTTTGATAGGTGTTTCAAAATCACC
S-R230G-F	CACTTTAATAAGATGGGAGAGTCATTGGG
S-R230G-R	CCCAATGACTCTCCCATCTTATTAAAGTG

Construction of a suicide strain

The suicide strain was constructed by allelic replacement as previously described (97). PCR was performed with Phusion DNA Polymerase (Thermo Scientific) unless stated otherwise. The genomic context upstream of *hrtAB* was amplified using primers MS0001b and MS019 and the downstream fragment was amplified using primers MS020 and MS006b. The fragments were fused by PCR SOEing to create an NdeI site between the upstream and downstream fragments (98). The 3' adenosine overhangs were added by incubation with ExTaq (TaKaRa) for 20 minutes at 72°C. The resulting product was ligated into PCR2.1 according to manufacturer's instructions (Life Technologies). *relE* was amplified from *E. coli* DH5α using primers MS023 and MS024. The plasmid and PCR products were digested with NdeI (New England Biolabs) and ligated with T4 DNA Ligase (New England Biolabs) to insert the toxin gene between upstream and downstream fragments. The plasmid DNA was isolated from transformants and a strain harboring two copies of *relE* in the correct orientation was selected for downstream applications. Using this plasmid as a template, primers MS001 and MS006 were used to amplify the suicide construct. This was inserted into pKORI and allelic exchange was performed as previously described (97).

Isolation of spontaneous resistant mutants

Overnight bacterial cultures of suicide strain or Δ*hrtB* were subcultured 1:100 into 5 mL of TSB and grown for 8 hours. One hundred μL of a 1:40,000 dilution were plated on media containing '882 (5 to 15 μM) or heme (0.5 or 1 μM). The resistant colonies were passaged twice on TSA to ensure resistance was genetically stable, and re-

challenged by plating on heme or ‘882. The colonies that retained resistance were used for downstream analysis.

Sequence analysis

Strains maintaining resistance were sequenced to determine mutations in the *hssRS* and P_{hrt} regions. The mutations were mapped to a template containing the sequence of *hrtAB::relE* in this region. The mutations were analyzed using Lasergene 13 (DNASTAR).

Cloning

The plasmid pMS001 was created by restriction digest of plasmid pES006 (containing P*lgt.hssS-myc* and P*hrt.xylE*) to remove *hssS-myc* (47). Digested plasmid was purified using a Gel Extraction Kit (Qiagen). The sequence for *hssR-myc* was excised from a plasmid previously created and purified (pES008, unpublished). Ligation was performed with T4 DNA Ligase (NEB) according to the manufacturer’s instructions, creating pMS001. Plasmids were purified from transformants and moved into *S. aureus* through standard protocols. The point mutations were created in pES006 and pMS001 utilizing Pfu mutagenesis with primers described in Table 3 (99).

Promoter activity assay

Promoter activity assay was performed as previously described (44). Briefly, p*hrtAB.xylE* was electroporated into the strains as previously described (47).

Immunoblot for HssR and HssS

Immunoblots for HssR-myc and HssS-myc were performed in *S. aureus* strains containing pMS001 and pES006 as previously described to determine expression levels at a 1:10,000 dilution of the α-myc antibody (47).

RESULTS

Construction of a suicide strain

To interrogate the *S. aureus* heme sensing system, a suicide strain was employed enabling selection of *S. aureus* strains that are unresponsive to exogenous heme or '882-induced endogenous heme synthesis. *S. aureus hrtAB* was replaced with two copies of the gene encoding the *Escherichia coli* RNA interferase toxin RelE under the control of the native *hrtAB* promoter to inhibit growth upon activation of HssRS (Figure 4a). Dual copies of *relE* were used to avoid selection of toxin-inactivating mutations, thereby ensuring selection of strains with mutations in HssRS or P_{hrt}. *S. aureus hrtAB::relE* grows equivalently to WT in the absence of heme or '882. Upon HssRS induction by heme or '882, *hrtAB::relE* is unable to grow (Figure 4b). A strain lacking the *hrtB* permease (Δ*hrtB*) was used to ensure that heme or '882 do not induce toxicity from heme accumulation at tested concentrations. These results demonstrate that the suicide strain may be used to identify suppressor mutants unresponsive to heme or '882.

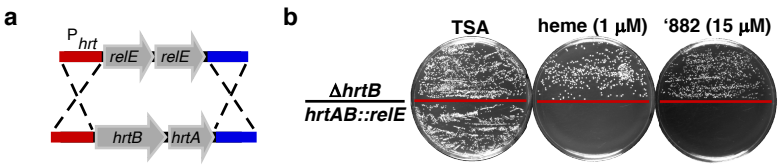

Figure 4. Construction of a suicide strain to select strains unresponsive to heme or ‘882.
(a) To create a P_{hrt} suicide strain, the *hrtAB* genes were replaced with two copies of the *E. coli* gene encoding the RNA interferase toxin RelE. (b) Upon heme or ‘882 stimulation, toxicity is induced in *hrtAB::relE*. A version of this figure is under review at Nature Chemical Biology for inclusion in “Antibacterial photosensitization through activation of coproporphyrinogen oxidase.”

Identification of residues required for HssRS and P_{hrt} function

Isolates of *hrtAB::relE* exhibiting spontaneous resistance to heme and ‘882 were identified. The stability of resistance was ensured through serial passage in plain media followed by challenge by heme or ‘882 a second time. Genomic DNA was isolated from strains retaining resistance to heme or ‘882 in the *hrtAB::relE* background. In order to identify mutations providing resistance to heme- or ‘882-induced activation of HssRS, the *hssRS*/P_{hrt} locus of resistant strains was sequenced. Approximately 90% of the mutations identified in this analysis were in *hssRS/*P_{hrt}. Mutations were identified throughout the *hssRS* locus and the *hrtAB* promoter (Figure 5, Figure 6).

With regards to HssS, mutations were found in almost every domain, suggesting that all portions of the histidine kinase are required for function (Figure 5). Interestingly, mutations were not identified in the two transmembrane domains, suggesting mutations in these regions do not affect function of this particular histidine kinase. Importantly, intracellular and extracellular mutations were identified using heme or ‘882, consistent with both domains being required for exogenous and endogenous heme sensing. All of the mutations identified utilizing heme as an activator, also provided resistance to ‘882 upon re-challenge, and vice versa (data not shown). These data suggest the mechanism by which exogenous and endogenous heme are sensed in *S. aureus* is through a similar mechanism. Future studies will saturate selection of strains resistant to these compounds allowing further conclusions to be drawn.

As expected, HssR mutations were identified in both the receiving and DNA-binding domains (Figure 5). Mutations in these domains likely affect phospho-acceptance from HssS and DNA-binding, however, further studies will need to be performed to

confirm this hypothesis. Finally, mutations in P_{hrt} were identified that lie within the known direct repeat where HssR is known to bind (44). In addition, mutations outside the direct repeat were also identified, suggesting a more complex regulatory network is required for P_{hrt} activation.

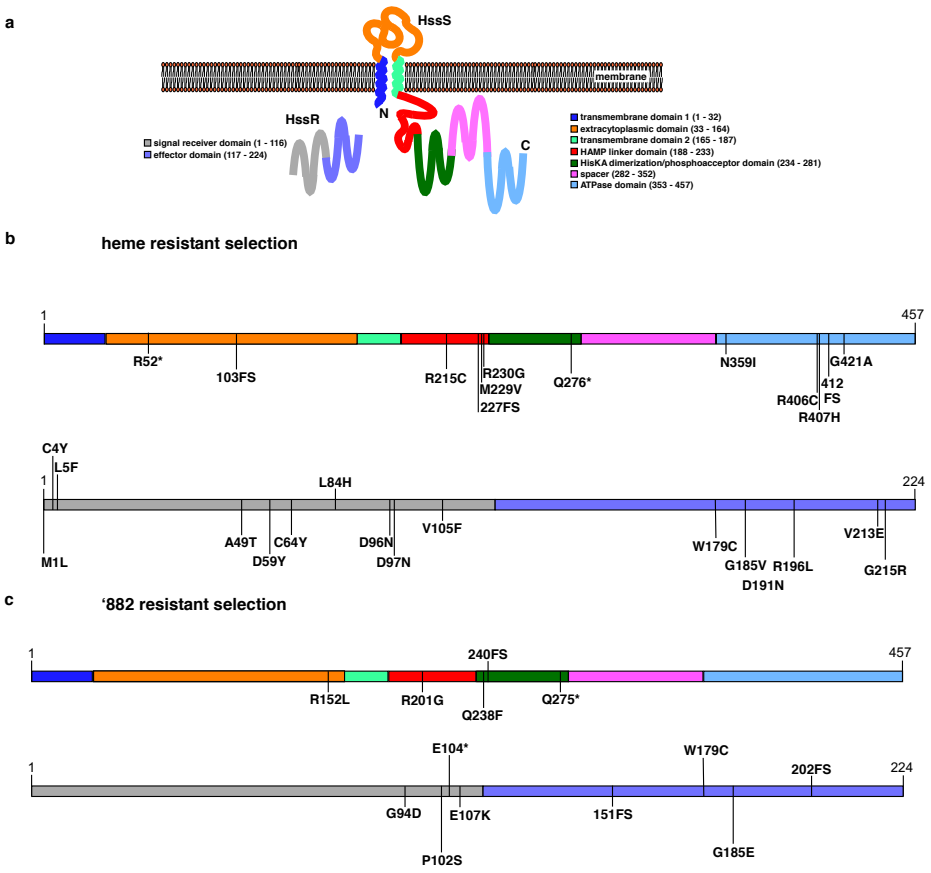

Figure 5. Mutations in HssRS identified in suicide selection.

(a) Cartoon representation of HssRS structure with domains, adapted from (44, 93). (b) Amino acid residues identified in sequencing of *hssRS* in heme resistant *hrtAB::relE* isolates. (b) Amino acid residues identified in sequencing of *hssRS* in '882 resistant *hrtAB::relE* isolates.

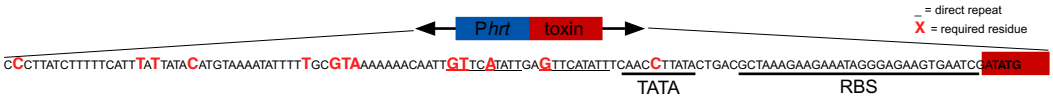

Figure 6. Mutations in P_{hrt} identified in suicide selection.

The wild-type sequence of the promoter of *hrtAB* is shown. Nucleic acid residues identified in sequencing of P_{hrt} in heme and ‘882 resistant *hrtAB::relE* isolates are highlighted in red.

Verification of the suicide selection to interrogate two-component systems

To confirm the suicide strain selection identifies mutations altering HssRS activation, strains lacking *hssR* (Δ*hssR*) or *hssS* (Δ*hssS*) were complemented *in trans* with a vector expressing *hssR* or *hssS*, respectively, harboring the identified mutations. Upon stimulation of strains expressing the HssR or HssS mutants, reduced activation was seen by both heme and ‘882 in all of the mutants (Figure 7). Importantly, regardless of the compound used to select the mutation, all the mutations provided resistance to both compounds upon re-challenge. In addition, background levels of activation are reduced in the HssR mutant strains, further confirming reduced levels of HssRS signaling in these strains (Figure 7). Taken together, these data validate the use of *hrtAB::relE* selection as a valuable tool to interrogate two-component system activation and regulation.

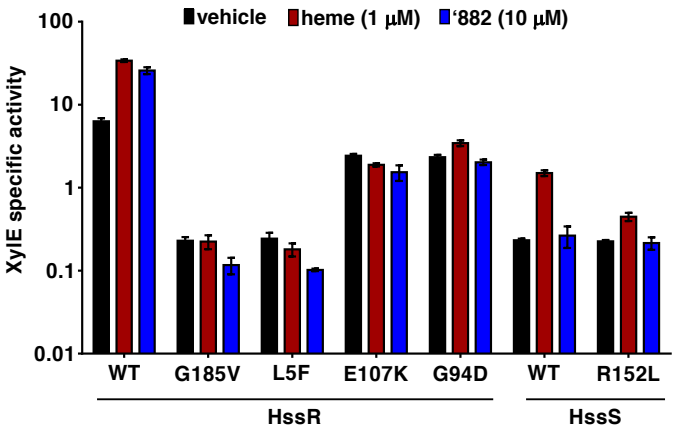

Figure 7. Mutations in HssRS affect *hrtAB* activation.

S. aureus Δ*hssR* or Δ*hssS* complemented *in trans* with a vector expressing *hssR* or *hssS* harboring the identified mutations were analyzed to determine P_{hrt} activation. Strains resistant to '882 or heme exhibit decreased activation of P_{hrt} when exposed to heme or '882.

Mutations in HssRS can decrease protein abundance

Mutations in HssRS and P_{hrt} may disrupt HssRS function through a variety of mechanisms. In order to interrogate the effect of these mutations on HssRS activation, a workflow was developed to interrogate and classify the mutations based upon their functional effects (Figure 8). Four classes were chosen to categorize the identified mutations: (i) altered protein abundance, (ii) decreased autophosphorylation of HssS, (iii) decreased phosphotransfer from HssS to HssR, and (iv) decreased DNA-binding by HssR.

In order to begin interrogating these residues, protein expression was measured by immunoblot. Of the mutations tested, six mutations in HssR (C4Y, L5F, A49T, E107K, G185V, R196L) led to decreased protein abundance, providing a mechanism for how these mutations provide resistance in the *hrtAB::relE* strain (Figure 9). The remaining mutations interrogated in this preliminary study were produced to equal levels of WT HssS or HssR. Mutations that do not affect protein abundance will be further interrogated to determine their effect on autophosphorylation, phosphotransfer, and DNA-binding.

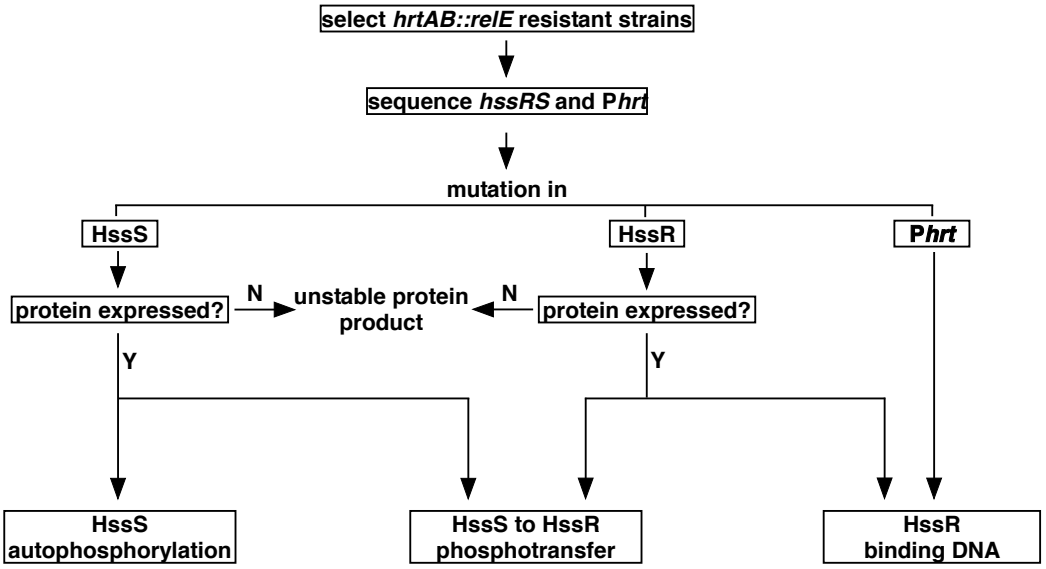

Figure 8. Workflow for interrogation of HssRS and P_{hrt} mutations.

Mutations identified in the selection of *hrtAB::relE* strains will be classified into: (i) altered protein expression, (ii) decreased autophosphorylation of HssS, (iii) decreased phosphotransfer from HssS to HssR, and (iv) decreased DNA-binding by HssR.

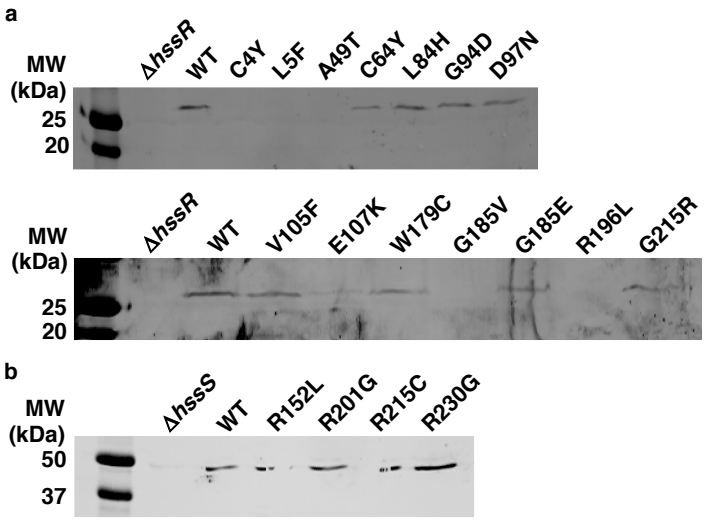

Figure 9. Immunoblots identify mutations disrupting protein expression

S. aureus Δ*hssR* (a) or Δ*hssS* (b) complemented *in trans* with a vector expressing *hssR-myc* or *hssS-myc* harboring the identified mutations were analyzed by immunoblotting for the Myc tag. Immunoblots were performed by Reece Knippel.

DISCUSSION

Here we report the construction of a suicide strain selection strategy to interrogate two-component system structure and function. Isolation of spontaneous resistant strains has identified numerous residues that, when mutated, affect HssRS function. The mutations were verified to affect levels of *hrtAB* activation, and this work has begun to dissect the mechanisms through which each mutation affects the function of HssRS. Further studies will saturate the selection by identifying more mutations, as well as continue to dissect mechanisms by which each mutation affects HssRS function.

Mutations in HssRS have potential to affect protein abundance, autophosphorylation, phosphotransfer from HssS to HssR, or HssR binding DNA (Figure 8). Despite not having saturated the selection, some insights are becoming clear. Heme- and ‘882-resistant strains were identified with mutations in both the extracellular and intracellular domains. Furthermore, mutations identified in HssS or HssR using heme or ‘882 provide resistance to the other compound, suggesting that exogenous and endogenous heme may be sensed through a similar mechanism. Upon selecting mutants to a point of saturation of this system, a better understanding of the mechanism of heme sensing will be uncovered.

Promoter mutations may also affect HssR binding, thereby decreasing activation of P_{hrt}. Consistent with this, mutations were identified within the promoter of *hrtAB*. As discussed in the Introduction to this chapter, HssR binds a direct repeat sequence upstream of *hrtAB*. Previous studies have characterized the HssR binding location by sequential shortening of the promoter region (44). Here we report the identification of

mutations using the suicide strain in the direct repeat, consistent with previous studies. Interestingly, mutations outside this region were also identified, suggesting promoter regulation is more complex and therefore likely requires additional factors to ensure proper gene expression. Future studies will continue to identify mutations required for P_{hrt} activation and interrogate their effect on HssR binding.

A previous high-throughput screen has identified numerous molecules that activate HssRS (47). Identifying targets of small molecules remains a significant challenge (50-52). Many approaches have been developed to identify small molecule targets, however, each has limitations. In order to successfully identify a target, many approaches must be taken. One approach that has proven successful is identification of spontaneously resistant strains to small molecules that induce growth arrest (53, 55). Genome sequencing of DNA from resistant isolates allows for the identification of mutations that providing resistance to the molecule of interest. Many molecules induce phenotypes other than growth inhibition. ‘882 induces HssRS activation, and therefore could not be used in WT bacteria to identify spontaneous resistant isolates. The P_{hrt} driven suicide strain overcomes this obstacle by engineering toxicity when exposed to a non-toxic small molecule. The suicide strain has identified mutations providing resistance to small molecule activators of HssRS. This suggests that identifying strains lacking mutations in *hssRS* and P_{hrt} can be further subjected to whole genome sequencing to identify mutations throughout the genome. This will provide insight into the potential target of ‘882, which will be discussed in Chapter III.

Taken together, this work has generated an unbiased *in vivo* strategy to interrogate the structure and function of HssRS. Importantly, the success of this approach suggests

this may be applied to other two-component systems in order to further our understanding of this essential bacterial signaling process. Specifically, the suicide strain approach allows for unbiased *in vivo* identification of mutations required for sensing without directed mutagenesis. Upon completion of this work, a stronger understanding of heme sensing in bacterial pathogens will be uncovered.

CHAPTER III. ANTIBACTERIAL PHOTOSENSITIZATION THROUGH ACTIVATION OF COPROPORPHYRINOGEN OXIDASE

INTRODUCTION

Skin and soft tissue infections (SSTIs) account for a majority of visits to hospitals and clinics in the United States, accounting for approximately 14 million ambulatory care visits each year (15). Furthermore, approximately 10% of hospitalized patients suffer from an SSTI (15). These infections are typically caused by Gram-positive bacteria. Etiological agents include *Staphylococcus aureus*, *Staphylococcus epidermidis*, *Propionibacterium acnes*, and *Bacillus anthracis*, the causative agents of "Staph infections," hospital acquired infections, acne, and cutaneous anthrax, respectively (9, 14, 15, 60). *S. aureus* and *P. acnes* are the most prevalent causative agents of SSTIs (9, 14, 15, 60). In fact over 90% of the world's population will suffer from acne over the course of their lifetime, leading to annual direct costs of over $3 billion (14-16, 18). The threat of these pathogens is compounded by the tremendous rise in antibiotic resistance, reducing the efficacy of the existing antibacterial armamentarium (9, 15, 60). Identifying new drug targets to treat SSTIs is paramount to enable the development of novel therapeutics.

Heme biosynthesis is conserved across all Kingdoms of life and heme is utilized for a diverse range of processes within cells. Until recently, it was thought that the heme biosynthesis pathway was conserved across all species, limiting its utility as a potential therapeutic target to treat infectious diseases. However, Dailey *et al.* discovered that

Gram-positive bacteria utilize a distinct pathway to synthesize the critical cellular cofactor heme (Figure 1a) (32, 33). Specifically, Gram-positive heme biosynthesis diverges at the conversion of coproporphyrinogen III (CPGIII) to coproporphyrin III (CPIII) through a six-electron oxidation by coproporphyrinogen oxidase (HemY), as opposed to being converted to protoporphyrin IX (PPIX) in the classical pathway by a distinct series of enzymes (21, 32). The divergence of the heme biosynthesis machinery between humans and Gram-positive bacteria provides a unique opportunity for the development of new antibiotics targeting this pathway as a strategy to treat infections.

Small molecule '882 was previously identified in a screen for activators of the *S. aureus* heme sensing system two-component system (HssRS) (Figure 13b) (44, 46, 47). Upon activation, HssRS induces the expression of the heme-regulated transporter (HrtAB) to alleviate heme toxicity (44, 46, 47). HssRS activation is triggered by massive accumulation of heme in '882-exposed bacteria; however, the mechanism by which '882 activates heme biosynthesis has not been uncovered (47).

We report here the identification of the cellular target of '882, a small molecule activator of heme biosynthesis, through the use of a P_{hrt} driven suicide strain. '882 activates coproporphyrinogen oxidase (HemY) from Gram-positive bacteria, an enzyme essential for heme biosynthesis. Activation of HemY induces accumulation of the product of the reaction, coproporphyrin III (CPIII), a photoreactive molecule of demonstrated utility in treating bacterial infections (16, 63, 100). Photodynamic therapy (PDT) utilizes a photosensitizing molecule activated by a specific wavelength of light to produce reactive oxygen species that leads to cell death (16). The only US Food and Drug Administration approved photosensitizers are aminolevulinic acid (ALA) derivatives,

which serve as prodrugs through their conversion to porphyrins in the heme biosynthetic pathway (16). Utilizing ‘882 to activate HemY, CPIII accumulates in a similar manner, inducing photosensitization specifically in Gram-positive bacteria, and ‘882-PDT reduces bacterial burden and tissue ulceration in murine models of SSTI. Thus, small molecule activation of HemY represents a promising strategy for the development of light-based antimicrobial therapies.

METHODS

Bacterial strains and growth conditions

Cloning was performed in *Escherichia coli* DH5α (Invitrogen™). Strains, plasmids, and primers used are described in Table 4, Table 5, Table 6, and Table 7. All proteins were expressed using *E. coli* strain BL21(DE3) pREL (47). All *S. aureus* and *S. epidermidis* strains were grown in tryptic soy broth (TSB) or agar (TSA), *E. coli* and *B. anthracis* were grown in lysogeny broth (LB) or agar (LBA), and *P. acnes* in brain heart infusion (BHI) broth or agar unless otherwise stated.

Table 4. Bacterial strains used in Chapter III.

Bacterial Strain	Description	Reference
Wild-type	*Staphylococcus aureus* strain Newman	(94)
Δ*hrtB*	In-frame deletion of *hrtB* in Newman background	(95)
RN4220	*S. aureus* cloning intermediate	(96)
hrtAB::relE	*S. aureus* strain Newman expressing two copies of *relE* at the *hrtAB* locus	This study
hemY.T183K	*S. aureus* strain Newman harboring a T183K mutation in HemY	This study
Δ*hemY*	*S. aureus* strain Newman harboring a transposon interrupting *hemY* expression	This study
Δ*hssRS*	In-frame deletion of *hssRS* in Newman background	(93)
Staphylococcus epidermidis	Strain NRS6	BEI
Bacillus anthracis	Strain Sterne	(101)
Propionibacterium acnes	ATCC® 6919™	ATCC

Table 5. Expression constructs used in Chapter III.

Protein	Expression Vector	Reference
Wild-type *Staphylococcus aureus* HemY	pET15b	This study
T183K *S. aureus* HemY	pET15b	This study
N186F *S. aureus* HemY	pET15b	This study
N186Y *S. aureus* HemY	pET15b	This study
Y171A *S. aureus* HemY	pET15b	This study
D450Y *S. aureus* HemY	pET15b	This study
F187W *S. aureus* HemY	pET15b	This study
F184A *S. aureus* HemY	pET15b	This study
M167F *S. aureus* HemY	pET15b	This study
V146M *S. aureus* HemY	pET15b	This study
***Bacillus subtilis* HemY**	pTrcHisA	(34)
***Homo sapiens* HemY**	pTrcHisB	(102)
***Propionibacterium acnes* HemY**	pTrcHisA	(34)

Table 6. Plasmids used in Chapter III.

Plasmids	Reference
p***hrt.xylE***	(46)
pKORI	(97)

Table 7. Primers used in Chapter III.

Primer Name	Sequence
SA_hemY_T183K_T	AGTTTGATGAGTACGTTTCCTAATTTTAAAG
SA_hemY_T183K_B	CTTTAAAATTAGGAAACGTACTCATCAAACT
N186Y_T_NWMN1723	GTTTGATGAGTACGTTTCCTTATTTTAAAGAAAAAGAAGAGGC
N186Y_B_NWMN1723	GCCTCTTCTTTTTCTTTAAAATAAGGAAACGTACTCATCAAAC
N186F_T_NWMN1723	GTTTGATGAGTACGTTTCCTTTTTTTAAAGAAAAAGAAGAGGC
N186F_B_NWMN1723	GCCTCTTCTTTTTCTTTAAAAAAAGGAAACGTACTCATCAAAC
SA_Y171A_T	CCTTTAATGGGTGGTATTGCTGGTACCGATATTG
SA_Y171A_B	CAATATCGGTACCAGCAATACCACCCATTAAAGG
SA_D450Y_T	GCGGTTGGACTACCTTATTGTATTACGCAAGG
SA_D450Y_B	CCTTGCGTAATACAATAAGGTAGTCCAACCGC
SA_F187W_T	GAGTACGTTTCCTAATTGGAAAGAAAAAGAAGAGGCATTCGG
SA_F187W_B	CCGAATGCCTCTTCTTTTTCTTTCCAATTAGGAAACGTACTC
SA_F184A_T	GTTTGATGAGTACGGCTCCTAATTTTAAAGAAAAAGAAGAGGC
SA_F184A_B	GCCTCTTCTTTTTCTTTAAAATTAGGAGCCGTACTCATCAAAC
SA_M167F_T	GAGAATTTAATAGAGCCTTTATTTGGTGGTATTTATGG
SA_M167F_B	CCATAAATACCACCAAATAAAGGCTCTATTAAATTCTC
SA_V146M_T	GGATGGTGACATTTCTATGGGTGCATTTTTCAGAGC
SA_V146M_B	GCTCTGAAAAATGCACCCATAGAAATGTCACCATCC
MS001	GGGGACAAGTTTGTACAAAAAAGCAGGCTGATTTGCTTAGGACGTGCTGC
MS001b	GATTTGCTTAGGACGTGCTGC
MS019	GCGTCTTTACAAGCCACATATGGATTCACTTCTCCCTATTTCTTC
MS020	GGGAGAAGTGAATCCATATGTGGCTTGTAAAGACGC
MS006	GGGGACCACTTTGTACAAGAAAGCTGGGTGGCCAACTTAAGCCAGG
MS006b	GGCCAACTTAAGCCAGG
MS023	GCGGCGCATATGGCGTATTTTCTGGATTTTGACG
MS024	CGCCGCCATATGGCTTTGGTTCAGAGAATGCG
pet15_hemYF1	GCGGCAGCCATATGGTGACTAAATCAGTGGCTATTATAG
pet15_hemYF2	GCGGCAGCCATATGCTAGTGACTAAATCAGTGGCTATTATAG
pet15_hemYR	GCTTTGTTAGCAGCCGTTACAACTCTGCGATTACTTC
pKOR1_hemY_FattB	GGGGACAAGTTTGTACAAAAAAGCAGGCTGTGACTAAATCAGTGGCTATTATAG
pKOR1_hemY_RattB	GGGGACCACTTTGTACAAGAAAGCTGGGTTTACAACTCTGCGATTACTTC

Strain construction

*S. aureus s*train *hemY::ermC* was described previously and the *hemY::ermC* allele was transduced into strain Newman using the Φ-85 bacteriophage (29, 103). To create an *S. aureus* strain harboring the T183K mutation in HemY, *hemY* was amplified from the point mutant isolated in the suicide selection using primers pKORI_hemY_FattB and pKORI_hemY_RattB. This construct was moved into pKORI and allelic replacement was utilized as previously described (97).

Suicide strain selection

Overnight bacterial cultures of suicide strain or Δ*hrtB* were subcultured 1:100 into 5 mL of TSB and grown for 8 hours. One hundred μL of a 1:40,000 dilution were plated on media containing ‘882 (5 to 15 μM). The resistant colonies were passaged twice on TSA to ensure resistance was genetically stable, and re-challenged by plating on heme or ‘882. The colonies that retained resistance to ‘882 but were sensitive to heme were used for downstream analysis.

Genome sequencing and analysis

Genomic DNA was isolated from mutant strains using the Wizard® Genomic Kit (Promega) and sequenced to identify mutations in *hssRS*/P_{hrt}*/relErelE.* Strains containing mutations in this locus were eliminated from subsequent analyses. The genomes from strains lacking mutation in this locus were sequenced by Perkin Elmer on the MiSeq Platform.

Whole genome sequencing analysis was automated with a tool written by Pedro Teixeira in the Python programming language. The input files were the Newman genome (.fas) and the mutations file (.csv). The program iterates through each mutation determining the mutation type and resultant amino acid change if applicable. The input .csv is preprocessed to combine proximal mutations in the same strain as both must be considered due to their combined codon effect. The script also includes options to specify the organism ID, the base pair radius around the mutation to use for genome matching, an e-value threshold for allowable search results, and a customizable delimiter character for visualization. The program takes into account both strand directions when searching to ensure complete coverage as well as potential missed search matches at the edges of the genome. All mutations are classified based on their effect – silent, substitution, frame shift, truncation, or deletion.

The Bacterial, Archaeal and Plant Plastid Code (transl_table=11) was used as our translation table, more information can be found at http://www.ncbi.nlm.nih.gov/Taxonomy/Utils/wprintgc.cgi.

Mutations in non-coding regions or that produced silent mutations in the amino acid sequence were removed. Mutations were compared to a control suicide strain not subjected to selection to eliminate mutations present in the parent strain. The genes identified in this analysis were re-sequenced in the relevant strain to confirm the presence of the mutation.

Heme precursor quantification

Cells were grown in TSB overnight in the presence or absence of 40 μM ‘882. The cells were pelleted and lysed as previously described (47). PBG was quantified from lysate as previously described (104). For HPLC analysis, protoplast lysates were incubated with Dianon HP20 beads for 1 hour at 4°C. Hydrophobic molecules were eluted from the beads with 3 mL of acetone. The samples were protected from light. The hydrophobic molecules were concentrated *in vacuo* for 24 hours at room temperature. The samples were resuspended in 200 μL 1:1 water:acetonitrile with 0.1% trifluoroacetic acid. High performance liquid chromatography was performed as previously described (105). Absorbance was measured at a wavelength of 400 nm to identify heme precursor molecule peaks. The fractions corresponding to the retention time of CPIII and heme standards were collected and lyophilized. The lyophilized fractions were resuspended in 100 μL 1:1 water:acetonitrile and analyzed by liquid chromatography tandem mass spectrometry as previously described (105). HPLC and mass spectrometry was performed by Lisa Lojek.

Promoter activity assay

Promoter activity assay was performed as previously described (44). Briefly, p*hrtAB.xylE* was electorporated into the strain *hemY.T183K*. The other strains used have been previously described (47). Overnight cultures were diluted 1:100 into TSB supplemented with 10 μg/mL chloramphenicol under the following conditions: vehicle (DMSO), 1 μM heme, or 10 μM ‘882. Cells were grown for 6 hours and assayed as previously described (46). The experiment was performed in triplicate on three separate

days (n=9). Data are presented as mean ± SEM. Student's t-test was performed to determine significance.

S. aureus HemY expression construct

S. aureus HemY was amplified from either Newman or the suicide strain resistant to '882 containing the T183K mutation using primers pET15_hemYF1 and pET15_hemYR and inserted into pET15b using the Gibson Assembly® Cloning Kit (New England Biolabs). The point mutations in *hemY* were created utilizing Pfu mutagenesis with primers described in Table 7 (99).

Enzyme expression and purification

The plasmids described in Table 5 were transformed into BL21(DE3) pREL. An overnight of a strain harboring each HemY expression construct were diluted 1:100 into Terrific Broth (Fisher Scientific) supplemented with the appropriate antibiotics and 10 μg/mL riboflavin. Cells containing *H. sapiens* HemY were grown at 37°C overnight. The cells containing *S. aureus* and *P. acnes* HemY were grown at 37°C until they reached an OD_{600} of 0.7, induced with 0.1 mM IPTG, and grown at 30°C overnight. The cells containing *B. subtilis* HemY were grown at 37°C until they reached an OD_{600} of 0.7, induced with 0.1 mM IPTG, and grown for 5 hours 37°C. The cells were washed with PBS and stored at -80°C until protein was harvested. The cells were resuspended in lysis buffer (50 mM Tris-MOPS, pH 8.0, 0.1 M potassium chloride, and 1% sodium cholate hydrate supplemented with 1 mg/mL lysozyme and one Pierce Protease Inhibitor Tablet (Thermo Scientific)), homogenized using a Dounce homogenizer, and passed through an

EmulsiFlex (Avestin) four times. Lysate was centrifuged at 40,000 x g for one hour and filtered with a 0.22 μM filter.

S. aureus, *P. acnes*, and *H. sapiens* HemY were purified utilizing HisPur Cobalt Superflow Agarose (Thermo Scientific). The lysate was mixed with agarose and incubated at 4°C with rotating for 30 minutes. The lysate and beads were poured into a gravity column followed by washing with 10 column volumes of 5 mM imidazole in the lysis buffer. Proteins were eluted with 250 mM imidazole in lysis buffer in 5 column volumes. *B. subtilis* protein was purified on an AKTA FPLC (GE Healthcare Life Sciences) with a linear gradient from 0 mM to 500 mM imidazole in lysis buffer. Glycerol was added to 10% total volume and protein was aliquoted and stored at -80°C. A fresh aliquot was used each day for assays.

All purified enzymes were analyzed by SDS-PAGE and tested for activity to verify purity (Figure 10).

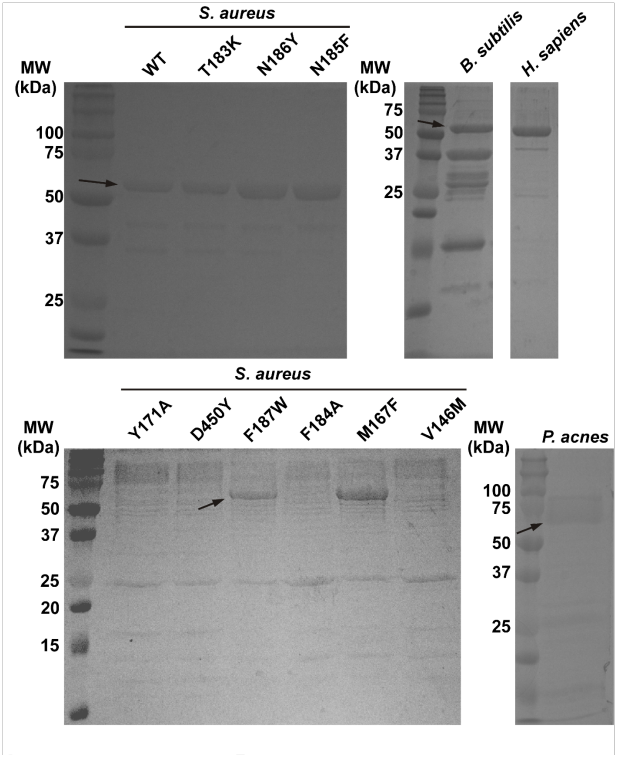

Figure 10. Purity of HemY used in biochemical assays.
After purification, each HemY was analyzed by SDS-PAGE to verify purity.

HemY activity assay

Purified HemY was assayed as previously described (106). The reactions were performed in 300 μL volume and incubated at room temperature for ten minutes before initiating the reaction. Reactions were monitored using a Cytation 5 (BioTek), and performed at least twice in triplicate. K_M and V_{max} values were determined by fitting data using the Michaelis-Menten equation in Prism (GraphPad) using 10.8 μg protein in each reaction. AC_{150} and activation (%) values were determined using Response vs. Log(substrate) in Prism (GraphPad). For *S. aureus* and *H. sapiens*, 10.8 μg of protein was used to determine the AC_{150}. For *B. anthracis* and *P. acnes*, 5.4 μg of protein was used to determine the AC_{150} to keep reactions in the linear range of the instrument. Data are represented as mean ± SEM.

'882-PAL labeling and protein detection

Overnight cultures of WT and Δ*hemY* in TSB supplemented with 1 μM heme were subcultured 1:50 into TSB supplemented with 1 μM heme and grown for 3 hours at 37°C. The cells were washed in PBS and resuspended in TSM (50 mM Tris-HCl pH 7.5, 0.5M sucrose, 10 mM $MgCl_2$) with 100 μg/mL lysostaphin and incubated at 37°C for 30 minutes. The protoplasts were pelleted by centrifugation at 20,000 x g for 20 minutes, washed once with TSM and resuspended in lysis buffer described above. The samples were sonicated three times at 80% for ten seconds while on ice. Cell debris was pelleted by centrifugation at 20,000 x g for 20 minutes.

The photolabeling and click reaction were performed similarly to what was previously described (107).The supernatant was diluted to 1 mg/mL, and '882-PAL was

added to 10 μM, incubated at room temperature for 2 hours on a rotating mixer in the dark, and exposed to UV light for 6 minutes (Deep Dome Lamp Fixture, Zoo Med Laboratories, Inc.). The samples were then diluted 1:14 in lysis buffer and reconcentrated to 1 mg/mL using an Amicon Ultra Centrifugal Filter Unit (Millipore) with a 3 kDa cutoff. $CuSO_4$, tris(3-hydroxypropyltriazolyl-methyl)amine (THPTA), sodium ascorbate, and biotin-azide were added to concentrations of 200, 200, 400 , and 50 μM, respectively, incubated for 2 hours on a rotating mixer in the dark, diluted and reconcentrated as before. The samples were separated on 15% SDS-PAGE gels and transferred to a nitrocellulose membrane using a Trans-Blot Turbo (BioRad) according to manufacturer's instructions. The membranes were stained with Ponceau S Solution (Sigma), imaged, and destained according to manufacturer's instructions. The membranes were blocked overnight at 4°C in PBS with 5% dry non-fat milk on a rocker, stained with IRDye 800CW Streptavidin (LI-COR) in PBS with 4% dry non-fat and 0.1% Tween-20 for two hours at room temperature on a rocker, washed three times with PBS with 0.1% Tween-20 for 5 minutes, and two times with PBS for five minutes. The membranes were imaged using an Odyssey infrared imaging system (LI-COR) at 800 nm.

Identification of additional mutations that affect '882 activity

In silico docking was performed by Raju Nagarajan and Ivelin S. Georgiev. Protoporphyrinogen oxidase structure (PDB-id: 3I6D, chain A) from *Bacillus subtilis* was used for the structural analysis. Molecular docking simulations with ligand '882 were performed using the AutoDock 4.2 and AutoDock tools (108). The protein was prepared for docking by assigning polar hydrogens, solvation parameters, and Kollman united

atom charges, whereas Gasteiger charges were assigned to the ligand. Water molecules were removed from the input structure. The ligand was modeled as flexible around rotatable bonds. The grid box was centered around residues T189 and Q192 (*S. aureus* T183 and N186). Flexible docking was performed by modeling as flexible these two residues, as well as the nearby Y177, F190 and F193. The default grid box size was adjusted to allow a free rotation of the ligand, and set at 70x70x70, with a grid spacing of 0.375 Å. Grid maps were generated using the AutoGrid program. The Lamarckian genetic algorithm (LGA) was used for the conformer search, with default parameters, including selection window (10 generations), population size (150) and maximum number of energy evaluations (2,500,000) (109). A total of 8,000 docked conformations were generated, and the 100 lowest-energy models were selected for further analysis. Potential mutations at residues, for which at least one ligand conformation (from the top 100) was within 4 Å, were modeled structurally, for selection of mutations to destabilize the interactions between the protein and the ‘882 ligand. Structural models were visualized using the PyMOL software. Two types of mutations were selected for experimental validation: (i) larger amino acid side chains that could sterically hinder ligand binding but that could be accommodated within the protein binding pocket, or (ii) Ala substitutions at residues that were found to have substantial ligand interactions in the docking models.

Light source and photosensitivity assays

A light source was engineered using an array of 135 individual 410 nm LED lights (Tianhui Electronic Co. Ltd) mounted in a custom laser-cut acrylic frame and

powered with a wall transformer to produce 1.41 mW/cm^2 over the entire surface of a 96-well plate. All light killing experiments were performed on three separate days and averaged. Student's *t*-test was performed to determine significance.

An overnight culture of *S. aureus* in RPMI supplemented with 1% casamino acids and 0.5 mM EDDHA was subcultured 1:50 into RPMI supplemented with 1% casamino acids and either 50 μM '882, 120 mM delta aminolevulinic acid hydrochloride (Frontier Biosciences), or a combination of the two. The culture was grown for 2 hours. An overnight of *S. epidermidis* in RPMI supplemented with 1% casamino acids was subcultured 1:50 into RPMI supplemented with 1% casamino acids and either 50 μM '882, 3.8 mM delta aminolevulinic acid hydrochloride (Frontier Biosciences), or a combination of the two. The culture was grown for 2 hours. Cells were diluted 1:10 into PBS. Twenty-five μL were transferred into a flat bottom 96 well plate and exposed to light to 0 or 2.5 J/cm^2.

An overnight culture of *B. anthracis* in RPMI supplemented with 1% casamino acids was subcultured 1:50 into RPMI supplemented with 1% casamino acids and either 50 μM '882, 3.8 mM delta aminolevulinic acid hydrochloride (Frontier Biosciences), or a combination of the two. The culture was grown for 5 hours, diluted 1:10 into PBS. Twenty-five μL were transferred into a flat bottom 96 well plate and exposed to light for to 0 or 2.5 J/cm^2. The bacteria were serially diluted, plated, and CFUs were counted after 20 hours of growth on LB agar.

A five-day anaerobic culture of *P. acnes* in BHI was removed from the anaerobic chamber (Coy) and subcultured 1:100 into BHI with either 50 μM '882, 230 μM delta aminolevulinic acid hydrochloride (Frontier Biosciences), or a combination of the two.

The culture was grown for 24 hours under anaerobic conditions. The culture was then removed from the anaerobic chamber and diluted 1:10 into PBS. Twenty-five μL were transferred into a flat bottom 96 well plate and exposed to light for to 0 or 5 J/cm^2. The bacteria were serially diluted, plated, and CFUs were counted after 5 days of growth on BHI agar. Data are represented as mean ± SEM.

Superficial skin infection

All mice were maintained in compliance with Vanderbilt's Institutional Animal Care and Use Committee regulations. Animals were infected as previously described using a tape-stripping model of infection (110). Six-to-eight week old female Balb/cJ mice or C57BL/6J mice were used for *S. aureus* and *P. acnes* infections, respectively. Briefly, stationary phase *S. aureus* cells grown in RPMI + 1% casamino acids + 0.5 mM EDDHA were washed with PBS, and approximately 2 x 10^8 CFU were inoculated in 5 μL of PBS. Twenty-four hours post infection, and each day thereafter, mice were left untreated, treated with 20 μL of 1 mM '882 in 2% Tween-80 in PBS with 2.5 J/cm^2 of 410 nm light two hours after exposure to compound. The size of each wound was calculated each day following infection by measuring dimensions on each animal and compared by Student's *t*-test. The presence of wound over the course of the infection was followed. Error and significance were determined using Prism's (GraphPad) function "Survival Curve Analysis."

Exponential phase *P. acnes* were washed in PBS and 2 x 10^8 CFU were inoculated in 5 μL of PBS. Thirty minutes post infection mice were untreated, or treated with either 50 μL 1.2 M ALA in 2% Tween-80 in PBS, 50 μL 1 mM '882 in 2% Tween-80 in PBS,

or 50 μL 1.2M ALA and 1 mM '882 in 2% Tween-80 in PBS. Two hours later mice were exposed to 2.5 J/cm^2 410 nm light. Mice were harvested 22 hours post infection. Skin samples containing the wound were homogenized using a Bullet Blender (Next Advanced) according to the manufacturer's instructions. The homogenate was serially diluted and plated. Data are represented as mean ± SEM. Student's *t*-test was performed to determine significance.

Chemical Synthesis

Chemical synthesis was performed by Brendan Dutter, PhD and Gary Sulikowski, PhD.

General Procedures: All non-aqueous reactions were performed in flame-dried flasks under an atmosphere of argon. Stainless steel syringes were used to transfer air- and moisture-sensitive liquids. Reaction temperatures were controlled using a thermocouple thermometer and analog hotplate stirrer. Reactions were conducted at room temperature (rt, approximately 23 °C) unless otherwise noted. Flash column chromatography was conducted using silica gel 230-400 mesh. Analytical thin-layer chromatography (TLC) was performed on E. Merck silica gel 60 F254 plates and visualized using UV and iodine stain.

Materials: All solvents and chemicals were purchased from Sigma-Aldrich unless otherwise noted. Dichloromethane (DCM) and tetrahydrofuran (THF) were used as received in a bottle with a SureSeal. Triethylamine was distilled from calcium hydride and stored over KOH. Deuterated solvents were purchased from Cambridge Isotope Laboratories. Trimethylsilylacetylene was purchased from Oakwood Chemicals. **S1** and

S3 were prepared using previously described procedures (111, 112). Biotin azide (PEG4 carboxamide-6-azidohexanyl biotin) was prepared by the Vanderbilt Institute of Chemical Biology chemical synthesis core. The preparation and characterization of '882 derivatives presented in Table 8, with exception of '882-PAL, has been previously described (49).

Instrumentation: ^{1}H NMR spectra were recorded on Bruker 400 or 600 MHz spectrometers and are reported relative to deuterated solvent signals. Data for ^{1}H NMR spectra are reported as follows: chemical shift (δ ppm), multiplicity (s = singlet, d = doublet, t = triplet, q = quartet, p = pentet, m = multiplet, br = broad, app = apparent), coupling constants (Hz), and integration. ^{13}C NMR spectra were recorded on Bruker 100 or 150 MHz spectrometers and are reported relative to deuterated solvent signals. ^{19}F NMR were recorded on a Bruker 376 MHz spectrometer. Low resolution mass spectrometry (LRMS) was conducted and recorded on an Agilent Technologies 6130 Quadrupole instrument.

Experimental Procedures:

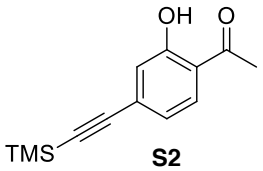

S2 **1-(2-hydroxy-4-((trimethylsilyl)ethynyl)phenyl)ethanone (S2).** To a stirred solution of 4-bromo-2-hydroxyacetophenone (**S1**) (220 mg, 1.02 mmol) in tetrahydrofuran (4 mL) was added triethylamine (284 µL, 2.04 mmol), bis(triphenylphosphine)palladium dichloride (36.0 mg, 0.051 mmol), copper(I) iodide (9.7 mg, 0.051 mmol), and trimethylsilylacetylene (216 µL, 1.53 mmol). The mixture was stirred overnight at room temperature under an atmosphere of argon until judged

complete by TLC. The reaction was filtered through Celite, concentrated, and purified by flash chromatography to provide 208 mg (88 %) of **S2** as white crystals. ^{1}H NMR (400 MHz, $CDCl_3$) δ 7.64 (d, J=8.24 Hz, 1H), 7.85 (d, J=1.40 Hz, 1H), 6.96 (dd, J=8.24 Hz, J=1.52 Hz, 1H), 2.61 (s, 3H), 0.23 (s, 9H); ^{13}C NMR (100 MHz, $CDCl_3$) δ 204.0, 162.1, 131.2, 130.6, 122.5, 121.7, 119.5, 103.7, 98.8, 26.8, -0.1; LRMS calculated for $C_{13}H_{17}O_2Si^+$ $(M+H)^+$ m/z: 233.1, measured 233.2.

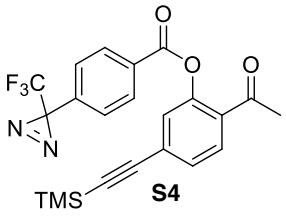

S4

2-acetyl-5-((trimethylsilyl)ethynyl)phenyl 4-(3-(trifluoromethyl)-3H-diazirin-3-yl)benzoate (**S4**). To a stirred solution of phenol **S2** (82.0 mg, 0.355 mmol) dissolved in dichloromethane (1 mL) was added triethylamine (54 μL, 0.390 mmol), one crystal of 4-dimethylaminopyridine, and benzoyl chloride **S3**[2] (97.0 mg, 0.390 mmol) dissolved in dichloromethane (0.5 mL). The reaction was stirred at room temperature for 1 h until judged complete by TLC analysis. The reaction was diluted with dichloromethane (20 mL), washed with saturated $NaHCO_3$, brine, dried ($MgSO_4$), and concentrated to provide 138 mg (86 %) of benozate **S4**. ^{1}H NMR (400 MHz, $CDCl_3$) δ 8.21 (dt, J=8.60 Hz, J=1.80 Hz, 2H), 7.80 (d, J=8.08 Hz, 1H), 7.44 (dd, J=8.08 Hz, J=1.52 Hz, 1H), 7.35 – 7.31 (m, 3H), 2.51 (s, 3H), 0.25 (s, 9H); ^{19}F NMR (376 MHz, $CDCl_3$) δ -67.9.

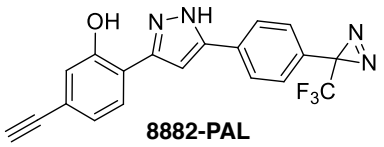

8882-PAL

5-ethynyl-2-(5-(4-(3-(trifluoromethyl)-3H-diazirin-3-yl)phenyl)-1H-pyrazol-3-yl)phenol (**'882-PAL**). To a stirred solution of

ester **S4** (138 mg, 0.310 mmol) dissolved in THF (1.5 mL) at 0 °C was added 0.5 M KHMDS in toluene (1.24 mL, 0.620 mmol). The reaction was maintained at 0 °C for 1.5 h at which point it was judged complete by TLC. The reaction was quenched by addition of 1 N HCl and the resulting mixture extracted with diethyl ether, concentrated, the residue flash filtered through silica gel with hexane/ethyl acetate (4:1), and concentrated again to provide 60.1 mg of crude diketone which was carried through to the next step without purification or characterization. The crude diketone (60.1 mg) was dissolved in 4.5 mL ethanol containing hydrazine hydrate (8.7 μL, 0.136 mmol). The reaction was maintained at room temperature until judged complete by LCMS (2 h). The reaction was concentrated and dissolved in methanol (1 mL) and potassium carbonate (19 mg, 0.136 mmol) was added. The reaction was stirred for 30 min until judged complete by LCMS. The reaction was partitioned between water and ethyl acetate. The organic layer was washed with brine, dried ($MgSO_4$), filtered and concentrated. The crude residue was purified by preparative scale reverse phase HPLC to provide 14.2 mg (12 % over 2 steps) of **'882-PAL** (Figure 11). ^{1}H NMR (600 MHz, CD_3OD) δ 7.88 (d, J=8.52 Hz, 2H), 7.66 (d, J=8.40 Hz, 1H), 7.32 (d, J=8.22 Hz, 2H), 7.16 (s, 1H), 7.03 – 7.00 (m, 2H), 3.50 (s, 1H); ^{13}C NMR (150 MHz, CD_3OD) δ 159.6, 133.9, 129.7, 127.3, 124.4, 123.6 (q, J=273.9 Hz), 120.7, 118.6, 101.9, 84.2, 78.9, 29.5 (q, J=40.4 Hz); ^{19}F NMR (376 MHz, CD_3OD) δ -67.0; LRMS calculated for $C_{19}H_{12}F_3N_4O^+$ $(M+H)^+$ m/z: 369.1, measured 369.2 (Figure 12).

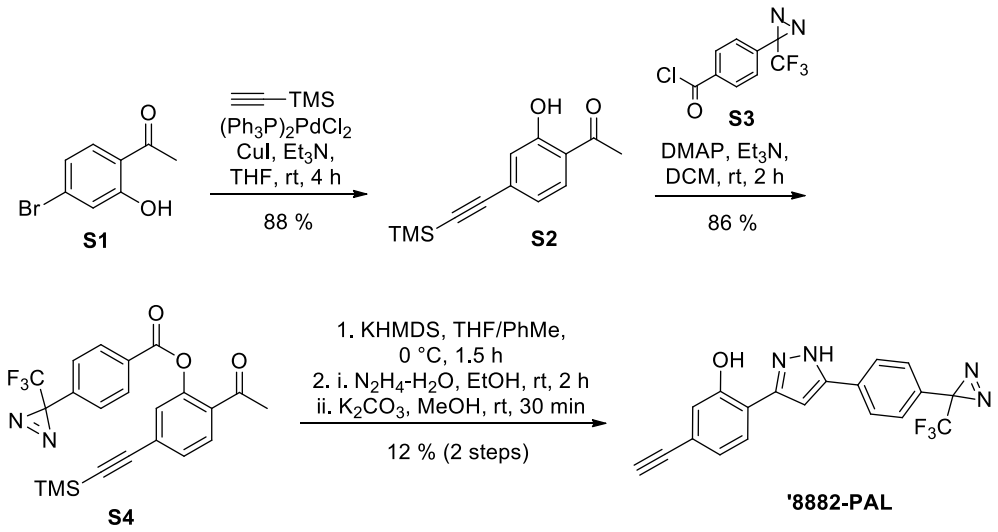

Figure 11. Synthesis of '882-PAL.

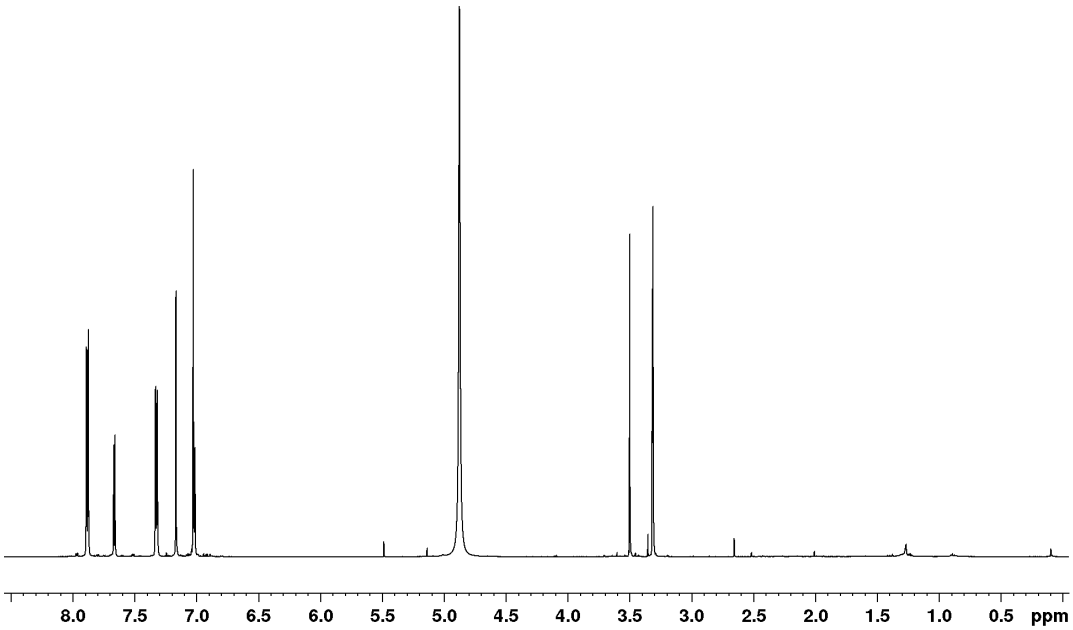

Figure 12. ^{1}H NMR spectrum of '882-PAL in CD_3OD.

RESULTS

Selection of ‘882-resistant suicide strains

The suicide strain was constructed as described in Chapter II (Figure 13c-d). Isolates of *hrtAB::relE* exhibiting spontaneous resistance to ‘882 were identified, and the stability of resistance was ensured through serial passage. Genomic DNA was isolated and the *hssRS/hrtAB* locus was sequenced. Whole genome sequencing was performed on isolates lacking mutations in *hssRS*/P*hrt* to identify mutations conferring resistance to ‘882 in the *hrtAB::relE* strain background. This analysis revealed a T183K mutation in HemY, an enzyme required for heme biosynthesis. The HemY T183K mutation was reconstructed in WT *S. aureus* (*hemY.T183K*), and this strain exhibits normal growth suggesting the HemY T183K mutation prevents the response of *S. aureus* to ‘882 without restricting heme biosynthesis, as seen in a strain lacking HemY (Δ*hemY*) (Figure 13e) (113). In addition, the T183K mutation abolished ‘882 sensing to the same level as Δ*hssRS*, while heme sensing remained intact (Figure 13f). Taken together, these results demonstrate that the HemY T183K mutation prevents ‘882-induced activation of *hrtAB* in *S. aureus*.

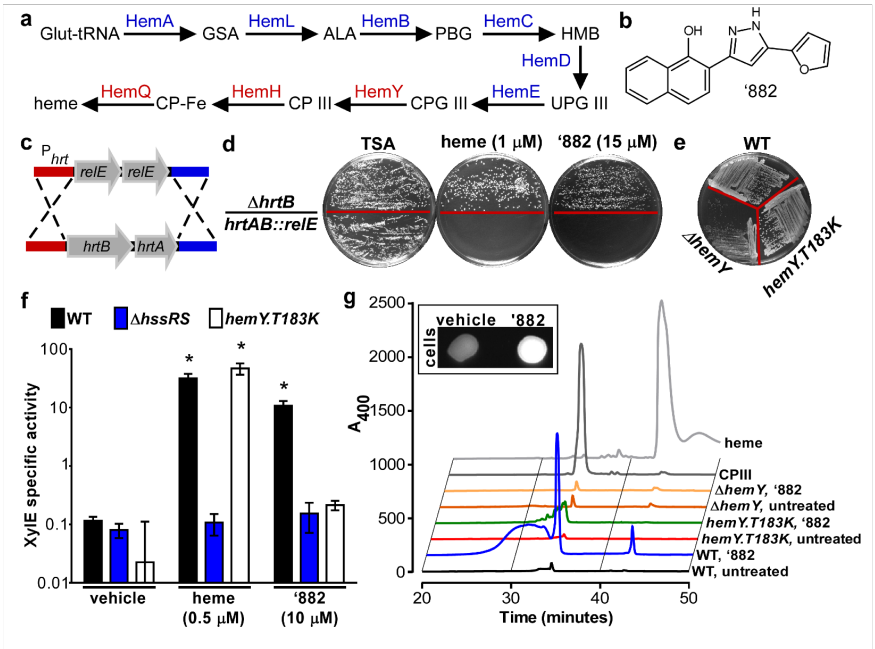

Figure 13. '882 exposure increases CPIII production in *S. aureus*.

(a) The terminal enzymes in the Gram-positive heme biosynthesis pathway (red) are distinct from other organisms. (b) '882 is a small molecule that increases heme biosynthesis in *S. aureus* (47). (c) To create a P_{hrt} suicide strain, the *hrtAB* genes were replaced with two copies of the *E. coli* gene encoding the RNA interferase toxin RelE. (d) Upon heme or '882 stimulation, toxicity is induced in *hrtAB::relE*. (e) Strain *hemY.T183K* exhibits a normal growth phenotype on TSA suggesting the HemY T183K does not restrict HemY function. (f) Strain *hemY.T183K* is unresponsive to '882, but retains the ability to respond to heme as measured by P_{hrt} activation. * denotes $p<0.001$ compared to vehicle treated for each strain. (g) HPLC analysis of WT, *hemY.T183K*, and Δ*hemY* ± '882. '882 increases CPIII production in WT cells but not in *hemY.T183K*. (Inset) '882-induced CPIII accumulation induces fluorescence in treated cells.

‘882 induces CPIII accumulation

To determine the impact of ‘882 on the heme biosynthesis pathway, intermediates of heme biosynthesis were quantified following ‘882 exposure. Porphobilinogen (PBG), an early heme biosynthetic precursor, is unaffected by ‘882 (Figure 13a, Figure 14). In contrast CPIII, the product of HemY, is greatly increased following ‘882 treatment (Figure 13a, g). Notably, CPIII accumulation is not observed in *hemY.T183K* or Δ*hemY* upon ‘882 treatment (Figure 13g). CPIII is the only fluorescent molecule in the heme biosynthesis pathway and ‘882 exposure triggers dramatic fluorescence in *S. aureus* (Figure 13g, inset). The HPLC fraction corresponding to the elution time of the CPIII standard was analyzed by LC-MS/MS and confirmed to be CPIII (Figure 15). These results demonstrate that ‘882 exposure leads to accumulation of CPIII in *S. aureus* and implicate HemY as a candidate target of the molecule.

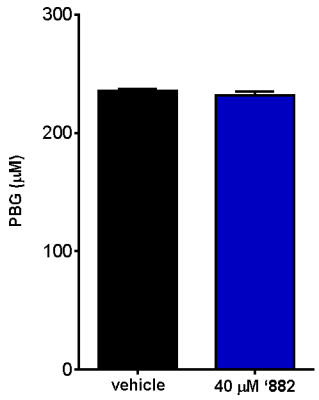

Figure 14. '882 does not affect early heme biosynthesis.

Porphobilinogen (PBG) was quantified to determine '882-induced effects on early heme biosynthesis intermediates. No effect on PBG was seen.

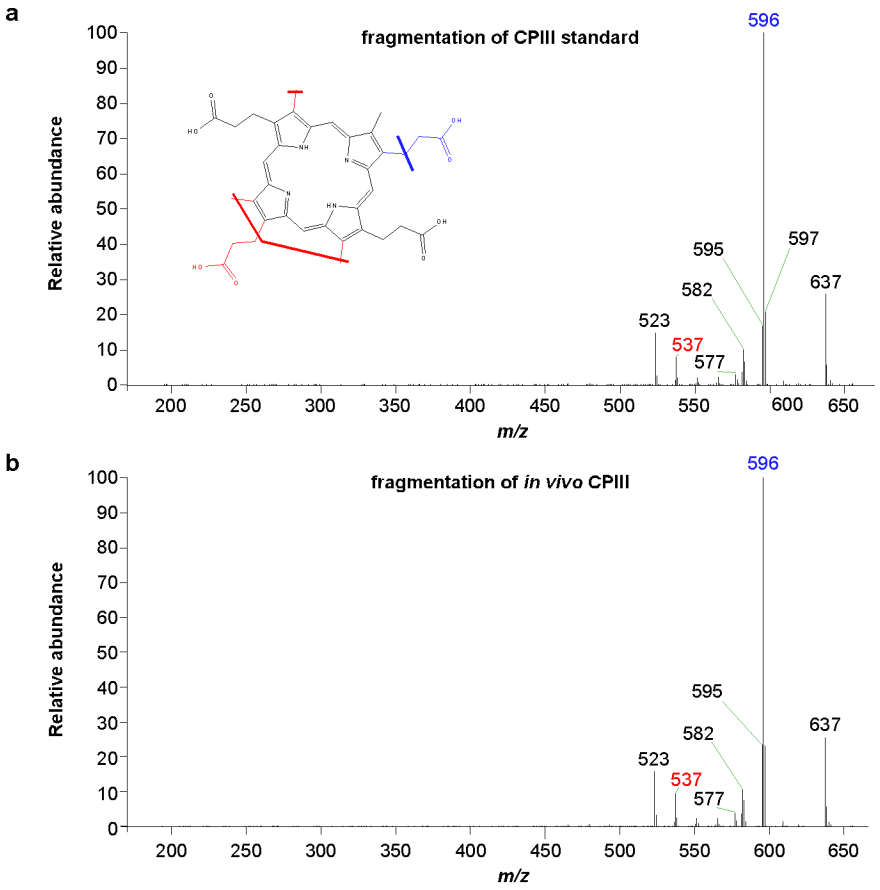

Figure 15. ‘882 induces accumulation of CPIII.

HPLC fractions containing either the CPIII standard peak or the corresponding fraction from ‘882 treated WT cells were analyzed by LC-MS/MS. MS/MS fragmentation of the peak at *m/z* 654.340, the mass of CPIII, is shown. The MS/MS fragmentation of this peak in both samples is nearly identical and consistent with expected major fragments, positively identifying the peak within these fractions as CPIII.

‘882 activates HemY from Gram-positive bacteria *in vitro*

To determine whether ‘882 directly activates *S. aureus* HemY, recombinant *S. aureus* WT HemY and HemY T183K were purified. Importantly, these two enzymes display similar K_M and V_{max} values, demonstrating the T183K mutation does not affect baseline HemY activity (Figure 16g, Figure 17a). Upon treatment with ‘882, WT HemY displayed 205% activity with an AC_{150} of 92 nM, whereas the T183K mutant did not respond to ‘882 at concentrations up to 10 μM (Figure 16a, g). These data establish ‘882 as a small molecule activator of HemY.

To determine if ‘882 retains activity against HemY from other Gram-positive organisms, recombinant *Bacillus subtilis* and *P. acnes* HemY were purified (32). K_M and V_{max} values were determined to characterize baseline activity of the enzymes, and each was tested for ‘882-induced activation (Figure 16b and g, Figure 17b). ‘882 activates HemY from *B. subtilis* and *P. acnes* with AC_{150} values of 42 and 16 nM, respectively (Figure 16b, g). Importantly, human HemY, a protoporphyrinogen oxidase as opposed to a coproporphyrinogen oxidase, did not respond to ‘882 treatment (Figure 16c, Figure 17c). These results establish ‘882 as a small molecule activator of HemY from Gram-positive bacteria.

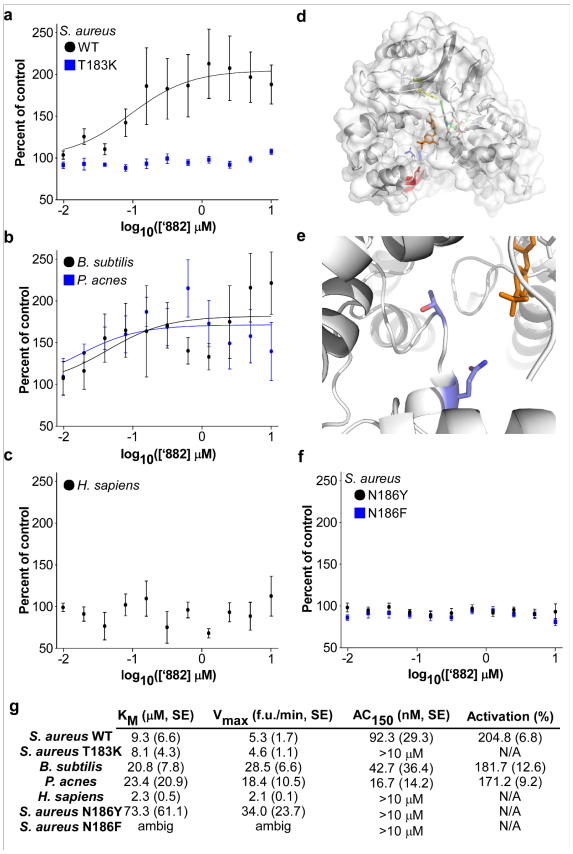

g

	K_M (μM, SE)	V_{max} (f.u./min, SE)	AC_{150} (nM, SE)	Activation (%)
***S. aureus* WT**	9.3 (6.6)	5.3 (1.7)	92.3 (29.3)	204.8 (6.8)
***S. aureus* T183K**	8.1 (4.3)	4.6 (1.1)	>10 μM	N/A
B. subtilis	20.8 (7.8)	28.5 (6.6)	42.7 (36.4)	181.7 (12.6)
P. acnes	23.4 (20.9)	18.4 (10.5)	16.7 (14.2)	171.2 (9.2)
H. sapiens	2.3 (0.5)	2.1 (0.1)	>10 μM	N/A
***S. aureus* N186Y**	73.3 (61.1)	34.0 (23.7)	>10 μM	N/A
***S. aureus* N186F**	ambig	ambig	>10 μM	N/A

Figure 16. ‘882 activates HemY from Gram-positive bacteria and identification of a region important for regulation of HemY.

(a-b, f) HemY activity was assayed with increasing ‘882 concentrations and 5 μM CPGIII. (c) HemY activity was assayed with increasing ‘882 concentrations and 5 μM PPGIX. (d) The residue of *B. subtilis* HemY homologous to *S. aureus* T183 (blue) is located in a region distinct from the active site (Y366, yellow) (114, 115). *B. subtilis* HemY shares 46% identity with *S. aureus* HemY. A residue homologous to *S. aureus* N186 (red) faces a cleft leading into the active site. (e) Magnified view of residues homologous to *S. aureus* T183 and N186 residues (carbon in light blue, nitrogen in dark blue, and oxygen in red). (g) K_M, V_{max}, AC_{150}, and activation (%) for each enzyme were determined.

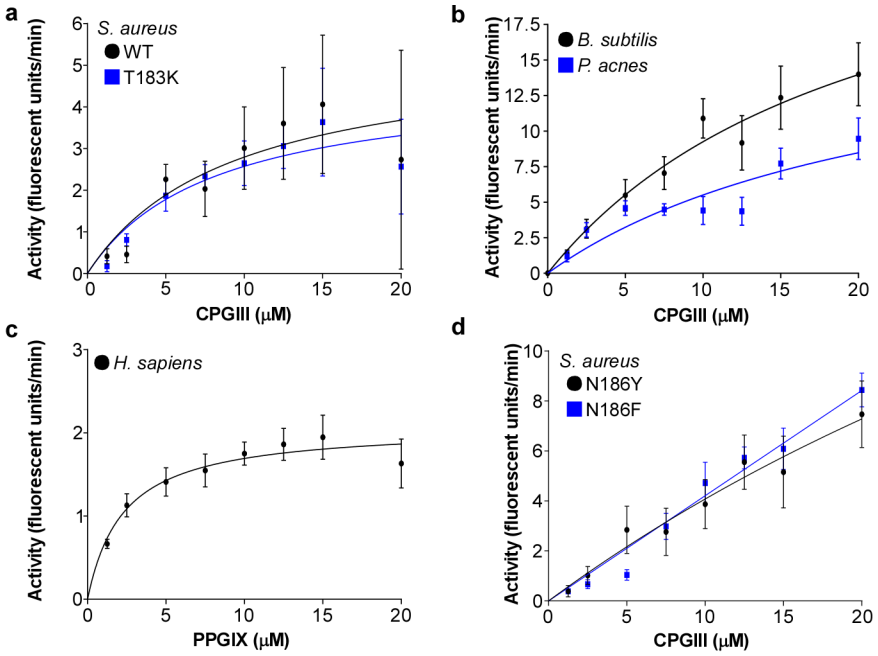

Figure 17. Characterization of HemY activity from Gram-positive bacteria and *H. sapiens*.
(a-d) Activities of recombinant HemY from *S. aureus* (WT, T183K, N186Y, N186F), *B. subtilis*, *P. acnes*, and *H. sapiens* with varying concentrations of coproporphyrinogen III (CPGIII) for Gram-positive HemY and protoporphyrinogen IX (PPGIX) for *H. sapiens* HemY to determine K_M and V_{max}.

Structure activity relationship (SAR) studies of ‘882

Recently a series of structural analogs of ‘882 were prepared and screened in a phenotypic HssRS activation assay using a XylE reporter gene to monitor transcription of *hrtAB* as a response to heme accumulation (Table 8) (49). These analogs were assayed in the HemY activation assay using WT and T183K mutant enzymes (Table 8). Three analogs (74-1B, VU0420372, 74-1A) proved superior or comparable to ‘882 as HemY activators *in vitro*. Notably, none of these more potent activators exhibit increased ability to trigger *hrtAB* expression in *S. aureus* over that of ‘882, suggesting that these compounds do not efficiently enter the bacterial cell. In addition, these ‘882 derivatives are also inactive against the T183K mutant suggesting all four diarylpyrazoles share a common binding site. The remaining eight diarylpryazoles were equally inactive when assayed against HemY or the T183K mutant. Collectively these SAR studies support activation of HemY by a common allosteric binding site.

Table 8. Structural analogs of '882 activate HemY.

Structure	Compound	*In vivo* activity: % activity of '882 at 50 µM (SEM)	*In vitro* activity: % activity of WT HemY at 1 µM (SEM)	*In vitro* activity: % activity of T183K HemY at 1 µM (SEM)
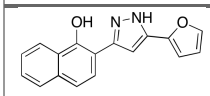	VU0038882	100 (9)[#]	192 (21)	69.3 (8.8)
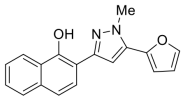	74-1B	0.335 (0.276)[#]	300 (42)	72.3 (11.5)
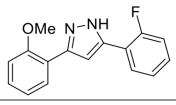	VU0420372	1.67 (0.55)[#]	230 (40)	72.1 (7.5)
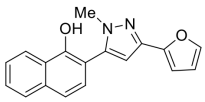	74-1A	0.206 (0.113)[#]	153 (15)	35.7 (4.7)
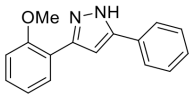	VU0420382	0.812 (0.297)[#]	128 (12)	78.3 (7.9)
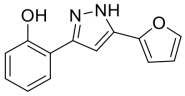	VU0125897	28.2 (0.8)[#]	112 (16)	110 (19)
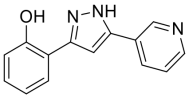	VU0476720	0.392 (0.146)[#]	111 (13)	95.6 (9.7)
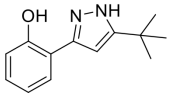	VU0476725	0.299 (0.188)[#]	109 (17)	137 (12)
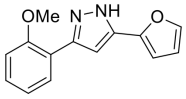	VU0366053	0.715 (0.093)[#]	89.6 (11.4)	106 (12)
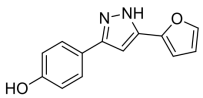	VU0404345	1.19 (0.31)[#]	81.9 (24.4)	75.8 (10.0)
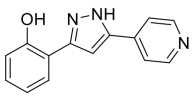	VU0476722	0.286 (0.136)[#]	79.4 (9.0)	95.2 (15.2)
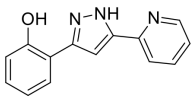	82A	0.245 (0.036)[#]	77.8 (14.9)	72.1 (9.5)
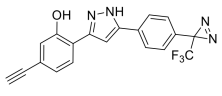	'882-PAL	59.0 (2.5) *	165 (26)	125 (35)

Previously published data (49).

* '882-PAL was tested at 10 µM in XylE assay and compared to 10 µM '882.

‘882-photoaffinity probe interacts with HemY in *S. aureus* lysates

Guided by the SAR data, an ‘882 photoaffinity probe (‘882-PAL) incorporating an alkyne moiety for click chemistry was prepared and confirmed to be active in *S. aureus* (Table 8). To determine if ‘882 directly interacts with HemY, lysates from WT and Δ*hemY* were prepared and treated with ‘882-PAL followed by photocrosslinking and then Cu catalyzed ligation of an azido-biotin reporter to the photolabelled proteins. A band corresponding to the molecular weight of HemY (52 kDa) was identified by detection of the biotin tag ligated to ‘882-PAL (Figure 18). This band is not present in lysate from Δ*hemY*, and is dependent upon the addition of the biotin tag (Figure 18). These results establish that ‘882 specifically interacts with HemY from *S. aureus* lysates.

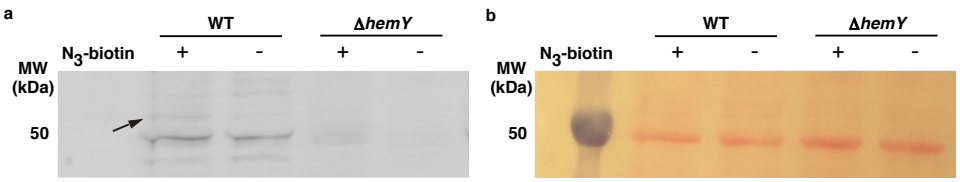

Figure 18. '882-PAL is active and identifies HemY in *S. aureus* lysate.

(a) '882-PAL was incubated with lysate from *S. aureus* and photocrosslinked. Click reaction was performed to add the biotin tag. Detection of biotinylated proteins was performed using a streptavidin conjugated fluorophore. A band at the approximate molecular weight (arrow, 52 kDa) of HemY was identified in WT lysate and not in Δ*hemY* lysate or in the absence of the biotin tag. (b) Ponceau S stain to verify protein loading was consistent across samples.

Structural analysis of the ‘882-HemY interaction

To gain insight into the potential binding site of ‘882 within HemY, the previously solved crystal structure of *B. subtilis* HemY was interrogated (Figure 16d) (115). Based on the location of *S. aureus* T183 within HemY, a nearby amino acid, N186, was implicated as potentially important due to its proximity on a short helix facing a cleft leading into the active site (Figure 16d, e). The N186 residue was altered to tyrosine or phenylalanine and the activity of the resulting enzyme variant was examined in the presence or absence of ‘882 (Figure 16f and g, Figure 17d). HemY N186Y and HemY N186F exhibit increased baseline activity relative to WT HemY, suggesting this region is important for positive enzyme regulation (Figure 16g, Figure 17d). Consistent with this, both mutations abolishes the ability of HemY to respond to ‘882 treatment (Figure 16f, g). Importantly, the helix containing these residues is in a distinct region from the active site of the molecule (Figure 16d). Taken together, these data support a model whereby ‘882 binds to the region of HemY containing residues 183 to 186 and acts as an allosteric modulator of enzyme activity. Mutations in this portion of the enzyme may mimic ‘882-induced changes in tertiary structure leading to enzyme activation.

***In silico* docking identifies a functional domain important for ‘882 activation**

To further our understanding of the functional domain required for ‘882 activity, the ‘882-HemY interaction was modeled by *in silico* docking to identify additional residues that may be required for ‘882-induced activity of HemY. Based upon this analysis, six more residues within HemY were selected for mutational analysis to interrogate their importance for ‘882-dependent activation (Figure 19a). Mutations were

made in *S. aureus hemY* creating the enzyme variants V146M, M167F, Y171A, F184A, F187W, and D450Y. Upon induction, V146M, Y171A, F184A, and D450Y led to unstable enzymes that could not be purified (Figure 10). HemY M167F and F187W expressed equivalently to WT (Figure 10), were purified, and interrogated for ‘882-induced activation. Both mutations inhibited the activation of HemY by ‘882 (Figure 19b). Taken together, these data begin to define a pocket within HemY that appears to be required for ‘882-dependent activation of the enzyme (Figure 19c).

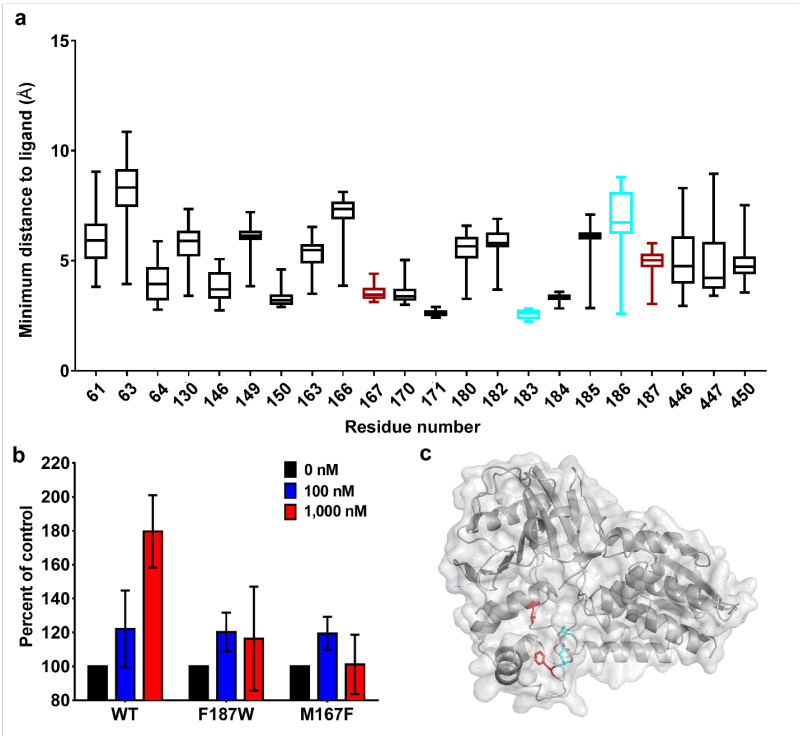

Figure 19. Identification of additional mutations that affect '882 activity.

(a) Distribution of ligand-residue distances for the subset of protein residue positions for which at least one of the top 100 ligand conformations was within 4 Å, shown as boxplots (box represents 25th and 75th percentile, and the horizontal line inside the box represents the median; vertical bars span between the min and max values). The two residues used to guide the docking are shown in cyan, whereas the two additional residues that were identified by the modeling approach and confirmed to have the desired disruption of '882 activity are shown in red. Structural analysis was performed on the *B. subtilis* crystal structure, homologous residue numbers to the *S. aureus* sequence are displayed (115). (b) HemY activity was assayed with '882 and 5 µM CPGIII. (c) Structural model highlighting the same four residues as in the boxplot in the *B. subtilis* structure (115).

HemY activation induces photosensitization of Gram-positive bacteria

Photodynamic therapy (PDT) is frequently used to treat bacterial skin infections and involves the use of a photosensitizer and a light source to destroy cells through the production of reactive oxygen species (16). Porphyrin intermediates of the heme biosynthesis pathway are the most common photosensitizers used in clinics. The production of porphyrin intermediates is often upregulated through the addition of aminolevulinic acid (ALA), the first committed precursor in the heme biosynthetic pathway (Figure 13a). A major limitation of ALA-PDT for the treatment of infectious diseases is the lack of specificity of this therapy, which induces photosensitivity in both bacterial and human cells. Due to the specificity of ‘882 for HemY from Gram-positive bacteria, this molecule should selectively sensitize bacteria to light while avoiding host toxicity. To test this hypothesis, S. aureus grown in the presence of ALA or ‘882 were exposed to 410 nm light, the excitation maximum for CPIII. Both ALA and ‘882 treatment led to significant growth inhibition of S. aureus following exposure to 2.5 J/cm2 of light (Figure 20a). A synergistic effect was seen when ‘882 and ALA were added together, likely due to ALA increasing precursor availability for HemY. Notably, ALA and ‘882 combined decreased *S. aureus* viability by four logs compared to untreated cells (Figure 20a). The toxicity of ‘882-PDT is conserved across some of the most important causes of human skin infections, including *S. epidermidis*, *B. anthracis*, and *P. acnes* (Figure 20b-d). These results establish the utility of ‘882-PDT as a potential therapeutic for the treatment of skin infections, most often caused by Gram-positive bacteria.

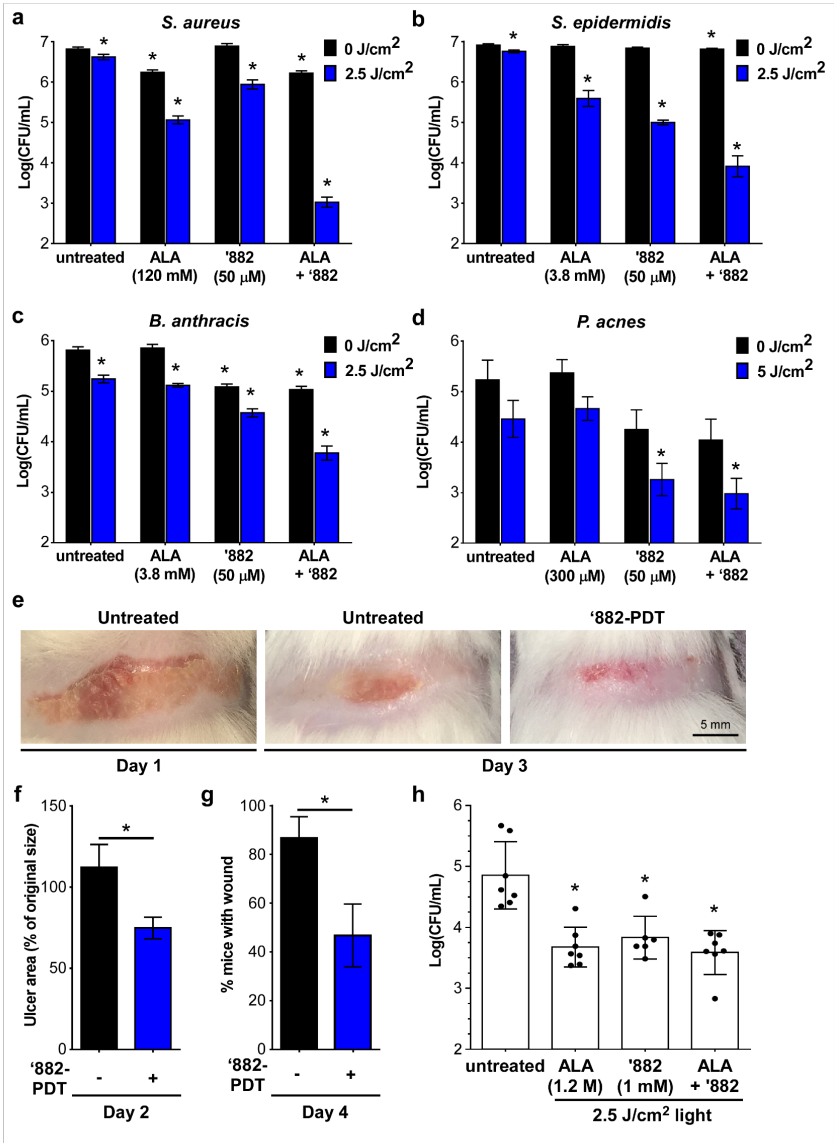

Figure 20. '882 induces photosensitivity in Gram-positive pathogens.

(a-d) *S. aureus*, *S. epidermidis*, *B. anthracis*, and *P. acnes* were exposed to ALA, '882, or ALA+'882 in the presence or absence light. * denotes $p<0.05$ compared to untreated. (e) Mice infected with *S. aureus* were treated daily with '882 ± 2.5 J/cm^2 light. Wound size was imaged three days post infection. (f) Wound size was quantified two days post infection. n=22, * denotes $p<0.05$. (g) Mice with wounds were quantified over the course of infection. n=15, * denotes $p<0.05$. (h) Mice infected with *P. acnes* were treated and bacteria quantified in the wound 22 hours post infection. * denotes $p<0.01$ compared to untreated.

‘882-PDT increases wound healing and decreases bacterial burdens *in vivo*

To determine the *in vivo* efficacy of ‘882-PDT, a murine model of cutaneous *S. aureus* infection was employed, which leads to considerable skin ulceration (Figure 20e) (110). Mice infected with *S. aureus* and treated with ‘882-PDT exhibited a 37% reduction in ulcer size following infection as compared to untreated animals (Figure 20e, f). Furthermore, ‘882-PDT increases healing rates, with 54% of mice having no visible lesion within four days (Figure 20g). To evaluate the broad utility of ‘882-PDT as a therapy for common skin infections, the efficacy of ‘882-PDT in a murine model of *P. acnes* infection was determined. ‘882-PDT led to a significant decrease in bacterial burden, highlighting the utility of ‘882 as a novel compound for the treatment of acne (Figure 20h). Taken together, these findings establish photodynamic therapy coupled with small molecule activation of HemY as an effective therapeutic strategy to specifically target Gram-positive pathogens.

DISCUSSION

These results define the small molecule ‘882 as an activator of Gram-positive HemY. Residues required for ‘882-induced activation have been identified, thereby revealing a functional domain involved in the activation of HemY. In addition, treatment with ‘882 leads to photosensitization of Gram-positive bacteria, reducing tissue ulceration and bacterial burdens *in vivo*. Taken together, these results establish ‘882 as an activator of Gram-positive HemY and provide proof-of-principle for small molecule activation of HemY as a potential therapeutic strategy for the treatment of bacterial infections.

Synthetic small molecule activators are rare, with only a handful identified to date (116). Identifying the targets of small molecules is a major obstacle in biomedical research (50-52). Phenotypic high-throughput screens utilizing small molecule libraries often result in the identification of numerous molecules with unknown targets. Several approaches have been successful in identifying intracellular targets of small molecules (53-59). Here we report a genetic selection strategy based on the creation of a suicide-strain that enables the identification of spontaneous resistant mutants to an activating compound that is typically non-toxic. This strategy can be adapted to a variety of systems where a small molecule activates a specific gene expression program, and may enable the identification of targets for numerous small molecule activators.

The mechanisms by which heme biosynthesis is regulated in Gram-positive bacteria are largely unknown (21). The identification of ‘882 as an activator of HemY establishes this molecule as a valuable tool for interrogating the heme biosynthetic

pathway in Gram-positive bacteria to further understand the synthesis of this essential cofactor. Interestingly, it has previously been demonstrated that HemY activity is modulated *in vitro* to a similar extent by addition of HemQ, the terminal enzyme in the Gram-positive heme biosynthesis pathway(34). This suggests that the interaction of HemY with ‘882 may not be a random occurrence, but may represent an inappropriate hijacking of a normal *in vivo* regulatory mechanism. ‘882-dependent activation of heme biosynthesis represents a valuable tool for studying the regulation of heme biosynthesis in Gram-positive bacteria.

Notably, enzyme activators have numerous properties that make them ideal therapeutics (116). Whereas inhibitors often require the ability to inhibit the enzyme by 90%, activators can induce phenotypes with small increases in enzyme activity, indicating that derivatives of ‘882 with slight increases in activity could lead to dramatic increases in CPIII accumulation and therefore antibacterial properties (116). Specifically, this has been seen with small molecule activators of glucokinase, where a 1.5-fold increase in enzymatic activity has shown significant effects *in vivo*. These molecules are now used as therapeutics for diabetes (117).

In addition, inhibitors often bind active sites of enzymes, which are typically well conserved across homologous enzymes. In contrast, activators often bind allosteric sites, which are less well conserved across enzymes thus increasing specificity and limiting off-target effects (116-118). Structural analysis of the ‘882-HemY interaction has identified a functional domain of HemY that suggests an allosteric mechanism of action for ‘882-induced activation (Figure 16, Figure 19). In addition, we have identified specific residues that when altered increase activity, further supporting that this portion of the

enzyme is important in positive regulation (Figure 17). Therefore, ‘882 and its derivatives have value as both probes of heme biosynthesis as well as small molecule photosensitizers for the treatment of bacterial infections.

The use of PDT has begun to expand beyond SSTIs. Gastrointestinal endoscopes have been developed that emit wavelengths that activate porphyrins in patients to detect cancer, and similar strategies have been interrogated for their ability to treat gastrointestinal infections (68, 69). Osteomyelitis and contamination of orthopedic devices are some of the most common invasive bacterial infections, and PDT strategies to combat these infections are being developed (66, 70-75). Finally, PDT-based strategies are in development for a variety of other diseases including parasitic, dental, and sinus infections (67, 76). As the utility of PDT-based therapies expands, so too will the potential clinical utility of small molecule activators of HemY.

The ability of ‘882 to specifically photosensitize Gram-positive bacteria circumvents the non-specific nature of ALA-PDT, which has limited the value of ALA-PDT for the treatment of infectious diseases (16, 64, 65). Furthermore, this provides proof-of-concept that activation of bacterial porphyrin production through specific activation of HemY is a viable therapeutic strategy that could be adapted to Gram-negative bacteria and other infectious diseases (16, 63, 67). Therefore, the development of ‘882-PDT has the potential to significantly expand the value of light-based therapies for the treatment of the most common causes of skin infections.

A version of the following section (Chapter IV, Bacterial nitric oxide synthase is required for the *Staphylococcus aureus* response to heme stress) was previously published in American Chemical Society Infectious Diseases.

Reprinted and adapted with permission from:
Bacterial Nitric Oxide Synthase is Required for the *Staphylococcus aureus* Response to Heme Stress
ACS Infect. Dis., **2016**, *2* (8), pp 572–578
DOI: 10.1021/acsinfecdis.6b00081
Publication Date (Web): June 28, 2016

CHAPTER IV. BACTERIAL NITRIC OXIDE SYNTHASE IS REQUIRED FOR THE *STAPHYLOCOCCUS AUREUS* RESPONSE TO HEME STRESS

INTRODUCTION

Staphylococcus aureus is a Gram-positive pathogen that causes significant morbidity and mortality worldwide (5-8). Diseases caused by *S. aureus* range from superficial skin infections to invasive disease with considerable mortality. In this regard, *S. aureus* is a leading pathogen associated with life-threatening blood stream infections (3). Furthermore, recent isolates exhibit significantly decreased susceptibility to the current antibacterial armamentarium (119). This has led to efforts focused on an increased understanding of the pathogenesis of this organism in order to identify novel therapeutic targets for the treatment of staphylococcal infection.

In order to colonize the vertebrate host, *S. aureus* requires numerous nutrients, such as heme (120). The heme requirement can be satisfied through two distinct mechanisms: importing exogenous heme through dedicated machinery or synthesizing endogenous heme *de novo* from metabolic precursors. Both heme acquisition and heme synthesis are required for full virulence of *S. aureus* (26, 27). Once acquired, heme is used for various processes in the cell. Intact heme is utilized as a cofactor for enzymes including cytochromes in the electron transport chain, catalase for the detoxification of reactive oxygen species, and bacterial nitric oxide synthase (bNOS). Heme can also be employed as a nutrient iron source for bacteria, through degradation by heme oxygenases to release free iron (31).

Although required to colonize the host, excess heme is toxic to bacteria. Thus, the ability to sense and detoxify heme is critical to many pathogens (46). Specifically, multiple Gram-positive pathogens sense heme through the heme sensor system (HssRS) two-component system (44, 46). Upon activation, HssRS induces the expression of the heme-regulated transporter (*hrtAB*), which encodes an efflux pump that alleviates heme toxicity (44, 45). The coordinated efforts of HssRS and HrtAB enable these pathogens to grow in the presence of high heme concentrations. Deletion of components of this pathway affect the virulence of *S. aureus* (46). Understanding the mechanism of HssRS activation will provide insight into the ability of pathogens to sense this required cofactor and survive within the hostile environment of the vertebrate host.

Recent studies have found that bacterial nitric oxide (NO) synthesis is important for bacterial survival in the host, and suggest multiple roles for NO during bacterial infections (121). Bacterial pathogens encode genes similar to mammalian nitric oxide synthases, which led to the characterization of the bacterial nitric oxide synthase (bNOS) hemoprotein (30). The critical role of bNOS has been established in a number of organisms including *S. aureus* and *Bacillus anthracis*, where bNOS has been shown to protect against various antibiotics and oxidative stress (121-124). Considering its contribution to virulence of these organisms, bNOS has been identified as a potential drug target for the treatment of infections (125).

We have previously reported a high-throughput screen (HTS) for activators of staphylococcal HssRS (47). This screen resulted in the identification of multiple chemical probes that activate HssRS (47, 49). One such probe, VU0038882 (‘882), activates staphylococcal heme biosynthesis, providing a powerful tool for understanding heme

biosynthesis in the context of heme sensing and infection (47). In this manuscript, we describe the mechanism of HssRS activation by VU0043981 (‘3981), a second compound identified in the same HTS. Importantly, in contrast to ’882, ‘3981 activates HssRS independently of heme accumulation, providing a unique probe to interrogate the heme sensing system. In this regard, a transposon screen utilizing a ‘3981-derived probe uncovered bNOS as crucial to the heme stress response, providing evidence that nitric oxide and heme sensing are linked in staphylococci.

METHODS

Bacterial strains, growth conditions, and plasmids

Cloning was performed in *Escherichia coli* DH5α (Invitrogen™). *S. aureus* strains were grown in tryptic soy broth (TSB) or agar (TSA), and *E. coli in* lysogeny broth (LB) or agar (LBA). Strains and plasmids used in this study are described in Table 9 and Table 10, respectively.

S. aureus strain allele *nos::*ermC was described previously and was transduced into Newman using the ϕ85 bacteriophage (creating Δ*nos*) or strain Δ*hrtB* (creating Δ*hrtB*/Δ*nos*) (29, 103).

A complementation construct for *nos* was created by PCR-amplifying *nos* using Newman genomic DNA as a template, and cloning into pOS1.p*lgt*.

Table 9. Bacterial strains used in Chapter IV.

Bacterial Strain	Description	Reference
Wild-type	Staphylococcus aureus strain Newman	(94)
USA300 JE2	Staphylococcus aureus strain USA300 JE2	(126)
RN4220	*S. aureus* cloning intermediate	(96)
Δ*hssRS*	In-frame deletion of *hssRS* in Newman background	(93)
Δ*hssS*	Transposon integration into *hssS* in Newman, PhiNE 01562 (SAV2362)	(46)
Δ*hemB*	Transposon integration disrupting *hemB*, *hemB::*ermC, in Newman	(47)
Δ*menB*	In-frame deletion of *menB* in Newman	(127)
Δ*nos*	Transposon integration disrupting bNOS, *nos::*ermC in Newman	This study
Δ*hrtB*	In-frame deletion of *hrtB* in Newman background	(95)
Δ*hrtB*/Δ*nos*	Transposon integration disrupting bNOS, *nos::*ermC in Δ*hrtB*	This study

Table 10. Plasmids used in Chapter IV.

Plasmids	Reference
pOS1	(128)
pOS1.Plgt	(129)
phrt.xylE	(46)
plgt.xylE	(44)
plgt.nos	This study

Promoter activity assay

Promoter activity assay was performed as previously described (44). Briefly, p*hrtAB.xylE* was electroporated into the strain Δ*nos*. The other strains used have been previously described (47). Overnight cultures were diluted 1:100 into TSB supplemented with 10 μg/mL chloramphenicol and grown for 24 hours and assayed as previously described (46). The experiment was performed in triplicate on three separate days (*n*=9). Data are presented as mean +/- SEM. Student's *t*-test was performed to determine significance.

IC_{50} determination

To determine toxicity of the compounds, *S. aureus* overnight cultures were diluted 1:100 into a 96-well plate containing 200 μL of TSB with or without supplementation of compound. Cultures were grown at 37°C for 7 hours (stationary phase of untreated bacteria) and the OD_{600} was determined. Data were transformed to percent growth of untreated bacteria, concentrations of compound were log transformed, and fitted using GraphPad (Prism).

Heme quantification

Quantification of intracellular heme was performed as previously described (47). The experiment was performed in triplicate on three separate days (*n*=9). Data are presented as mean +/- SEM. Student's *t*-test was performed to determine significance.

Heme adaptation

Heme adaptation assays were performed similar to previously described (46, 47). The assay was performed in 96-well plates with pretreatments with vehicle (DMSO), heme, or a '3981 derived compound. Briefly, colonies were selected into 150 μL TSB in a 96-well plate and grown for 6 hours with shaking at 37°C. Cultures were subcultured 1:150 into the condition being tested and grown overnight. In the morning, cultures were subcultured again 1:150 into the heme concentration being interrogated or vehicle control and grown 6 hours. OD_{600} were determined and compared. The experiment was performed in triplicate on three separate days (n=9). Data are presented as mean +/- SEM. Student's t-test was performed to determine significance.

Transposon mutant screen

The staphylococcal Nebraska Transposon Mutant Library was screened using the protocol described above (126). Cultures were pretreated with '7501 overnight, and subcultured into 50 μM heme. Hits were identified as those that were greater than two standard deviations below the mean growth of the plate being tested.

Chemical Synthesis

Chemical synthesis was performed by Brendan Dutter, PhD and Gary Sulikowski, PhD.

General: Room temperature was approximately 23°C. Analytical thin-layer chromatography (TLC) was performed on E. Merck silica gel 60 F254 plates and visualized using UV light. All solvents and chemicals were purchased from Sigma-

Aldrich except 3-methoxybenzylamine (Combi-Blocks). Deuterated acetone was purchased from Cambridge Isotope Laboratories. ^{1}H NMR spectra were recorded on a Bruker 400 MHz spectrometer and are reported relative to deuterated solvent signals. Data for ^{1}H NMR spectra are reported as follows: chemical shift (δ ppm), multiplicity (s = singlet, d = doublet, t = triplet, dd = doublet of doublets, m = multiplet, br = broad, app = apparent), coupling constants (Hz), and integration. ^{13}C NMR spectra were recorded on a Bruker 100 MHz spectrometer and are reported relative to deuterated solvent signals. Low resolution mass spectrometry (LRMS) was conducted and recorded on an Agilent Technologies 6130 Quadrupole instrument.

Synthesis of Thioureas: Syntheses of '3981 and '7501 were adapted from a previously described procedure (130). To a stirred solution of 4-phenoxyaniline (1.0 eq) in dichloromethane (0.20 M) was added an equal volume of saturated sodium bicarbonate. The resulting biphasic mixture was cooled to 0 °C and stirred vigorously. Thiophosgene (1.0 eq) dissolved in a minimal amount of dichloromethane was added dropwise to the mixture. Once addition was complete, the mixture was stirred vigorously for 30 min at 0 °C. 4-fluorobenzylamine (for '3981) or 3-methoxybenzylamine (for '7501) (1.05 eq) was added to the reaction neat and the mixture was allowed to warm to room temperature with vigorous stirring. When the reaction was judged complete (TLC or LCMS), it was diluted with dichloromethane, the aqueous layer removed, the organic layer washed with 1 N HCl (1x), brine (1x), dried ($MgSO_4$), filtered, and the solvent removed *in vacuo*. The residue was purified by recrystallization from isopropanol. Yields were in the range of 50 – 60 % and compound purity was determined by ^{1}H NMR and LC-MS.

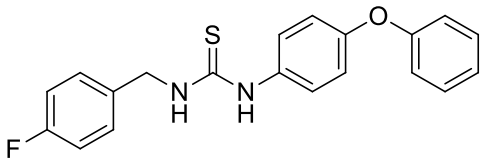

1-(4-fluorobenzyl)-3-(4-phenoxyphenyl)thiourea (**'3981**). Light yellow crystals; ^{1}H NMR (400 MHz, acetone-d6) δ 8.87 (br s, 1H), 7.57 (br s, 1H), 7.47 – 7.34 (m, 6H), 7.14 (t, J=7.40 Hz, 1H), 7.10 – 7.04 (app t, 2H), 7.02 – 6.96 (m, 4H), 4.87 (d, J=5.16 Hz, 2H); ^{13}C NMR (100 MHz, acetone-d6) δ 183.1, 164.0, 161.6, 158.1, 155.8, 136.3, 134.7, 130.8, 130.45, 130.37, 127.5, 124.3, 120.1, 119.6, 115.8, 115.6, 48.0; LRMS calculated for $C_{20}H_{17}FN_2OS$ $(M+H)^+$ *m/z*: 353.1, measured 353.1.

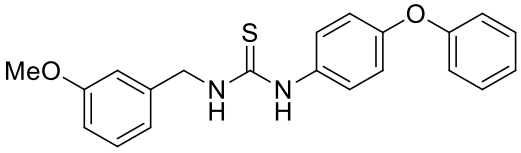

1-(3-methoxybenzyl)-3-(4-phenoxyphenyl)thiourea (**'7501**). Yellow crystals**;** ^{1}H NMR (400 MHz, acetone-d6) δ 8.90 (br s, 1H), 7.50 (br s, 1H), 7.46 – 7.35 (m, 4H), 7.22 (t, J=7.86 Hz, 1H), 7.13 (t, J=7.38 Hz, 1H), 7.03 – 6.92 (m, 6H), 6.81 (dd, J=8.16 Hz, J=1.68 Hz, 1H), 4.86 (d, J=5.68 Hz, 2H), 3.77 (s, 3H); ^{13}C NMR (100 MHz, acetone-d6) δ 183.0, 160.7, 158.1, 155.7, 141.6, 134.7, 130.8, 130.2, 127.5, 124.3, 120.5, 120.0, 119.5, 114.0, 113.2, 55.4, 48.8; LRMS calculated for $C_{21}H_{20}N_2O_2S$ $(M+H)^+$ *m/z*: 365.1, measured 365.1.

RESULTS AND DISCUSSION

‘3981 activates HssRS and is toxic to *S. aureus*

A high-throughput screen (HTS) was performed to identify small molecule activators of *S. aureus* HssRS (47). Compound VU0043981 (‘3981) was identified in this HTS as an activator of *S. aureus* HssRS (Figure 21A, inset). ‘3981 activates HssRS in a dose dependent manner, and this activation is dependent upon the two-component system (Figure 21A). These results demonstrate that ‘3981 is an activator of HssRS leading to activation of *hrtAB* expression in *S. aureus*.

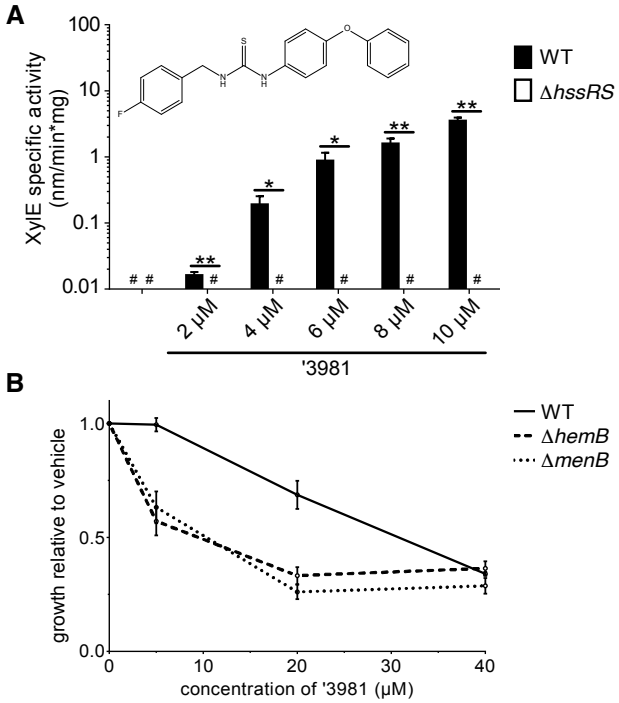

Figure 21. '3981 activates HssRS and is toxic to *S. aureus*.

(A) Compound '3981 was identified in a HTS for activators of HssRS. *S. aureus* WT and Δ*hssRS* harboring p*hrt.xylE* were treated with increasing concentrations of '3981. '3981 activates HssRS in a dose-dependent manner requiring the HssRS two-component system. Inset, structure of '3981. * denotes $p < 0.05$, ** denotes $p < 0.0001$. # denotes data are below the limit of detection. (B) WT, Δ*hemB* and Δ*menB* were treated with increasing concentrations of '3981.

‘3981 inhibits growth of *S. aureus*.

Previously identified small molecule activators of HssRS exhibit toxicity to fermenting *S. aureus*, although the mechanism of toxicity is yet to be determined (47, 49). In order to probe the toxicity of ‘3981 to *S. aureus*, WT and two respiration deficient strains, Δ*hemB* and Δ*menB*, were grown in the presence of increasing concentrations of ‘3981. Δ*hemB* and Δ*menB* strains are deficient in production of heme and menaquinone, respectively, both of which are required for bacterial respiration (113). Therefore these strains must generate energy through fermentation. Compound ‘3981 is toxic to both WT and fermenting *S. aureus* strains (Figure 21B). Taken together, these data suggest that ‘3981 activates HssRS and is toxic to fermenting and respiring *S. aureus*.

‘3981 activates HssRS independent of heme accumulation

Heme is the only identified activator of HssRS (44, 46, 47, 93). To determine if ‘3981 activates HssRS through increasing endogenous heme biosynthesis, heme accumulation was quantified upon exposure to increasing concentrations of ‘3981 in the absence of exogenous heme. Heme accumulation was not observed in ‘3981-treated cells, suggesting that ‘3981 does not trigger HssRS through activation of heme biosynthesis. This is in contrast to ‘882, a previously identified activator of HssRS that induces heme biosynthesis (Figure 22) (47). Therefore, ‘3981 represents a small molecule that activates HssRS independently of heme accumulation, providing a unique tool to interrogate the heme sensing system in *S. aureus*.

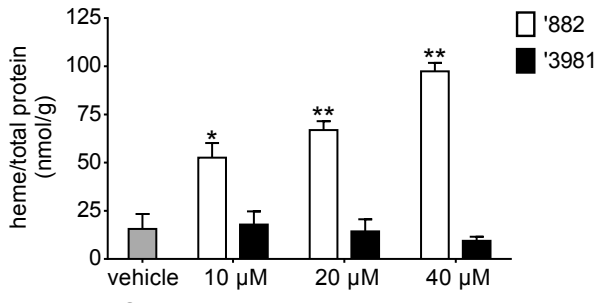

Figure 22. '3981 does not increase endogenous heme biosynthesis.

S. aureus was grown in the presence of '882 and '3981 and the absence of any exogenous heme source. '882 activates heme biosynthesis leading to heme accumulation (47). '3981 does not activate heme biosynthesis, suggesting '3981 activates HssRS through a mechanism distinct from increased heme production. Significance was determined in comparison with vehicle treatment. * denotes $p < 0.05$, ** denotes $p < 0.0001$.

‘3981 activity requires aerobic respiration

Although ‘3981 does not increase heme biosynthesis, heme could be required for ‘3981-mediated activation of HssRS. Heme is utilized for numerous processes within the cell, including as a required cofactor for cytochromes and bacterial nitric oxide synthase (26, 30, 113, 123). To test the requirement for heme biosynthesis in ‘3981-dependent HssRS activation, the activity of ‘3981 was measured in a heme biosynthesis mutant (Δ*hemB)*. Upon treatment of Δ*hemB* with ‘3981, activation of HssRS was not detected (Figure 23A). As heme is required for respiration, the requirement for aerobic respiration to the activity of ‘3981 was interrogated. Respiration can be disrupted through either inactivation of heme biosynthesis, or by growing bacteria in an anaerobic environment in the absence of a terminal electron acceptor. *S. aureus* was treated with either ‘882 or ‘3981 during anaerobic growth. Whereas ‘882 activates HssRS in respiration defective strains, ‘3981 does not (Figure 23B). In order to control for growth differences between strains, a plasmid constitutively expressing *xylE* was included (p*lgt*.*xylE*). Taken together these data suggest that ‘3981 does not activate heme biosynthesis, but its mechanism of action requires aerobic respiration.

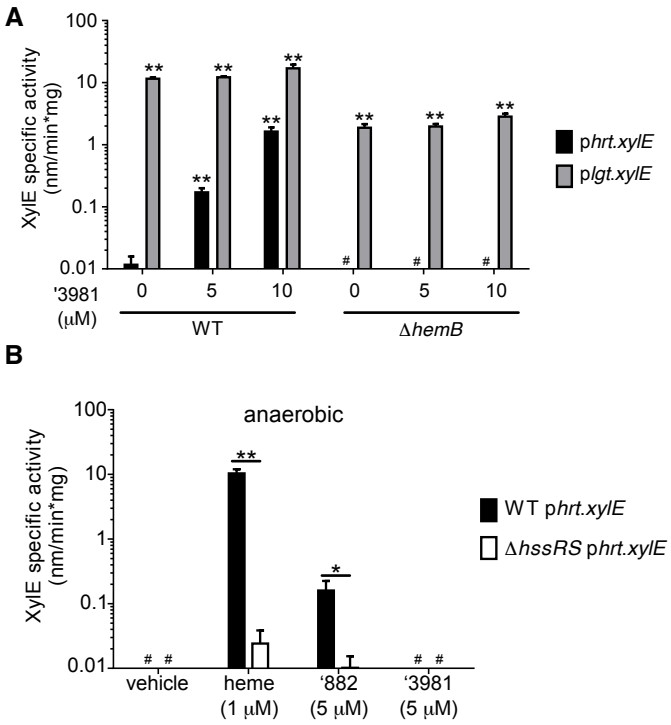

Figure 23. '3981 activity is dependent on aerobic respiration.

(A) To determine the requirement of heme synthesis for HssRS activation, *S. aureus* WT and Δ*hemB* harboring p*hrt.xylE* were treated with increasing concentrations of '3981. Activation of HssRS was not seen in the Δ*hemB* strain. Significance was determined in comparison with vehicle treatment of p*hrt.xylE*. (B) As heme is required for many cellular processes, including respiration, the ability of '3981 to activate HssRS in an anaerobic environment was tested. WT harboring p*hrt.xylE* were treated with heme, '882, or '3981. '3981 activity is dependent upon intact respiration. * denotes $p < 0.05$, ** denotes $p < 0.0001$. # denotes the data are below the limit of detection.

Structure activity relationship studies identify ‘3981 derivatives with increased activity

The general toxicity of ‘3981 towards *S. aureus* hindered its use as a probe of heme sensing. Using this structure as a starting point, a library of derivatives was generated to determine structure-activity relationships (SAR, Table 11) and to identify compounds exhibiting increased HssRS activation (Figure 24A, Figure 25, Figure 26). The 4-biaryl ether system was determined to be required for HssRS activation as replacement with smaller biaryl, aryl or aliphatic groups resulted in loss of activity. The benzylic carbon is also required for activity as replacement the 4-fluorobenzyl with a 4-fluorophenyl group resulted in an inactive compound. Several derivatives were synthesized with various substituents on the benzylamine moiety. Removal of the electron withdrawing 4-fluorine and substitution with an electron rich methyl ether at the 3-position resulted in a compound, VU0047501 (‘7501), with 4x the activity of the parent molecule (Figure 24A, B). In addition to increased HssRS activation, ‘7501 was considerably less toxic than ‘3981 (Figure 24C). Furthermore, ‘7501 retained identical phenotypes to ‘3981 in regards to an inability to induce heme accumulation and a requirement for aerobic respiration (Figure 27). Due to the increased activity and lack of toxicity, ‘7501 was utilized to probe the heme stress response without confounding effects due to the toxicity of the parent molecule.

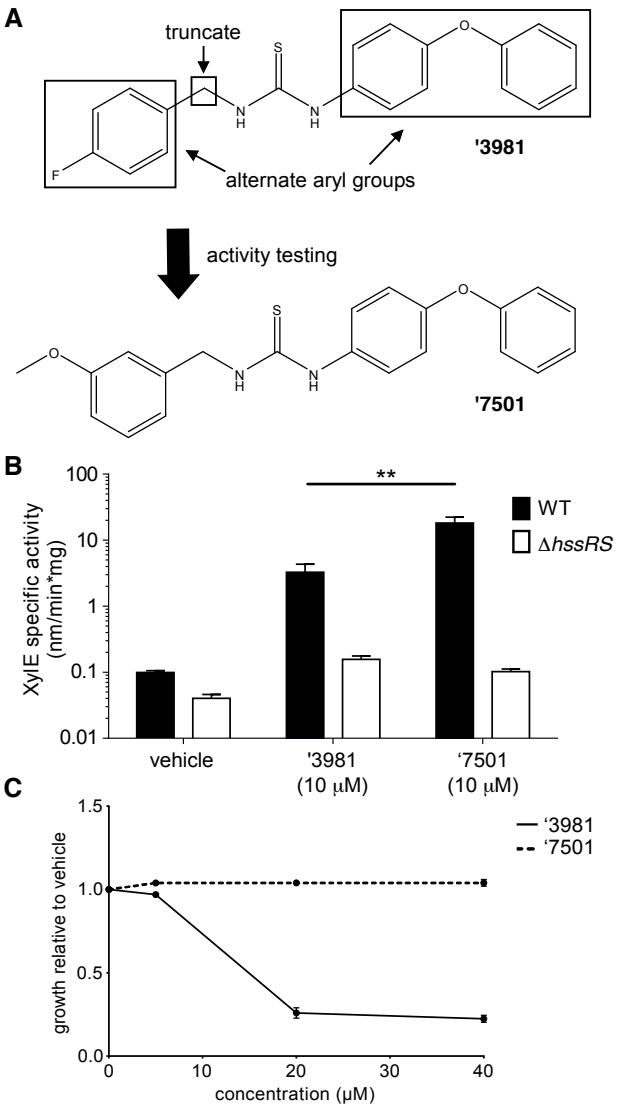

Figure 24. '3981-derivatives were identified with increased HssRS activation and decreased toxicity.
(A) Systematic modification identified important characteristics of '3981, leading to identification of compound '7501 with increased ability to activate HssRS while lacking toxicity of the parent compound. (B) WT harboring p*hrt*-*xylE* were treated with equivalent concentrations of '3981 and '7501. '7501 shows 4-fold increased activity compared to the parent molecule. * denotes $p < 0.05$, ** denotes $p < 0.0001$. (C) Growth inhibition of '3981 and '7501 were determined. Whereas '3981 inhibits growth of WT bacteria, '7501 lacks toxicity.

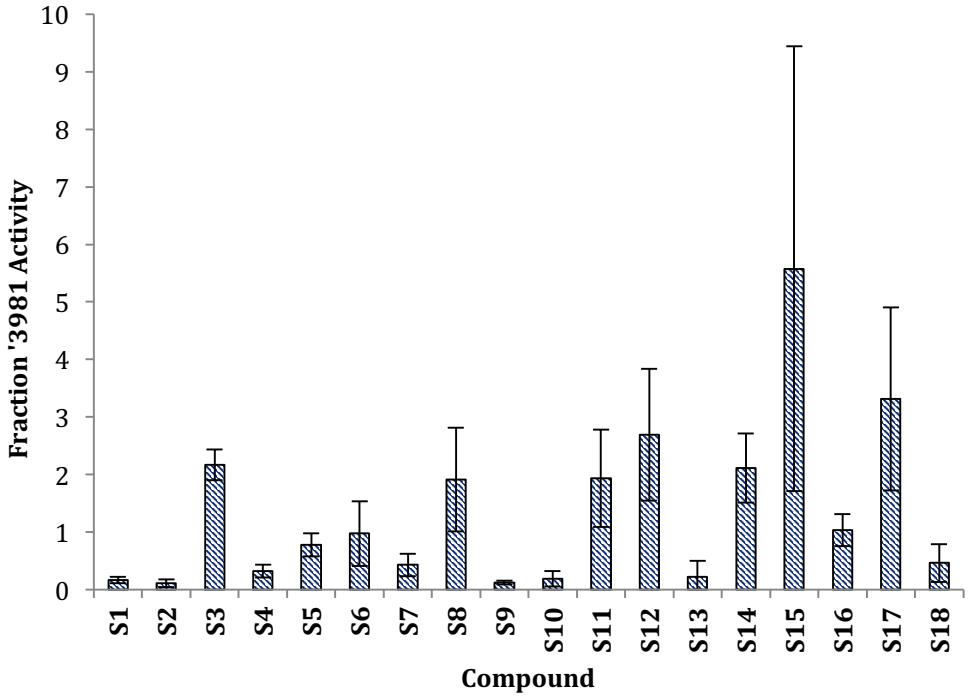

Figure 25. Activation of HssRS by S1 – S18 at 10 µM relative to '3981.

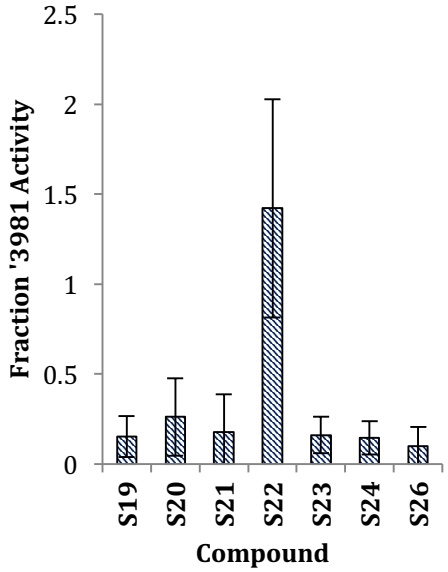

Figure 26. Activation of HssRS by S19 – S26 at 10 µM relative to '3981.
S25 is excluded because data could not be obtained due to toxicity under the assay conditions.

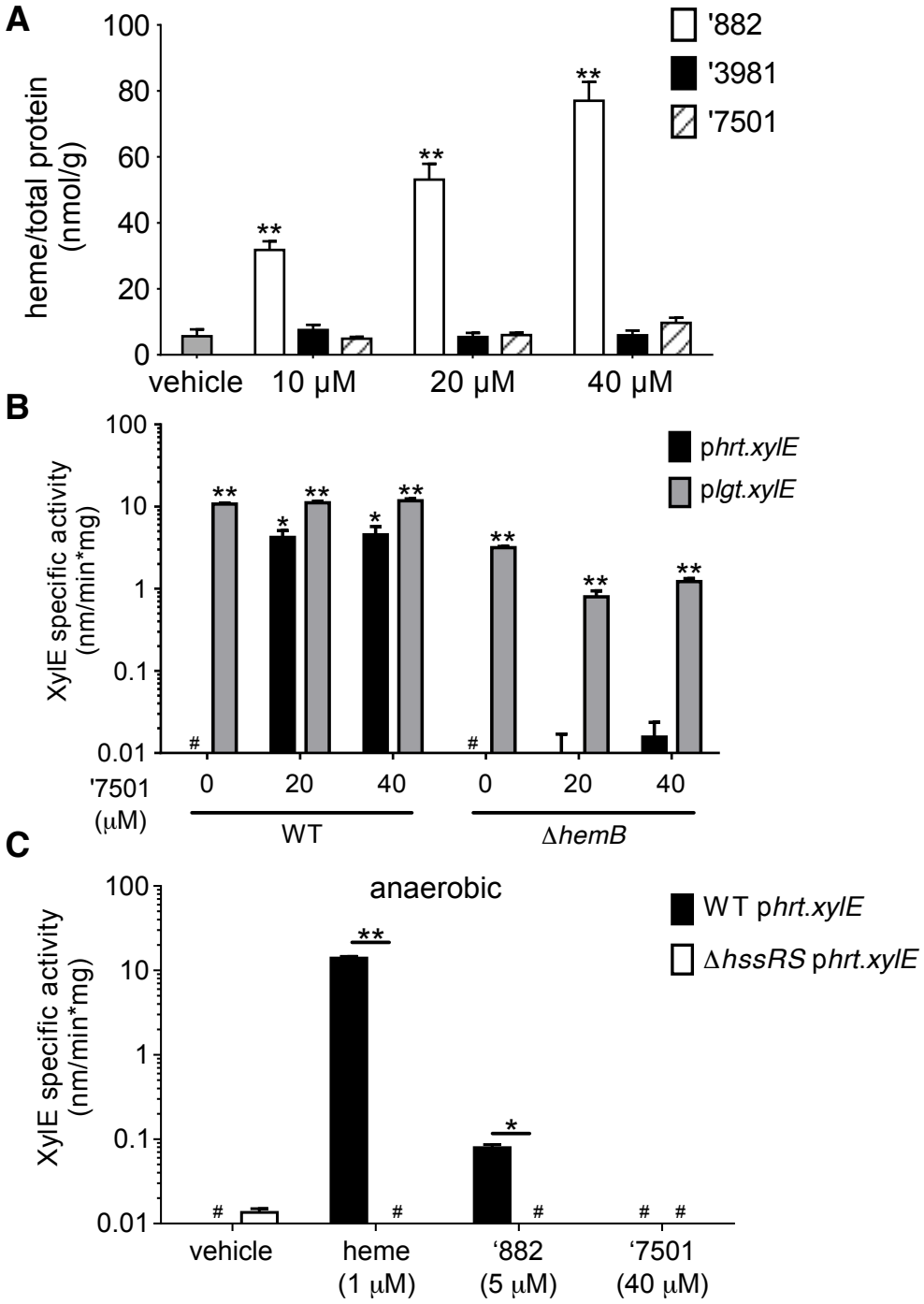

Figure 27. '7501 activity is identical to '3981.

(A) *S. aureus* was grown in the presence of '882, '3981, and '7501 and the absence of any exogenous heme source. While '882 activates heme biosynthesis, neither '3981 nor '7501 activate heme biosynthesis. Significance was determined in comparison with vehicle treatment. (B) *S. aureus* WT and Δ*hemB* harboring p*hrt.xylE* were treated with increasing concentrations of '7501. No activation of HssRS was seen in the Δ*hemB* strain. Significance was determined in comparison with vehicle treatment of p*hrt.xylE*. (C) WT harboring p*hrt.xylE* were treated with heme, '882, or '7501 in an anaerobic environment. '7501 activity is dependent upon intact respiration. * denotes $p < 0.05$, ** denotes $p < 0.0001$.

Table 11. General synthesis for SAR studies around '3981 structure.

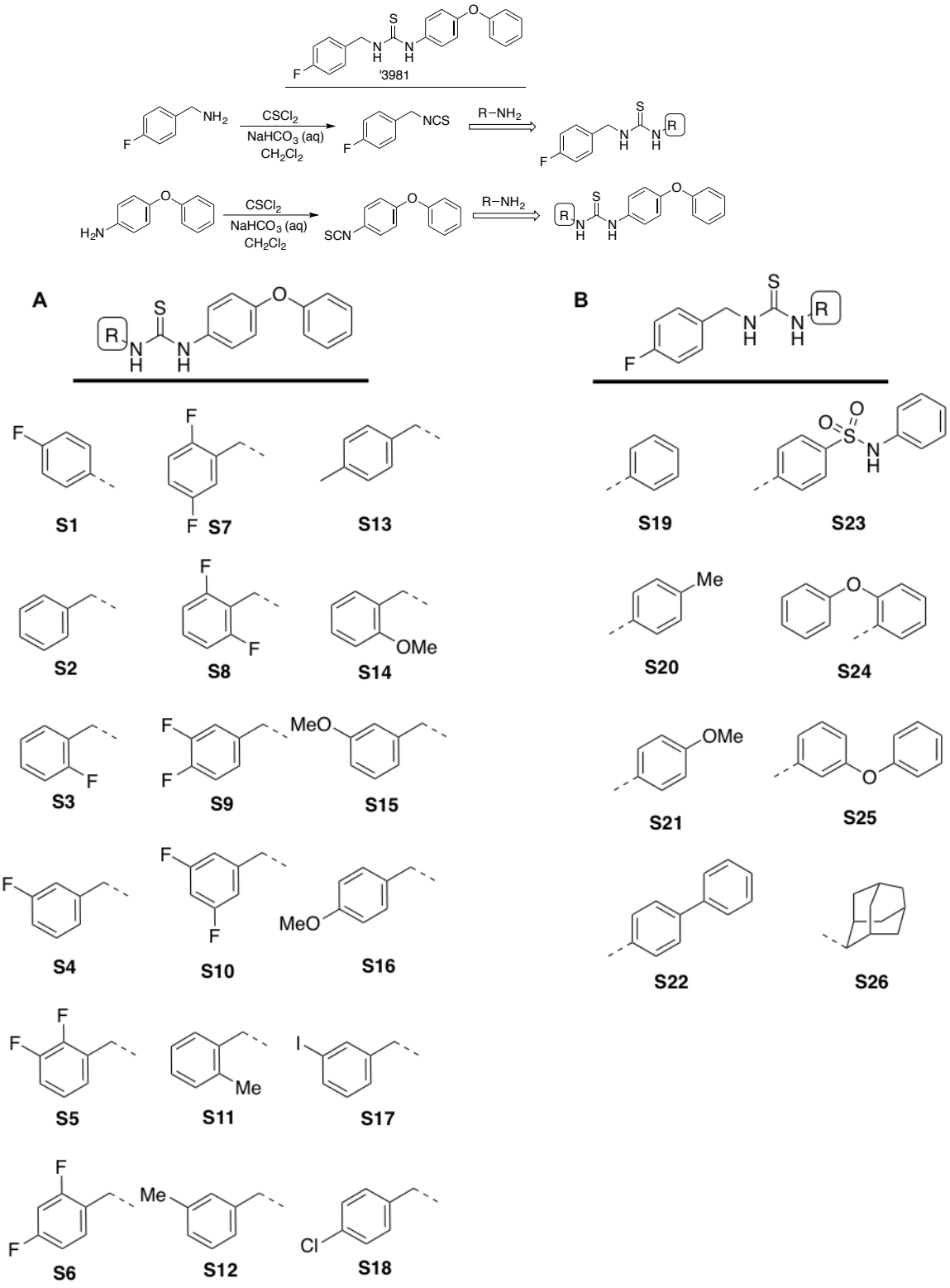

A transposon screen identifies bacterial nitric oxide synthase as required for the heme stress response

‘7501 exhibits increased activation of HssRS relative to ‘3981, therefore the ability of ‘7501 to adapt *S. aureus* to heme toxicity was tested (46, 47). Indeed, ‘7501 adapts *S. aureus* to the toxic effects of heme. This result implies that HssRS activation was sufficient to upregulate HrtAB expression to enable the bacteria to subsequently cope with toxic concentrations of heme (Figure 28A). Using ‘7501-dependent heme adaptation as an assay platform, the Nebraska Transposon Mutant Library, consisting of approximately 2,000 strains of *S. aureus* with single, defined inactivating mutations, was screened to identify genes required for ‘7501 activity. Multiple genes were identified that are required for the ability of ‘7501 to activate the HssRS-HrtAB heme stress response (Table 12). Importantly, a number of these genes, including the gene encoding cytochrome protein Qox, are required for respiration, consistent with data presented in Figure 28 (Table 12). In addition, a number of the identified genes are in the pathway for production of NO directly through inactivation of bNOS, or for enzymes involved in pathways leading to NO formation (Figure 28B). This suggests that NO synthesis and the bacterial heme stress response are linked within *S. aureus*. Heme serves as a cofactor for bNOS implying the possibility of a functional link between these two systems.

To verify that bNOS is required for the ability of *S. aureus* to adapt to heme stress, the *nos::*ermC mutation was transduced into *S. aureus* strain Newman (Δ*nos*). As expected, interruption of *bNOS* led to decreased resistance to heme toxicity (Figure 29). Furthermore, this decreased resistance of Δ*nos* to heme can be restored by providing a

full length copy of *nos in trans* (Figure 29). Taken together, these results demonstrate that bNOS is required for adaptation to heme toxicity.

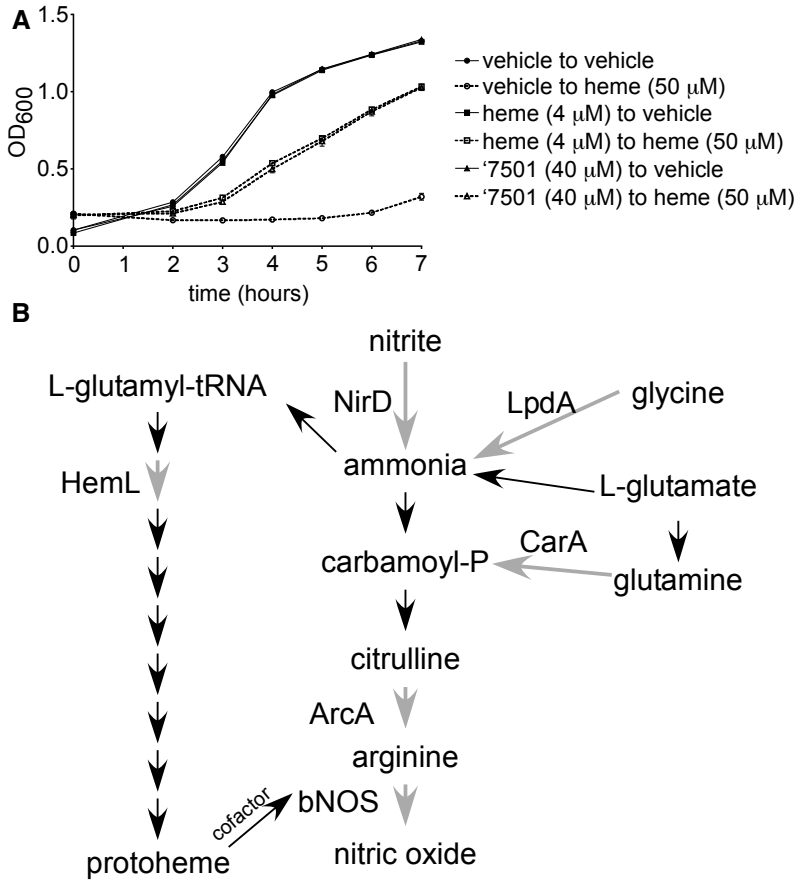

Figure 28. An adaptation screen uncovers the importance of nitric oxide to the heme stress response. (A) *S. aureus* strain USA300 JE2 was pretreated with '7501 followed by exposure to toxic concentrations of heme. '7501 adapts *S. aureus* to heme toxicity. (B) The Nebraska Transposon Mutant Library was screened to identify strains that could not be adapted to heme toxicity using '7501. Many strains disrupted in genes encoding nitric oxide synthesis proteins were identified (gray, bold).

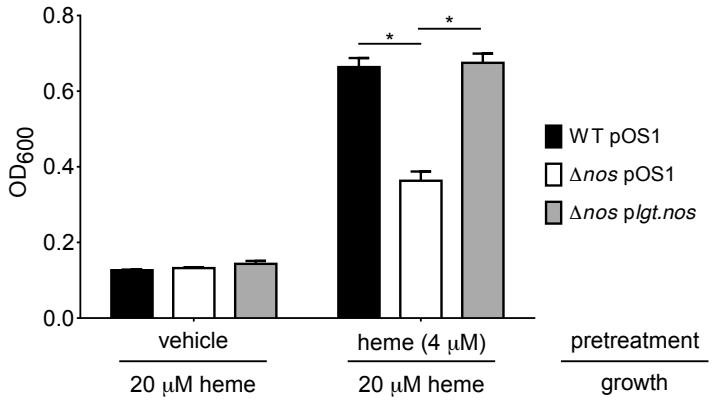

Figure 29. Bacterial nitric oxide synthase is required for adaptation to heme toxicity.

S. aureus WT harboring pOS1.P*lgt*, Δ*nos* harboring pOS1.P*lgt*, and Δ*nos* harboring p*lgt.nos* were pretreated with heme followed by exposure to toxic concentrations of heme. WT is adapted to the toxic effects of heme, whereas Δ*nos* is significantly impaired when treated with toxic concentrations of heme. This phenotype is complemented by addition of *nos* expressed *in trans*. Data shown are a representative sample. * denotes $p < 0.05$.

Table 12. Genes identified in '7501-induced adaptation to heme toxicity.

Accession Number	Gene name	Gene description
SAUSA300_0505	*pdxT*	glutamine amidotransferase subunit PdxT
SAUSA300_0191	*ptsG*	PTS system, glucose-specific IIBC component domain protein
SAUSA300_0561	-	hypothetical protein
SAUSA300_1271	-	hydrolase-like protein
SAUSA300_0616		putative Na+/H+ antiporter, MnhG component
SAUSA300_2371	*bioB*	biotin synthase
SAUSA300_1458		glyoxalase family protein
SAUSA300_0996	*lpdA*	dihydrolipoamide dehydrogenase
SAUSA300_1089	*lspA*	lipoprotein signal peptidase
SAUSA300_0759	*gpmI*	phosphoglyceromutase
SAUSA300_0539	*ilvE*	branched-chain amino acid aminotransferase
SAUSA300_0272		conserved hypothetical protein
SAUSA300_1095	*carA*	carbamoyl phosphate synthase small subunit
SAUSA300_0633	*fhuA*	ferrichrome transport ATP-binding protein fhuA
SAUSA300_2438	*sarU*	staphylococcal accessory regulator U
SAUSA300_2395	-	amino acid permease
SAUSA300_0980	-	hypothetical protein
SAUSA300_1614	*hemL*	glutamate-1-semialdehyde-2,1-aminomutase
SAUSA300_0305	-	formate/nitrite transporter family protein
SAUSA300_1684	-	hypothetical protein
SAUSA300_0545	-	hypothetical protein
SAUSA300_0559		putative substrate--CoA ligase
SAUSA300_2025	*rsbU*	sigma-B regulation protein
SAUSA300_1428	-	hypothetical protein
SAUSA300_0597	-	putative endonuclease III
SAUSA300_0847		conserved hypothetical protein
SAUSA300_1948	-	phi77 ORF069-like protein
SAUSA300_1148	*codY*	transcriptional repressor CodY
SAUSA300_2309	*hssS*	sensor histidine kinase (HssS)
SAUSA300_1169	*ftsK*	DNA translocase FtsK
SAUSA300_2219	*moaA*	molybdenum cofactor biosynthesis protein A

SAUSA300_1792	-	hypothetical protein
SAUSA300_0945	-	isochorismate synthase family protein
SAUSA300_2033	*kdpB*	K+-transporting ATPase, B subunit
SAUSA300_1842		transcriptional regulator, Fur family
SAUSA300_0918	-	diacylglycerol glucosyltransferase
SAUSA300_1003		conserved hypothetical protein
SAUSA300_2353		conserved hypothetical protein
SAUSA300_0963	*qoxA*	quinol oxidase, subunit II
SAUSA300_1867		conserved hypothetical protein
SAUSA300_0384	-	hypothetical protein
SAUSA300_1185	*miaB*	(dimethylallyl)adenosine tRNA methylthiotransferase
SAUSA300_1628	*lysP*	lysine-specific permease
SAUSA300_1895	*NOS*	nitric oxide synthase oxygenase
SAUSA300_2540		fructose-bisphosphate aldolase class-I
SAUSA300_1558	*mtnN*	5'-methylthioadenosine/S-adenosylhomocysteine nucleosidase
SAUSA300_2291	*gltS*	sodium/glutamate symporter
SAUSA300_0924	-	sodium transport family protein
SAUSA300_0958	-	hypothetical protein
SAUSA300_2312	*mqo*	malate:quinone oxidoreductase
SAUSA300_1182	-	pyruvate ferredoxin oxidoreductase, alpha subunit
SAUSA300_1866	*vraS*	two-component sensor histidine kinase
SAUSA300_1865	*vraR*	DNA-binding response regulator
SAUSA300_1544	*lepA*	GTP-binding protein LepA
SAUSA300_2345	*nirD*	nitrite reductase [NAD(P)H], small subunit
SAUSA300_2542	-	putative AMP-binding enzyme
SAUSA300_1092	*pyrP*	uracil permease
SAUSA300_0694		putative membrane protein
SAUSA300_1648		putative NADP-dependent malic enzyme

bNOS contributes to heme sensing and detoxification independent of *hrtAB*

The mechanism by which bNOS protects *S. aureus* from heme toxicity could be due to activation of HssRS or general protection from heme toxicity through an HssRS-independent mechanism. To determine if bNOS contributes to heme sensing through HssRS, WT and Δ*nos* were treated with either vehicle, heme, or '7501 and the response of the *hrt* reporter was measured as described above. Interestingly, Δ*nos* exhibits a significant decrease in activation of the *hrt* promoter; however, the magnitude of this change does not fully account for the differences in response to heme (Figure 30A). Based on these observations, we hypothesized that in addition to an involvement in sensing heme toxicity, bNOS is involved in resisting heme toxicity in a mechanism distinct from HssRS activity. To test this hypothesis, an *hrtB/bNOS* double mutant was constructed to determine if this strain is more sensitive to heme toxicity than inactivation of *hrtB* alone. A strain lacking the heme efflux system (Δ*hrtB*) is more resistant to heme toxicity than an *hrtB/bNOS* double mutant, implicating bNOS in protecting *S. aureus* from heme toxicity independently of *hrtB* (Figure 30B). Taken together, these data suggest that bNOS both affects sensing of heme by HssRS and protects *S. aureus* from heme toxicity through a mechanism distinct from the actions of HssRS and HrtAB.

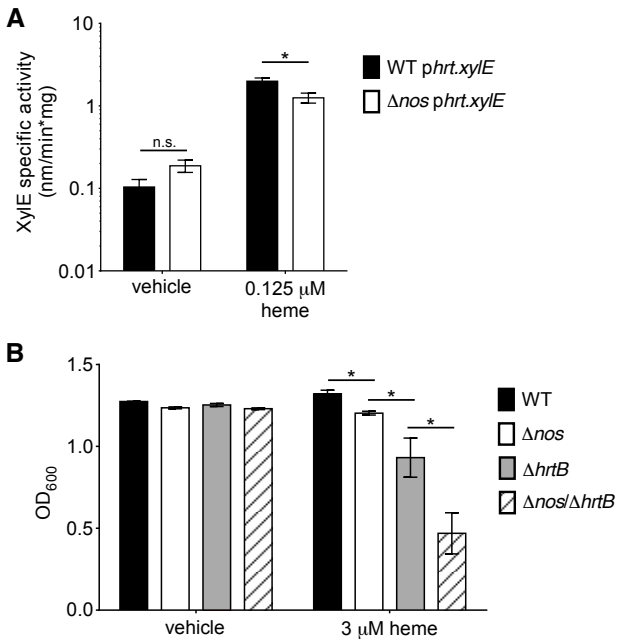

Figure 30. Bacterial nitric oxide synthase affects heme sensing and protects *S. aureus* from heme toxicity independently of *hrtAB*.

(A) To determine if bNOS contributes to heme sensing, *S. aureus* WT and Δ*bnos* harboring p*hrt.xylE* were treated with heme. The Δ*bnos* strain shows a significant decrease in the ability to sense heme, suggesting bNOS plays a role in heme sensing in *S. aureus*. (B) To determine if bNOS contributes to protection from heme toxicity independent of HssRS/HrtAB, strains WT, Δ*bnos,* Δ*hrtB,* Δ*bnos*/Δ*hrtB* were grown in the presence of low concentrations of heme. Strain Δ*bnos*/Δ*hrtB* has a significant growth defect compared to Δ*hrtB* suggesting bNOS contributes to the protection from heme toxicity independent of HssRS/HrtAB. * denotes $p < 0.05$, ** denotes $p < 0.0001$.

CONCLUSIONS

Maintaining correct heme homeostasis is crucial for the survival of bacterial pathogens within the host (46, 131). Heme is a required molecule for many processes within the cell; however, it is also toxic to the organism. This concept has been termed the "heme paradox" (131). Therefore, being able to sense and respond to increased heme levels is vital for organisms to survive in the diverse environments experienced within the host. Understanding the mechanisms by which these bacterial pathogens sense and respond to heme stress has the potential to uncover novel targets for therapeutic development, as altering the ability of *S. aureus* to sense heme affects virulence of this organism (46).

Understanding the specific requirements of two-component system activation remains a challenge (40). In order to further our understanding of the heme stress response and the mechanisms of HssRS activation, this work utilized a small molecule activator of the heme sensing system. Previously identified small molecule activators of HssRS have multiple activities within the cell, and have provided a more thorough understanding of the mechanisms behind heme homeostasis within the bacterial cell (47, 49). Consistent with this, here we report that '3981 is both toxic to *S. aureus* and activates HssRS in a respiration-dependent manner (Figure 21 and Figure 23). Structure activity relationship studies have separated these activities (Figure 24), thereby providing '3981-derivatives that lack toxicity, and thus enhancing the ability of this scaffold to interrogate the heme stress response.

Heme is the canonical activator of HssS in *S. aureus* (44, 46, 47). Small molecule activators provide an opportunity to interrogate two-component system activation. Importantly, ‘3981 does not induce heme accumulation within *S. aureus* (Figure 22). These data support the possibility that there may be multiple ligands required for HssS activation. Activation by multiple ligands is not unprecedented. In *Mycobacterium tuberculosis*, DosS and DosT are histidine kinases that sense heme and their activity is modulated by other ligands, including CO, NO, and O_2 (132). This leads to the exciting hypothesis that perhaps HssS senses heme in complex with another intracellular molecule to modulate the response to heme stress.

Previous work has shown the importance of bNOS in survival in the host, as well as resistance to various antibiotics and oxidative stress (123). The importance of endogenous nitric oxide production has been demonstrated in numerous organisms, including the pathogens *S. aureus* and *B. anthracis* (123). Taken together, bNOS has been proposed as a viable antibacterial target (125). Consistent with this, utilizing ‘3981 has identified another role for bNOS in *S. aureus*, specifically in resistance to heme stress. Although bNOS contributes slightly to heme sensing, it plays a crucial role in resisting heme stress independently of the HssRS-HrtAB heme stress response (Figure 30). Heme induces significant oxidative stress in *S. aureus* (127). It is likely that bNOS protects *S. aureus* from the oxidative stress imposed by heme, as bNOS protects bacteria from oxidative stress. Targeting bNOS for antibiotic development has the potential to affect a number of systems within the bacteria, and therefore significantly impact virulence of this pathogen.

Overall, this work has provided a unique look into the heme stress response in *S. aureus*. SAR separated two phenotypes induced by ‘3981, ultimately providing probes with significantly increased ability to activate the bacterial heme stress response. In addition, these probes activate the heme sensing system independently of heme accumulation, suggesting that heme may not be the only molecule required for HssRS activation. Finally, these probes have identified bNOS as required for the heme stress response, uncovering another important role of nitric oxide synthesis in bacterial pathogens and highlighting bNOS as a target for antibacterial development.

CHAPTER V. SUMMARY AND SIGNIFICANCE

S. aureus is a major human pathogen that causes significant morbidity and mortality worldwide (2-4, 91). Furthermore, the levels of antibiotic resistance in bacterial pathogens is increasing. It is estimated that if the antimicrobial resistance problem is not tackled, it will result in over $100 trillion in losses by 2050, and cause over 10 million deaths annually (133). Understanding the pathogenesis of bacterial pathogens is vital to our continued treatment of infectious agents. The work presented in Chapters II through IV deepen our understanding of various aspects of bacterial survival and treatment in the host.

UNDERSTANDING HEME SENSING AND DETOXIFICATION IN *S. AUREUS*

Understanding mechanisms by which bacteria respond to their environment is crucial for understanding bacterial physiology and will aid in the identification of potential therapeutic targets. During infection of the host, bacteria experience to a large array of stressors. Two-component systems are a major mechanism by which bacteria sense and respond to their environment (38-41). Specifically, bacteria require proper heme homeostasis to survive and cause disease. Although required, heme is also toxic to the bacteria. *S. aureus* encodes the heme sensing system (HssRS) in order to sense and respond to heme toxicity within the host. The specific mechanisms by which heme is sensed and whether it physically interacts with HssS remains unknown.

New tools are needed to interrogate two-component system signaling (38, 80, 90). Many of the current methods require a directed approach to select residues to mutate to

determine their effect on two-component system function. Chapter II describes the development of a suicide strain to interrogate two-component systems. The unbiased selection strategy was applied to the *S. aureus* HssRS two-component system. Preliminary results have identified numerous mutations that decrease HssRS function. These data suggest that endogenous and exogenous heme are sensed through a similar mechanism. Upon saturation of this system, a stronger understanding of the residues required for HssRS and P_{hrt} function will be gained. The success of the suicide strain strategy suggests it can be used to interrogate additional two-component systems, which will further our understanding of the mechanisms by which numerous pathogens sense and respond to their environment. Finally, the suicide strain can be utilized to identify small molecule targets in bacterial pathogens, the topic of Chapter III.

Chapter IV utilized a second activator of HssRS to further interrogate the mechanisms of heme sensing and detoxification. Importantly, SAR studies on molecule '3981 was able to separate two phenotypes induced by the parent molecule: HssRS activation and toxicity. Based upon these data, a non-toxic and more potent HssRS activator, '7501, was synthesized. Using a genetic screen, a role for bNOS was identified in resisting heme toxicity. Nitric oxide synthesis contributes to HssRS activation, as well as detoxification through a mechanism independent of HssRS and HrtAB. Heme toxicity is induced in bacterial cells through production of significant oxidative stress (127). bNOS has been previously reported to increase resistance to oxidative stress (125, 134). In keeping with this, it is possible that bNOS protects *S. aureus* from heme toxicity through increasing resistance to oxidative stress. Alternatively, bNOS requires heme as a cofactor and could serve as a heme sink within bacterial cells, thereby reducing free heme

in the cell that contributes to toxicity (30, 134, 135). Consistent with the work presented in Chapter IV, there are likely many mechanisms in place for *S. aureus* and other pathogens to resist heme toxicity. As heme sensing and detoxification systems are conserved across numerous pathogens, the data presented in Chapters II and IV have furthered our understanding of the mechanisms by which bacteria sense and respond to heme.

DEVELOPING PROBES TARGETING HEME BIOSYNTHESIS

Heme biosynthesis occurs in organisms from all kingdoms of life. Recently, it was discovered that Gram-positive bacteria utilize a noncanonical pathway to synthesize this essential cofactor, stimulating interest in development of therapeutics targeting heme biosynthesis to treat bacterial infections. In addition, regulation of this pathway is not well understood, highlighting the need for validated probes to interrogate heme biosynthesis. Previously small molecule activators of HssRS were identified in order to interrogate heme homeostasis in *S. aureus*. Small molecule '882 increases endogenous heme biosynthesis, although the mechanism by which '882 functions remained unknown (47, 49). Chapter III describes the use of a P_{hrt} driven suicide strain as a strategy to identify the target of '882. Analysis of suppressor mutants resistant to '882, in combination with follow-up studies, identified that '882 activates HemY, a coproporphyrinogen oxidase specific to Gram-positive bacteria.

Small molecule activators are rare, with only a handful identified to date (116). Many groups focus efforts on enzyme inhibition through binding of and inhibiting the active site of the enzyme. Active sites are often conserved across classes of enzymes and

well characterized, aiding in the process of targeting these sites. Enzyme activation occurs through a different mechanism, one of the most common of which is through small molecule-binding to an allosteric site (116). In keeping with this, enzymes that contain allosteric sites may have evolved such a site for natural regulation of the enzyme (116). Therefore, identification of small molecule activators provides imporant insight into enzyme regulation. With regards to heme biosynthesis, the regulation of the pathway remains largely unknown (21, 136, 137). Taken together, insights gained utilizing ‘882 will aid in elucidating regulation of heme biosynthesis in Gram-positive bacteria.

Small molecule activators also have numerous properties that make them ideal therapeutics (116). As described above, allosteric sites are less well conserved across classes of enzymes than is the conservation of active sites, thus limiting off-target effects of small molecule activators that bind allosteric sites. In addition, inhibitors often require the ability to inhibit an enzyme by 90% to induce a strong phenotype (116). In contrast, small molecule activators can induce significant phenotypes with small modulations in enzyme activity, suggesting that SAR studies that leads to synthesis of derivatives with small increases in activity may lead to dramatic increases in therapeutic effects (116). An example of the success of enzyme activation in therapeutics can be seen in glucokinase activators, which are now used in clinics to treat diabetes (116, 117).

PDT involves the use of a photosensitizer in the presence of light to induce cell death (16). As a therapeutic strategy, PDT has been successful in the treatment of numerous diseases. To date, the application of PDT has been limited against bacterial infections as the only FDA approved therapy consists of ALA, an early precursor in heme biosynthesis. With the identification of the noncanonical heme biosynthesis pathway

utilized by Gram-positive bacteria, targeting bacterial heme biosynthesis in combination with light is a promising strategy. ‘882 specifically activates HemY from Gram-positive bacteria, and does not activate HemY from *H. sapiens*. The product of HemY from Gram-positive bacteria is CPIII, a well characterized photosensitizer (16, 61, 100). Chapter III describes the successful application of ‘882-PDT against Gram-positive bacteria *in vitro* and *in vivo*. Taken together, the identification of ‘882 as a small molecule activator of HemY will allow for further interrogation of the regulation of heme biosynthesis, as well as providing proof-of-concept that HemY activation in combination with light is a viable therapeutic strategy to treat infectious diseases.

CHAPTER VI. FUTURE DIRECTIONS

To continue the battle against bacterial pathogens, a more complete understanding of bacterial physiology is necessary to identify novel therapeutic targets. The work presented in Chapters II-IV provide a more in depth understanding of various aspects of bacterial physiology, disease, and treatment. Nonetheless, a number of questions remain to be addressed.

UNDERSTANDING MECHANISMS OF HEME RESISTANCE: INTERROGATE THE STRUCTURE AND FUNCTION OF HSSRS.

Chapter II describes the development and verification of a suicide strain selection strategy as a method to interrogate two-component system structure and function. The use of the suicide strain has led to the identification of numerous residues required for HssRS and P_{hrt} function, although future work remains to obtain a full understanding of heme resistance in *S. aureus*.

Saturate the suicide strain selection.

Although a number of residues have been identified, the work presented in Chapter II is not a complete list of residues required for HssRS activation. Continued efforts should be focused on further selection until adequate coverage has been obtained, ideally when no new residues are being identified in the selections. Upon completion, there will be many opportunities to further the understanding of the mechanism of heme sensing in *S. aureus*.

First, mutations in HssRS should be interrogated to determine their effects on protein expression through immunoblots as described in Chapter II. Those mutations that do not affect expression should be further interrogated to determine potential effects on autophosphorylation, phosphotransfer from HssS to HssR, or DNA-binding of HssR to P_{hrt}. Methods for interrogating mutations in these systems have been previously described (44, 93). Mutations in P_{hrt} should be interrogated to determine their effect on HssR binding. Completion of these studies will classify the mutations as described in Figure 8. Furthermore, since exogenous and endogenous heme are utilized in the suicide strain selections, insight into the mechanism by which these two heme sinks are sensed can be interrogated. Once the selections are completed, it is possible that the same residues will be identified with both ligands, suggesting that the two heme sinks are sensed through a similar mechanism. Interrogation of mutations specific to each should be performed to determine specific requirements of sensing each heme source.

Overall, identifying these residues aids in the understanding of two-component system signaling. First, identifying residues required for function provides an insight into the impact of each domain in HssRS function. The number of mutations identified in each domain will provide an understanding of the sensitivity of each domain to modulations in structure. For instance, current data suggests that mutations in membrane spanning domains of the histidine kinase are not required for function, as no mutations have been identified in these regions. In addition, identifying mutations in an unbiased manner allows for a functional analysis of each domain, allowing for further characterization of known domains. Finally, specificity of two-component signaling is not fully understood (41). Sequence analysis has shown that two-component systems

share high sequence homology, however, specificity for their cognate partners is retained. Identifying residues required for interaction of the histidine kinase and the response regulator can be further interrogated for their importance in providing specificity in the signaling pathway. Taken together, using an unbiased selection strategy provides a tool to interrogate two-component system function.

Obtain a crystal structure of HssR and HssS.

In addition to identifying residues, understanding the structural impact of these mutations is important to dissect two-component system structure and function. Therefore, HssS and HssR should be crystalized. Mapping mutations identified in the suicide strain selection will give a more complete understanding of their structural impact, combined with the functional impacts described in Section 1a. The completion of these studies will allow for a relationship between structural domains and their functional impact on HssRS activity.

Apply suicide strain strategy to other two-component systems.

The successful application of a suicide strain to HssRS signaling suggests this method can be adapted to study other two-component systems. *S. aureus* has sixteen two-component systems that should be interrogated through use of a suicide strain. As discussed in Chapter II, the mechanisms of signaling in these systems remains to be elucidated. Therefore, applying a suicide strain selection strategy to each two-component system has the potential to significantly increase our understanding of multiple signaling networks in *S. aureus*.

The use of a suicide strain is not limited to *S. aureus*. Many bacterial pathogens encode heme sensing two-component system (44, 46, 81, 93, 131, 138). A suicide selection strategy should be applied to each of these organisms. For example, *B. anthracis*, also encodes *hssRS*/*hrtAB* that shares high similarity with *S. aureus hssRS/hrtAB*. Comparing the structural and functional effects of mutations in HssRS in these two organisms will identify conserved determinants of heme sensing. Furthermore, utilizing a less similar heme sensing system, one can identify shared features required or specific to two-component systems from more diverse organisms. Taken together, the completion of these studies will provide insights into heme sensing by two-component systems across numerous medically relevant pathogens.

Dissect two-component system specificity.

The suicide selection should be adapted to dissect specificity of two-component system signaling as well. Two-component systems that sense diverse stimuli often share high sequence similarity. Numerous studies have attempted to understand how signaling specificity is conserved (41, 81, 139). In addition, there are many examples of cross-talk and cross-regulation among multiple two-component systems in which a histidine kinase or response regulator interacts with a component from a separate two-component system (38, 40, 41, 81). The suicide strain should be adapted to study cross-talk and cross-regulation. As an example, *B. anthracis* encodes a two-component system, HitRS, that exhibits cross-regulation with HssRS (81). Specific activators of both histidine kinases have been identified (81). Application of a P_{hrt} driven suicide strain using a specific activator of HitRS will identify residues required for HitRS-HssRS interactions.

Similarly, application of a P_{hit} driven suicide strain with an activator of HssRS will identify residues required for cross-regulation from HitRS to HssRS. Taken together, this work will identify features that provide specificity for two-component system interactions, and provide a stronger understanding of the mechanisms of cross-talk and cross-regulation.

Identify the ligands of two-component systems.

Identifying ligands of two-component systems remains a significant challenge (40). Heme is the canonical activator of HssS, however, a direct interaction has not been shown (44, 46, 135). Therefore, efforts should focus on identifying the ligand for HssS, and determine whether heme directly activates HssS. Previous methods to interrogate ligand-histidine kinase interactions should be performed, such as reconstitution of the recombinant HssS in liposomes and utilization of membrane vesicles from strains overexpressing HssS (42, 83). Autophosphorylation of HssS can be monitored in the presence of potential ligands to determine their effect on HssS. Heme should be utilized to determine if heme directly activates HssS. As described in Chapter IV, DosST from *M. tuberculosis* binds heme in combination with nitric oxide or carbon monoxide (132). Consistent with conclusions from Chapter IV, it is possible that nitric oxide may bind HssS as well. Therefore, nitric oxide and nitric oxide in combination with heme should be interrogated to determine their impact on HssS activation.

Finally, the suicide strain strategy should be utilized to identify additional genetic requirements of HssS activation. Utilizing the P_{hrt} driven suicide strain, heme resistant isolates should be identified that lack mutations in *hssRS*/P_{hrt}, as was performed with ‘882

in Chapter III. This will identify genetic elements required for heme-induced HssS activation. Pathway analysis of the mutations identified will provide insight into potential ligands of HssS. Molecules identified in this analysis should then be tested in the liposome and membrane vesicle phosphorylation experiments described above.

Determine mechanism of ‘3981-induced HssRS activation.

The canonical mechanism by which *S. aureus* alleviates heme toxicity is through activation of HssRS to increase *hrtAB* expression (44, 46). The work described in Chapter IV has identified bacterial nitric oxide production as a second mechanism of heme resistance, which contributes to heme sensing as well as detoxification. Further studies should investigate the mechanisms of ‘3981-induced adaptation to heme toxicity.

Identify the subcellular target of ‘3981

In order to obtain a full understanding of ‘3981-induced HssRS activation, the subcellular target of ‘3981 should be identified. Preliminary SAR studies presented in Chapter IV begin to determine molecular features required for ‘3981-induced HssRS activation. A series of SAR studies described in Chapter IV are ongoing and have identified structural elements necessary for ‘3981-induced activity. A subset of ‘3981 derivatives are shown in Table 11. Based upon these data and future SAR studies, biochemical and photoactive linkers should be attached to locations that do not affect ‘3981 activity, thereby creating live probes that bind the target(s) of ‘3981. Dead probes should also be synthesized that contain molecular features that inhibit the ability of ‘3981 to activate HssRS. Using bacterial cell lysates, a series of pull down experiments should

be performed. Proteins identified with the live probe that are not present in the dead probe experiments should be identified as potential targets. This approach should isolate targets that physically interact with ‘3981-derived probes. Confirmatory experiments should prioritize proteins with the highest abundance in the pull down experiments. The potential interaction with ‘3981-derived probes should be interrogated through a series of genetic and biochemical approaches that should be selected based upon the proteins identified.

Preliminary studies have tested ‘3981 in the *hrtAB::relE* strain to identify mutations providing resistance to ‘3981. Interestingly, ‘3981 did not induce growth arrest, suggesting the potency of ‘3981 is insufficient to induce sufficient *relE* expression to halt growth of the bacteria. Future studies should attempt to modify the suicide strain to induce increased levels of toxicity. For example, more copies of *relE* could be incorporated, or multiple different toxins could be incorporated into a single strain. ‘3981 should be tested using the new suicide strain to identify strains resistant to ‘3981 that lack mutations in HssRS/P_{hrt} (47). Taken together the completion of these studies will provide a characterization of binding partners of ‘3981, and mechanisms of resistance to ‘3981-induced HssRS activation. Furthermore, the analysis of these data will provide the foundation for identifying the target of ‘3981.

Determine the mechanism by which bNOS alters heme detoxification.

The results presented in Chapter IV suggest that bacterial nitric oxide is important in heme sensing by HssRS, as well as detoxification through a mechanism distinct from HssRS/HrtAB. To interrogate the role of nitric oxide in HssRS activation, future studies should interrogate the possibility of nitric oxide, or a nitric oxide-heme complex in binding HssS. In addition, future studies should determine the mechanism by which bNOS contributes to resisting heme stress independent of HssRS/HrtAB. Previously it has been shown that bNOS provides resistance to oxidative stress (122, 125, 134, 140). Consistent with this, the primary mechanism by which heme induces toxicity in *S. aureus* is through the production of oxidative stress (127). Therefore, future studies should address the hypothesis that bNOS protects *S. aureus* from the oxidative stress induced by heme. Alternatively, bNOS may protect *S. aureus* from heme induced toxicity through other mechanisms. bNOS utilizes heme as a cofactor (134). Future studies should interrogate whether bNOS can serve as a heme sink within the cell, thereby decreasing free heme and therefore reducing heme-induced toxicity. Taken together, completion of these studies will provide the mechanism by which bNOS affects heme sensing and detoxification.

DEVELOPMENT OF PROBES AND LIGHT-BASED THERAPEUTICS TARGETING HEME BIOSYNTHESIS

DEVELOP HEMY ACTIVATORS BASED UPON THE '882-SCAFFOLD.

Chapter III describes the identification of HemY as the target of '882. '882 represents a probe for interrogation of heme biosynthesis as well as a potential therapeutic.

Advance SAR studies around '882.

SAR studies presented in previous work and Chapter III have defined features of '882 that are required for activity (49). Based upon these SAR data, a new series of compounds should be developed to further characterize '882-induced HemY activation. These derivatives should be tested in the HemY activity assay for *in vitro* activity and the XylE activity assay for *in vivo* activity, as shown in Table 8.

Determine the mechanism of '882-induced activation of HemY.

'882 has been shown to directly interact with and activate HemY from Gram-positive bacteria. A functional domain has been identified that is required for '882-induced activation, however, whether '882 directly binds to the identified fictional domain remains unknown. To date, many attempts have been made to obtain a crystal structure of '882 bound to HemY. The *S. aureus* HemY-'882 complex has not crystalized, and the structures obtained from *B. subtilis* HemY have a set of flexible loops adjacent to the functional domain identified in Chapter III, preventing the successful determination of the '882-HemY structure. Importantly, previously published structures

of HemY are also incomplete in this region (36, 115). Clearly this is a dynamic part of the enzyme, consistent with it playing a role in enzyme activation. Future studies should continue crystallization efforts in order to obtain a structural understanding of ‘882-induced HemY activation. As ‘882 activates HemY from a variety of Gram-positive bacteria, HemY from other species should be purified, and crystallization efforts should include these enzymes as well.

Probe heme biosynthesis with ‘882 to understand regulation of this pathway.

The identification of a small molecule that activates HemY may not be a random occurrence. Interestingly, HemY activity is increased to a similar extent by *in vitro* interactions with HemQ, the terminal pathway enzyme in this heme synthesis pathway (34). This suggests that the interaction of HemY with ‘882 may represent an inappropriate hijacking of a normal *in vivo* regulatory mechanism. Future work should attempt to identify intracellular molecules that may activate HemY. Lysates from *S. aureus* should be fractionated and screened in the P*hrt*.*lux* assay as previously described (47). Efforts should then be focused on identifying specific molecules that activate HssRS. Compounds confirmed to activate HssRS should then be tested in the HemY activity assay to determine their direct effect on HemY activity.

Regulation of heme biosynthesis remains largely unknown (21). ‘882 leads to an accumulation of CPIII in bacterial cells. By modulating HemY activity, effects of increased CPIII production can be characterized through transcriptional and translational changes of the enzymes involved in heme biosynthesis, which will elucidate potential regulatory mechanisms in *S. aureus* heme biosynthesis. In addition, HemY activity

should be tested in the presence of precursors and products in the heme biosynthesis pathway to determine if HemY is modulated through feedback or feedforward regulation. Finally, it has previously been shown that *in vitro* addition of HemQ increases HemY activity (24, 32, 34). This suggests that HemY may interact with HemQ. Therefore, the HemY-HemQ interaction may be required for regulation of HemY activity. Therefore, molecules identified in the screen described above as well as intermediates in the heme biosynthesis pathway should also be tested in the presence of HemQ. Taken together, the completion of these studies will provide insights into the regulation of heme biosynthesis in Gram-positive bacteria.

THERAPEUTIC APPLICATION OF '882-BASED ANTIMICROBIALS.

Current antimicrobial PDT is limited due to non-specific effects of ALA, the only FDA approved photosensitizer (16). '882-PDT has been validated as a potential bacterial specific therapeutic strategy in Chapter III. Future studies should continue to develop '882-based therapeutics for treatment of infectious diseases.

Optimize application of the '882-based therapeutics.

In order to develop '882-based therapeutics, numerous studies should be performed. First, species that are responsive to '882 should be determined. HemY from addition Gram-positive bacterial species should be purified and tested for '882-induced activation as discussed in Chapter III. Based upon the results from this analysis, the range of species that may be sensitive to '882-PDT can be determined. Second, the SAR studies presented in Chapter III in combination with future studies should be utilized to design

superior ‘882 derivatives for *in vivo* testing. The most active probes should be tested for toxicity. In addition, drug metabolism and pharmacokinetic studies should be performed to identify probes that have favorable properties for *in vivo* testing. Finally, devices to deliver light to the site of infection should be optimized. The data presented in Chapter III utilizes 2.5 J/cm^2 of blue-light. Importantly, this dose of light is significantly lower than has previously been utilized in murine models of *S. aureus* infection treated with ALA-PDT (100). Limiting the intensity of light exposure decreases the possibility of off-target effects on mammalian skin. Taken together, optimizing ‘882-derivatives for therapeutic development, and optimizing light delivery is important in development of ‘882-based PDT.

Determine resistance frequency and mechanisms of resistance to ‘882-PDT.

An important limitation of current antimicrobial therapies is the development of resistance to antibiotics. To further characterize ‘882 as a potential therapeutic, the resistance frequency and the mechanisms of resistance should be determined. This will further define the utility of ‘882-PDT as a potential therapeutic option in treating infectious diseases. Researchers have attempted to determine the frequency of bacterial resistance to current PDT strategies. Interestingly, bacteria resistant to PDT have not been identified (16, 20, 141). Identifying the frequency and mechanisms of resistance to ‘882-PDT will characterize the long-term efficacy of ‘882-PDT as a therapeutic strategy.

Develop small molecule activators of HemY outside of Gram-positive organisms.

The successful application of ‘882 to modulate heme biosynthesis opens the doors for applications beyond Gram-positive bacteria. *H. sapiens* and Gram-negative Bactria encode HemY enzymes that serve as protoporphyrinogen oxidases, which although similar, are structurally distinct from HemY from Gram-positive organisms. Importantly, deficiencies of HemY in *H. sapiens* results in a disease known as variegate porphyria (137, 142). Upon obtaining a structure of the HemY-‘882 complex, structural relationships between HemY from Gram-positive bacteria, HemY from Gram-negative bacteria, and HemY from *H. sapiens* should be determined. Ultimately, this analysis will provide insight into developing small molecules that target HemY from *H. sapiens* and Gram-negative bacteria. Molecules targeting HemY from *H. sapiens* could provide insights into treatments for variegate porphyria. The success of ‘882-PDT in treating Gram-positive bacterial infections provides proof-of-concept that activation of porphyrin production induces toxicity in the presence of light. Therefore, small molecules that activate HemY from Gram-negative bacteria will allow for the development of small molecule based PDT strategies to treat Gram-negative bacterial infections. Taken together, future studies should focus on expanding the application of small molecule HemY activators.

REFERENCES

1. **Wertheim HFL**, **Melles DC**, **Vos MC**, **van Leeuwen W**, **van Belkum A**, **Verbrugh HA**, **Nouwen JL**. 2005. The role of nasal carriage in *Staphylococcus aureus* infections. Lancet Infect Dis **5**:751–762.

2. **Shorr AF**, **Tabak YP**, **Gupta V**, **Johannes RS**, **Liu LZ**, **Kollef MH**. 2006. Morbidity and cost burden of methicillin-resistant *Staphylococcus aureus* in early onset ventilator-associated pneumonia. Crit Care **10**:R97.

3. **Wisplinghoff H**, **Bischoff T**, **Tallent SM**, **Seifert H**, **Wenzel RP**, **Edmond MB**. 2004. Nosocomial bloodstream infections in US hospitals: analysis of 24,179 cases from a prospective nationwide surveillance study. Clin Infect Dis **39**:309–317.

4. **Shorr AF**, **Haque N**, **Taneja C**, **Zervos M**, **Lamerato L**, **Kothari S**, **Zilber S**, **Donabedian S**, **Perri MB**, **Spalding J**, **Oster G**. 2010. Clinical and economic outcomes for patients with health care-associated *Staphylococcus aureus* pneumonia. J Clin Microbiol **48**:3258–3262.

5. **Klevens RM**, **Edwards JR**, **Tenover FC**, **McDonald LC**, **Horan T**, **Gaynes R**, **National Nosocomial Infections Surveillance System**. 2006. Changes in the epidemiology of methicillin-resistant *Staphylococcus aureus* in intensive care units in US hospitals, 1992-2003. Clin Infect Dis **42**:389–391.

6. **Klevens RM**, **Morrison MA**, **Nadle J**, **Petit S**, **Gershman K**, **Ray S**, **Harrison LH**, **Lynfield R**, **Dumyati G**, **Townes JM**, **Craig AS**, **Zell ER**, **Fosheim GE**, **McDougal LK**, **Carey RB**, **Fridkin SK**, **Active Bacterial Core surveillance (ABCs) MRSA Investigators**. 2007. Invasive methicillin-resistant *Staphylococcus aureus* infections in the United States. JAMA **298**:1763–1771.

7. **DeLeo FR**, **Otto M**, **Kreiswirth BN**, **Chambers HF**. 2010. Community-associated meticillin-resistant *Staphylococcus aureus*. Lancet **375**:1557–1568.

8. **Graham PL**, **Lin SX**, **Larson EL**. 2006. A U.S. population-based survey of *Staphylococcus aureus* colonization. Ann Intern Med **144**:318–325.

9. **Otto M**. 2013. Community-associated MRSA: what makes them special? Int J Med Microbiol **303**:324–330.

10. **Harris SR**, **Feil EJ**, **Holden MTG**, **Quail MA**, **Nickerson EK**, **Chantratita N**, **Gardete S**, **Tavares A**, **Day N**, **Lindsay JA**, **Edgeworth JD**, **de Lencastre H**, **Parkhill J**, **Peacock SJ**, **Bentley SD**. 2010. Evolution of MRSA during hospital transmission and intercontinental spread. Science **327**:469–474.

11. **Pantosti A**, **Venditti M**. 2009. What is MRSA? Eur Respir J **34**:1190–1196.

12. **Fluit AC**, **Jones ME**, **Schmitz FJ**, **Acar J**, **Gupta R**, **Verhoef J**. 2000. Antimicrobial susceptibility and frequency of occurrence of clinical blood isolates in Europe from the SENTRY antimicrobial surveillance program, 1997 and 1998. Clin Infect Dis **30**:454–460.

13. **The Centers for Disease Control and Prevention**. 2013. Antibiotic Resistance Threats in the United States, 2013.

14. **Bhate K**, **Williams HC**. 2013. Epidemiology of acne vulgaris. Br J Dermatol **168**:474–485.

15. **Tognetti L**, **Martinelli C**, **Berti S**, **Hercogova J**, **Lotti T**, **Leoncini F**, **Moretti S**. 2012. Bacterial skin and soft tissue infections: review of the epidemiology, microbiology, aetiopathogenesis and treatment: a collaboration between dermatologists and infectivologists. J Eur Acad Dermatol Venereol **26**:931–941.

16. **Wan MT**, **Lin JY**. 2014. Current evidence and applications of photodynamic therapy in dermatology. Clin Cosmet Investig Dermatol **7**:145–163.

17. **Cunliffe WJ**. 1986. Acne and unemployment. Br J Dermatol **115**:386.

18. **Basra MKA**, **Shahrukh M**. 2009. Burden of skin diseases. Expert Rev Pharmacoecon Outcomes Res **9**:271–283.

19. **Walsh TR**, **Efthimiou J**, **Dréno B**. 2016. Systematic review of antibiotic resistance in acne: an increasing topical and oral threat. Lancet Infect Dis **16**:e23–33.

20. **Aslam I**, **Fleischer A**, **Feldman S**. 2015. Emerging drugs for the treatment of acne. Expert Opin Emerg Drugs **20**:91–101.

21. **Choby JE**, **Skaar EP**. 2016. Heme Synthesis and Acquisition in Bacterial Pathogens. Journal of Molecular Biology.

22. **Frankenberg N**, **Moser J**, **Jahn D**. 2003. Bacterial heme biosynthesis and its biotechnological application. Applied Microbiology and Biotechnology **63**:115–127.

23. **Haley KP**, **Skaar EP**. 2012. A battle for iron: host sequestration and *Staphylococcus aureus* acquisition. Microbes Infect **14**:217–227.

24. **Mayfield JA**, **Hammer ND**, **Kurker RC**, **Chen TK**, **Ojha S**, **Skaar EP**, **DuBois JL**. 2013. The chlorite dismutase (HemQ) from *Staphylococcus aureus* has a redox-sensitive heme and is associated with the small colony variant phenotype. Journal of Biological Chemistry **288**:23488–23504.

25. **Skaar EP**, **Schneewind O**. 2004. Iron-regulated surface determinants (Isd) of *Staphylococcus aureus*: stealing iron from heme. Microbes Infect **6**:390–397.

26. **Hammer ND**, **Reniere ML**, **Cassat JE**, **Zhang Y**, **Hirsch AO**, **Indriati Hood M**, **Skaar EP**. 2013. Two heme-dependent terminal oxidases power *Staphylococcus aureus* organ-specific colonization of the vertebrate host. mBio **4**:e00241–13–e00241–13.

27. **Torres VJ**, **Pishchany G**, **Humayun M**, **Schneewind O**, **Skaar EP**. 2006. *Staphylococcus aureus* IsdB is a hemoglobin receptor required for heme iron utilization. J Bacteriol **188**:8421–8429.

28. **Skaar EP**. 2010. The battle for iron between bacterial pathogens and their vertebrate hosts. PLoS Pathog **6**:e1000949.

29. **Mazmanian SK**, **Skaar EP**, **Gaspar AH**, **Humayun M**, **Gornicki P**, **Jelenska J**, **Joachmiak A**, **Missiakas DM**, **Schneewind O**. 2003. Passage of Heme-Iron Across the Envelope of *Staphylococcus aureus*. Science **299**:906–909.

30. **Holden JK**, **Li H**, **Jing Q**, **Kang S**, **Richo J**, **Silverman RB**, **Poulos TL**. 2013. Structural and biological studies on bacterial nitric oxide synthase inhibitors. Proc Natl Acad Sci USA **110**:18127–18131.

31. **Skaar EP**, **Gaspar AH**, **Schneewind O**. 2004. IsdG and IsdI, heme-degrading enzymes in the cytoplasm of *Staphylococcus aureus*. J Biol Chem **279**:436–443.

32. **Dailey HA**, **Gerdes S**, **Dailey TA**, **Burch JS**, **Phillips JD**. 2015. Noncanonical coproporphyrin-dependent bacterial heme biosynthesis pathway that does not use protoporphyrin. Proc Natl Acad Sci USA **112**:2210–2215.

33. **Lobo SAL**, **Scott A**, **Videira MAM**, **Winpenny D**, **Gardner M**, **Palmer MJ**, **Schroeder S**, **Lawrence AD**, **Parkinson T**, **Warren MJ**, **Saraiva LM**. 2015. *Staphylococcus aureus* haem biosynthesis: characterisation of the enzymes involved in final steps of the pathway. Mol Microbiol **97**:472–487.

34. **Dailey T**, **Boynton T**, **Albetel A-N**, **Gerdes S**, **Johnson M**, **Dailey H**. 2010. Discovery and Characterization of HemQ: an essential heme biosynthetic pathway component. J Biol Chem **285**:25978–86.

35. **Hansson M**, **Hederstedt L**. 1994. *Bacillus subtilis* HemY is a peripheral membrane protein essential for protoheme IX synthesis which can oxidize coproporphyrinogen III and protoporphyrinogen IX. J Bacteriol **176**:5962–5970.

36. **Corradi HR**, **Corrigall AV**, **Boix E**, **Mohan CG**, **Sturrock ED**, **Meissner PN**, **Acharya KR**. 2006. Crystal structure of protoporphyrinogen oxidase from *Myxococcus xanthus* and its complex with the inhibitor acifluorfen. J Biol Chem **281**:38625–38633.

37. **Dailey HA**, **Dailey TA**. 1996. Protoporphyrinogen oxidase of *Myxococcus xanthus*. Expression, purification, and characterization of the cloned enzyme. J Biol Chem **271**:8714–8718.

38. **Stock AM**, **Robinson VL**, **Goudreau PN**. 2000. Two-component signal transduction. Annu Rev Biochem **69**:183–215.

39. **Capra EJ**, **Laub MT**. 2012. Evolution of two-component signal transduction systems. Annu Rev Microbiol **66**:325–347.

40. **Perry J**, **Koteva K**, **Wright G**. 2011. Receptor domains of two-component signal transduction systems. Mol Biosyst **7**:1388–1398.

41. **Laub MT**, **Goulian M**. 2007. Specificity in two-component signal transduction pathways. Annu Rev Genet **41**:121–145.

42. **Bader MW**, **Sanowar S**, **Daley ME**, **Schneider AR**, **Cho U**, **Xu W**, **Klevit RE**, **Le Moual H**, **Miller SI**. 2005. Recognition of antimicrobial peptides by a bacterial sensor kinase. Cell **122**:461–472.

43. **Wolanin PM**, **Thomason PA**, **Stock JB**. 2002. Histidine protein kinases: key signal transducers outside the animal kingdom. Genome Biol **3**:REVIEWS3013.

44. **Stauff DL**, **Torres VJ**, **Skaar EP**. 2007. Signaling and DNA-binding activities of the *Staphylococcus aureus* HssR-HssS two-component system required for heme sensing. J Biol Chem **282**:26111–26121.

45. **Stauff DL**, **Bagaley D**, **Torres VJ**, **Joyce R**, **Anderson KL**, **Kuechenmeister L**, **Dunman PM**, **Skaar EP**. 2008. *Staphylococcus aureus* HrtA is an ATPase required for protection against heme toxicity and prevention of a transcriptional heme stress response. J Bacteriol **190**:3588–3596.

46. **Torres VJ**, **Stauff DL**, **Pishchany G**, **Bezbradica JS**, **Gordy LE**, **Iturregui J**, **Anderson KL**, **Dunman PM**, **Joyce S**, **Skaar EP**. 2007. A *Staphylococcus aureus* regulatory system that responds to host heme and modulates virulence. Cell Host and Microbe **1**:109–119.

47. **Mike LA**, **Dutter BF**, **Stauff DL**, **Moore JL**, **Vitko NP**, **Aranmolate O**, **Kehl-Fie TE**, **Sullivan S**, **Reid PR**, **DuBois JL**, **Richardson AR**, **Caprioli RM**, **Sulikowski GA**, **Skaar EP**. 2013. Activation of heme biosynthesis by a small molecule that is toxic to fermenting *Staphylococcus aureus*. Proc Natl Acad Sci USA **110**:8206–8211.

48. **Francis KP**, **Joh D**, **Bellinger-Kawahara C**, **Hawkinson MJ**, **Purchio TF**, **Contag PR**. 2000. Monitoring bioluminescent *Staphylococcus aureus* infections in living mice using a novel *luxABCDE* construct. Infect Immun **68**:3594–3600.

49. **Dutter BF**, **Mike LA**, **Reid PR**, **Chong KM**, **Ramos-Hunter SJ**, **Skaar EP**, **Sulikowski GA**. 2016. Decoupling Activation of Heme Biosynthesis from Anaerobic Toxicity in a Molecule Active in *Staphylococcus aureus*. ACS Chem Biol acschembio.5b00934.

50. **Lomenick B**, **Hao R**, **Jonai N**, **Chin RM**, **Aghajan M**, **Warburton S**, **Wang J**, **Wu RP**, **Gomez F**, **Loo JA**, **Wohlschlegel JA**, **Vondriska TM**, **Pelletier J**, **Herschman HR**, **Clardy J**, **Clarke CF**, **Huang J**. 2009. Target identification using drug affinity responsive target stability (DARTS). Proc Natl Acad Sci USA **106**:21984–21989.

51. **Ziegler S**, **Pries V**, **Hedberg C**, **Waldmann H**. 2013. Target identification for small bioactive molecules: finding the needle in the haystack. **52**:2744–2792.

52. **Burdine L**, **Kodadek T**. 2004. Target identification in chemical genetics: the (often) missing link. **11**:593–597.

53. **Palmer KL**, **Daniel A**, **Hardy C**, **Silverman J**, **Gilmore MS**. 2011. Genetic basis for daptomycin resistance in enterococci. Antimicrob Agents Chemother **55**:3345–3356.

54. **Kaatz GW**, **Lundstrom TS**, **Seo SM**. 2006. Mechanisms of daptomycin resistance in *Staphylococcus aureus*. Int J Antimicrob Agents **28**:280–287.

55. **Peleg AY**, **Miyakis S**, **Ward DV**, **Earl AM**, **Rubio A**, **Cameron DR**, **Pillai S**, **Moellering RC**, **Eliopoulos GM**. 2012. Whole genome characterization of the mechanisms of daptomycin resistance in clinical and laboratory derived isolates of *Staphylococcus aureus*. PLoS ONE **7**:e28316.

56. **Meredith TC**, **Wang H**, **Beaulieu P**, **Gründling A**, **Roemer T**. 2012. Harnessing the power of transposon mutagenesis for antibacterial target identification and evaluation. **2**:171–178.

57. **Wang H**, **Claveau D**, **Vaillancourt JP**, **Roemer T**, **Meredith TC**. 2011. High-frequency transposition for determining antibacterial mode of action. Nat Chem Biol **7**:720–729.

58. **Borden JR**, **Papoutsakis ET**. 2007. Dynamics of genomic-library enrichment and identification of solvent tolerance genes for *Clostridium acetobutylicum*. Appl Environ Microbiol **73**:3061–3068.

59. **Luesch H**, **Wu TYH**, **Ren P**, **Gray NS**, **Schultz PG**, **Supek F**. 2005. A genome-wide overexpression screen in yeast for small-molecule target identification. **12**:55–63.

60. **Dryden MS**. 2009. Skin and soft tissue infection: microbiology and epidemiology. Int J Antimicrob Agents **34 Suppl 1**:S2–7.

61. **Barra F**, **Roscetto E**, **Soriano AA**, **Vollaro A**, **Postiglione I**, **Pierantoni GM**, **Palumbo G**, **Catania MR**. 2015. Photodynamic and Antibiotic Therapy in Combination to Fight Biofilms and Resistant Surface Bacterial Infections. Int J Mol Sci **16**:20417–20430.

62. **Fu X-J**, **Fang Y**, **Yao M**. 2013. Antimicrobial Photodynamic Therapy for Methicillin-Resistant *Staphylococcus aureus* Infection. BioMed Research International **2013**:1–9.

63. **Maisch T**, **Hackbarth S**, **Regensburger J**, **Felgenträger A**, **Bäumler W**, **Landthaler M**, **Röder B**. 2011. Photodynamic inactivation of multi-resistant bacteria (PIB) - a new approach to treat superficial infections in the 21st century. J Dtsch Dermatol Ges **9**:360–366.

64. **Gholam P**, **Kroehl V**, **Enk AH**. 2013. Dermatology life quality index and side effects after topical photodynamic therapy of actinic keratosis. Dermatology (Basel) **226**:253–259.

65. **Clark C**, **Bryden A**, **Dawe R**, **Moseley H**, **Ferguson J**, **Ibbotson SH**. 2003. Topical 5-aminolaevulinic acid photodynamic therapy for cutaneous lesions: outcome and comparison of light sources. Photodermatol Photoimmunol Photomed **19**:134–141.

66. **Bisland SK**, **Chien C**, **Wilson BC**, **Burch S**. 2006. Pre-clinical *in vitro* and *in vivo* studies to examine the potential use of photodynamic therapy in the treatment of osteomyelitis. Photochem Photobiol Sci **5**:31–38.

67. **Dai T**, **Huang Y-Y**, **Hamblin MR**. 2009. Photodynamic therapy for localized infections—State of the art. Photodiagnosis and Photodynamic Therapy **6**:170–188.

68. **Choi S**, **Lee H**, **Chae H**. 2012. Comparison of *in vitro* photodynamic antimicrobial activity of protoporphyrin IX between endoscopic white light and newly developed narrowband endoscopic light against *Helicobacter pylori* 26695. J Photochem Photobiol B, Biol **117**:55–60.

69. **Hatogai K**, **Yano T**, **Kojima T**, **Onozawa M**, **Daiko H**, **Nomura S**, **Yoda Y**, **Doi T**, **Kaneko K**, **Ohtsu A**. 2016. Salvage photodynamic therapy for local failure after chemoradiotherapy for esophageal squamous cell carcinoma. Gastrointest Endosc **83**:1130–1139.e3.

70. **Cassat JE**, **Skaar EP**. 2013. Recent advances in experimental models of osteomyelitis. Expert Rev Anti Infect Ther **11**:1263–1265.

71. **Gerber JS**, **Coffin SE**, **Smathers SA**, **Zaoutis TE**. 2009. Trends in the incidence of methicillin-resistant *Staphylococcus aureus* infection in children's hospitals in the United States. Clin Infect Dis **49**:65–71.

72. **Campoccia D**, **Montanaro L**, **Arciola CR**. 2006. The significance of infection related to orthopedic devices and issues of antibiotic resistance. Biomaterials **27**:2331–2339.

73. **Bisland SK**, **Burch S**. 2006. Photodynamic therapy of diseased bone.

Photodiagnosis and Photodynamic Therapy **3**:147–155.

74. **Goto B**, **Iriuchishima T**, **Horaguchi T**, **Tokuhashi Y**, **Nagai Y**, **Harada T**, **Saito A**, **Aizawa S**. 2011. Therapeutic effect of photodynamic therapy using Na-pheophorbide a on osteomyelitis models in rats. Photomed Laser Surg **29**:183–189.

75. **Li X**, **Guo H**, **Tian Q**, **Zheng G**, **Hu Y**, **Fu Y**, **Tan H**. 2013. Effects of 5-aminolevulinic acid-mediated photodynamic therapy on antibiotic-resistant staphylococcal biofilm: an in vitro study. J Surg Res **184**:1013–1021.

76. **Krespi YP**, **Kizhner V**. 2011. Phototherapy for chronic rhinosinusitis. Lasers Surg Med **43**:187–191.

77. **Galperin MY**, **Nikolskaya AN**, **Koonin EV**. 2001. Novel domains of the prokaryotic two-component signal transduction systems. FEMS Microbiol Lett **203**:11–21.

78. **Lee H-N**, **Jung K-E**, **Ko I-J**, **Baik HS**, **Oh J-I**. 2012. Protein-protein interactions between histidine kinases and response regulators of *Mycobacterium tuberculosis* H37Rv. J Microbiol **50**:270–277.

79. **Barbieri CM**, **Wu T**, **Stock AM**. 2013. Comprehensive analysis of OmpR phosphorylation, dimerization, and DNA binding supports a canonical model for activation. Journal of Molecular Biology **425**:1612–1626.

80. **Scharf BE**. 2010. Summary of useful methods for two-component system research. Curr Opin Microbiol **13**:246–252.

81. **Mike LA**, **Choby JE**, **Brinkman PR**, **Olive LQ**, **Dutter BF**, **Ivan SJ**, **Gibbs CM**, **Sulikowski GA**, **Stauff DL**, **Skaar EP**. 2014. Two-component system cross-regulation integrates *Bacillus anthracis* response to heme and cell envelope stress. PLoS Pathog **10**:e1004044.

82. **Gao R**, **Stock AM**. 2009. Biological insights from structures of two-component proteins. Annu Rev Microbiol **63**:133–154.

83. **Kostakioti M**, **Hadjifrangiskou M**, **Pinkner JS**, **Hultgren SJ**. 2009. QseC-mediated dephosphorylation of QseB is required for expression of genes associated with virulence in uropathogenic Escherichia coli. Mol Microbiol **73**:1020–1031.

84. **Loomis WF**, **Shaulsky G**, **Wang N**. 1997. Histidine kinases in signal transduction pathways of eukaryotes. J Cell Sci **110 (Pt 10)**:1141–1145.

85. **Miller SI**, **Kukral AM**, **Mekalanos JJ**. 1989. A two-component regulatory system (phoP phoQ) controls *Salmonella typhimurium* virulence. Proc Natl Acad Sci USA **86**:5054–5058.

86. **Xu J**, **Fu S**, **Liu M**, **Xu Q**, **Bei W**, **Chen H**, **Tan C**. 2014. The two-component system NisK/NisR contributes to the virulence of *Streptococcus suis* serotype 2. Microbiol Res **169**:541–546.

87. **Chand NS**, **Hung DT**. 2011. The two-component sensor kinase KinB acts as a non-canonical switch between acute and chronic infection. Virulence **2**:553–558.

88. **Miller SI**, **Mekalanos JJ**. 1990. Constitutive expression of the phoP regulon attenuates Salmonella virulence and survival within macrophages. J Bacteriol **172**:2485–2490.

89. **Yarwood JM**, **Schlievert PM**. 2003. Quorum sensing in *Staphylococcus* infections. The Journal of clinical investigation **112**:1620–5.

90. **Barrett JF**, **Hoch JA**. 1998. Two-component signal transduction as a target for microbial anti-infective therapy. Antimicrob Agents Chemother **42**:1529–1536.

91. **Shorr AF**, **Combes A**, **Kollef MH**, **Chastre J**. 2006. Methicillin-resistant *Staphylococcus aureus* prolongs intensive care unit stay in ventilator-associated pneumonia, despite initially appropriate antibiotic therapy. Critical Care Medicine **34**:700–706.

92. **Wright JS**, **Lyon GJ**, **George EA**, **Muir TW**, **Novick RP**. 2004. Hydrophobic interactions drive ligand-receptor recognition for activation and inhibition of staphylococcal quorum sensing. Proc Natl Acad Sci USA **101**:16168–16173.

93. **Stauff DL**, **Skaar EP**. 2009. *Bacillus anthracis* HssRS signalling to HrtAB regulates haem resistance during infection. Mol Microbiol **72**:763–778.

94. **Duthie ES**, **Lorenz LL**. 1952. Staphylococcal coagulase; mode of action and antigenicity. J Gen Microbiol **6**:95–107.

95. **Attia AS**, **Benson MA**, **Stauff DL**, **Torres VJ**, **Skaar EP**. 2010. Membrane damage elicits an immunomodulatory program in *Staphylococcus aureus*. PLoS Pathog **6**:e1000802.

96. **Kreiswirth BN**, **Löfdahl S**, **Betley MJ**, **O'Reilly M**, **Schlievert PM**, **Bergdoll MS**, **Novick RP**. 1983. The toxic shock syndrome exotoxin structural gene is not detectably transmitted by a prophage. Nature **305**:709–712.

97. **Bae T**, **Schneewind O**. 2006. Allelic replacement in *Staphylococcus aureus* with inducible counter-selection. Plasmid **55**:58–63.

98. **Horton RM**, **Cai ZL**, **Ho SN**, **Pease LR**. 1990. Gene splicing by overlap extension: tailor-made genes using the polymerase chain reaction. BioTechniques **8**:528–535.

99. **Weiner MP**, **Costa GL**, **Schoettlin W**, **Cline J**, **Mathur E**, **Bauer JC**. 1994.

Site-directed mutagenesis of double-stranded DNA by the polymerase chain reaction. Gene **151**:119–123.

100. **Morimoto K**, **Ozawa T**, **Awazu K**, **Ito N**, **Honda N**, **Matsumoto S**, **Tsuruta D**. 2014. Photodynamic therapy using systemic administration of 5-aminolevulinic acid and a 410-nm wavelength light-emitting diode for methicillin-resistant *Staphylococcus aureus*-infected ulcers in mice. PLoS ONE **9**:e105173.

101. **Sterne M**. 1946. Avirulent anthrax vaccine. Onderstepoort J Vet Sci Anim Ind **21**:41–43.

102. **Dailey TA**, **Dailey HA**. 1996. Human protoporphyrinogen oxidase: expression, purification, and characterization of the cloned enzyme. Protein Sci **5**:98–105.

103. **Fey PD**, **Endres JL**, **Yajjala VK**, **Widhelm TJ**, **Boissy RJ**, **Bose JL**, **Bayles KW**. 2013. A genetic resource for rapid and comprehensive phenotype screening of nonessential *Staphylococcus aureus* genes. mBio **4**:e00537–12.

104. **Fujita H**. 2001. Measurement of δ-aminolevulinate dehydratase activity. Curr Protoc Toxicol **Chapter 8**:Unit 8.6.

105. **Reniere ML**, **Ukpabi GN**, **Harry SR**, **Stec DF**, **Krull R**, **Wright DW**, **Bachmann BO**, **Murphy ME**, **Skaar EP**. 2010. The IsdG-family of haem oxygenases degrades haem to a novel chromophore. Mol Microbiol **75**:1529–1538.

106. **Shepherd M**, **Dailey HA**. 2005. A continuous fluorimetric assay for protoporphyrinogen oxidase by monitoring porphyrin accumulation. Analytical biochemistry **344**:115–121.

107. **Wang F**, **Sambandan D**, **Halder R**, **Wang J**, **Batt SM**, **Weinrick B**, **Ahmad I**, **Yang P**, **Zhang Y**, **Kim J**, **Hassani M**, **Huszar S**, **Trefzer C**, **Ma Z**, **Kaneko T**, **Mdluli KE**, **Franzblau S**, **Chatterjee AK**, **Johnson K**, **Mikusova K**, **Besra GS**, **Fütterer K**, **Jacobs WR**, **Schultz PG**. 2013. Identification of a small molecule with activity against drug-resistant and persistent tuberculosis. Proc Natl Acad Sci USA **110**:E2510–7.

108. **Morris GM**, **Huey R**, **Lindstrom W**, **Sanner MF**, **Belew RK**, **Goodsell DS**, **Olson AJ**. 2009. AutoDock4 and AutoDockTools4: Automated docking with selective receptor flexibility. J Comput Chem **30**:2785–2791.

109. **Morris GM**, **Goodsell DS**, **Halliday RS**, **Huey R**. 1998. Automated docking using a Lamarckian genetic algorithm and an empirical binding free energy function. J Comput Chem **19**:1639–1662.

110. **Kugelberg E**, **Norström T**, **Petersen TK**, **Duvold T**, **Andersson DI**, **Hughes D**. 2005. Establishment of a superficial skin infection model in mice by using *Staphylococcus aureus* and *Streptococcus pyogenes*. Antimicrob Agents

Chemother **49**:3435–3441.

111. **Gao H**, **Su P**, **Shi Y**, **Shen X**, **Zhang Y**, **Dong J**, **Zhang J**. 2015. Discovery of novel VEGFR-2 inhibitors. Part II: Biphenyl urea incorporated with salicylaldoxime. Eur J Med Chem **90**:232–240.

112. **Bender T**, **Huss M**, **Wieczorek H**, **Grond S**, **Zezschwitz von P**. 2007. Convenient Synthesis of a [1-14C]Diazirinylbenzoic Acid as a Photoaffinity Label for Binding Studies of V-ATPase Inhibitors. European Journal of Organic Chemistry **2007**:3870–3878.

113. **Proctor RA**, **Eiff von C**, **Kahl BC**, **Becker K**, **McNamara P**, **Herrmann M**, **Peters G**. 2006. Small colony variants: a pathogenic form of bacteria that facilitates persistent and recurrent infections. Nat Rev Micro **4**:295–305.

114. **Sun L**, **Wen X**, **Tan Y**, **Li H**, **Yang X**, **Zhao Y**, **Wang B**, **Cao Q**, **Niu C**, **Xi Z**. 2009. Site-directed mutagenesis and computational study of the Y366 active site in *Bacillus subtilis* protoporphyrinogen oxidase. Amino Acids **37**:523–530.

115. **Qin X**, **Sun L**, **Wen X**, **Yang X**, **Tan Y**, **Jin H**, **Cao Q**, **Zhou W**, **Xi Z**, **Shen Y**. 2010. Structural insight into unique properties of protoporphyrinogen oxidase from *Bacillus subtilis*. J Struct Biol **170**:76–82.

116. **Zorn JA**, **Wells JA**. 2010. Turning enzymes ON with small molecules. Nat Chem Biol **6**:179–188.

117. **Grimsby J**, **Sarabu R**, **Corbett WL**, **Haynes N-E**, **Bizzarro FT**, **Coffey JW**, **Guertin KR**, **Hilliard DW**, **Kester RF**, **Mahaney PE**, **Marcus L**, **Qi L**, **Spence CL**, **Tengi J**, **Magnuson MA**, **Chu CA**, **Dvorozniak MT**, **Matschinsky FM**, **Grippo JF**. 2003. Allosteric activators of glucokinase: potential role in diabetes therapy. Science **301**:370–373.

118. **Howitz KT**, **Bitterman KJ**, **Cohen HY**, **Lamming DW**, **Lavu S**, **Wood JG**, **Zipkin RE**, **Chung P**, **Kisielewski A**, **Zhang L-L**, **Scherer B**, **Sinclair DA**. 2003. Small molecule activators of sirtuins extend *Saccharomyces cerevisiae* lifespan. Nature **425**:191–196.

119. **Stevens DL**, **Ma Y**, **Salmi DB**, **McIndoo E**, **Wallace RJ**, **Bryant AE**. 2007. Impact of antibiotics on expression of virulence-associated exotoxin genes in methicillin-sensitive and methicillin-resistant *Staphylococcus aureus*. J Infect Dis **195**:202–211.

120. **Skaar EP**, **Humayun M**, **Bae T**, **DeBord KL**, **Schneewind O**. 2004. Iron-source preference of *Staphylococcus aureus* infections. Science **305**:1626–1628.

121. **van Sorge NM**, **Beasley FC**, **Gusarov I**, **Gonzalez DJ**, **Köckritz-Blickwede von M**, **Anik S**, **Borkowski AW**, **Dorrestein PC**, **Nudler E**, **Nizet V**. 2013. Methicillin-resistant *Staphylococcus aureus* bacterial nitric-oxide synthase

affects antibiotic sensitivity and skin abscess development. Journal of Biological Chemistry **288**:6417–6426.

122. **Rafferty S**. 2011. Nitric Oxide Synthases of Bacteria - and Other Unicellular Organisms. The Open Nitric Oxide Journal **3**:25–32.

123. **Sudhamsu J**, **Crane BR**. 2009. Bacterial nitric oxide synthases: what are they good for? Trends Microbiol **17**:212–218.

124. **Shatalin K**, **Gusarov I**, **Avetissova E**, **Shatalina Y**, **McQuade LE**, **Lippard SJ**, **Nudler E**. 2008. *Bacillus anthracis*-derived nitric oxide is essential for pathogen virulence and survival in macrophages. Proc Natl Acad Sci USA **105**:1009–1013.

125. **Holden JK**, **Kang S**, **Beasley FC**, **Cinelli MA**, **Li H**, **Roy SG**, **Dejam D**, **Edinger AL**, **Nizet V**, **Silverman RB**, **Poulos TL**. 2015. Nitric Oxide Synthase as a Target for Methicillin-Resistant *Staphylococcus aureus*. Chem Biol **22**:785–792.

126. **Bose JL**, **Fey PD**, **Bayles KW**. 2013. Genetic tools to enhance the study of gene function and regulation in *Staphylococcus aureus*. Appl Environ Microbiol **79**:2218–2224.

127. **Wakeman CA**, **Hammer ND**, **Stauff DL**, **Attia AS**, **Anzaldi LL**, **Dikalov SI**, **Calcutt MW**, **Skaar EP**. 2012. Menaquinone biosynthesis potentiates haem toxicity in *Staphylococcus aureus*. Mol Microbiol **86**:1376–1392.

128. **Schneewind O**, **Model P**, **Fischetti VA**. 1992. Sorting of protein A to the staphylococcal cell wall. Cell **70**:267–281.

129. **Bubeck Wardenburg J**, **Williams WA**, **Missiakas D**. 2006. Host defenses against *Staphylococcus aureus* infection require recognition of bacterial lipoproteins. Proc Natl Acad Sci USA **103**:13831–13836.

130. **Manjula SN**, **Malleshappa Noolvi N**, **Vipan Parihar K**, **Manohara Reddy SA**, **Ramani V**, **Gadad AK**, **Singh G**, **Gopalan Kutty N**, **Mallikarjuna Rao C**. 2009. Synthesis and antitumor activity of optically active thiourea and their 2-aminobenzothiazole derivatives: a novel class of anticancer agents. Eur J Med Chem **44**:2923–2929.

131. **Anzaldi LL**, **Skaar EP**. 2010. Overcoming the heme paradox: heme toxicity and tolerance in bacterial pathogens. Infect Immun **78**:4977–4989.

132. **Kumar A**, **Toledo JC**, **Patel RP**, **Lancaster JR Jr**, **Steyn AJ**. 2007. *Mycobacterium tuberculosis* DosS is a redox sensor and DosT is a hypoxia sensor. Proc Natl Acad Sci USA **104**:11568–73.

133. **O'Neill J**. 2016. Tackling drug-resistant infections globally: final report and

recommendations. London: Wellcome Trust & HM Government.

134. **Sudhamsu J**, **Crane BR**. 2009. Bacterial nitric oxide synthases: what are they good for? Trends Microbiol **17**:212–8.

135. **Surdel MC**, **Dutter BF**, **Sulikowski GA**, **Skaar EP**. 2016. Bacterial Nitric Oxide Synthase Is Required for the *Staphylococcus aureus* Response to Heme Stress. ACS Infect Dis acsinfecdis.6b00081.

136. **Schobert M**, **Jahn D**. 2002. Regulation of heme biosynthesis in non-phototrophic bacteria. J Mol Microbiol Biotechnol **4**:287–294.

137. **Ajioka RS**, **Phillips JD**, **Kushner JP**. 2006. Biosynthesis of heme in mammals. Biochim Biophys Acta **1763**:723–736.

138. **Lechardeur D**, **Cesselin B**, **Liebl U**, **Vos MH**, **Fernandez A**, **Brun C**, **Gruss A**, **Gaudu P**. 2012. Discovery of intracellular heme-binding protein HrtR, which controls heme efflux by the conserved HrtB-HrtA transporter in *Lactococcus lactis*. Journal of Biological Chemistry **287**:4752–4758.

139. **Skerker JM**, **Perchuk BS**, **Siryaporn A**, **Lubin EA**, **Ashenberg O**, **Goulian M**, **Laub MT**. 2008. Rewiring the specificity of two-component signal transduction systems. Cell **133**:1043–1054.

140. **Gusarov I**, **Shatalin K**, **Starodubtseva M**, **Nudler E**. 2009. Endogenous nitric oxide protects bacteria against a wide spectrum of antibiotics. Science **325**:1380–1384.

141. **Cassidy CM**, **Donnelly RF**, **Tunney MM**. 2010. Effect of sub-lethal challenge with Photodynamic Antimicrobial Chemotherapy (PACT) on the antibiotic susceptibility of clinical bacterial isolates. J Photochem Photobiol B, Biol **99**:62–66.

142. **Qin X**, **Tan Y**, **Wang L**, **Wang Z**, **Wang B**, **Wen X**, **Yang G**, **Xi Z**, **Shen Y**. 2011. Structural insight into human variegate porphyria disease. FASEB J **25**:653–664.